Oil-Free Centrifugal Hydrogen Compression Technology Demonstration

Final Report

DOE Grant No.: DE-FG36-08GO18060

September 1, 2008 – May 31, 2014

MiTi® Project No.: 01W07-01-61208

Prepared for

Department of Energy

Hydrogen and Fuel Cells Program

Principal Investigator

Hooshang Heshmat, Ph.D.

Mohawk Innovative Technology, Inc.

1037 Watervliet-Shaker Rd.

Albany, NY 12205

1.0 Executive Summary

One of the key elements in realizing a mature market for hydrogen vehicles is the deployment of a safe and efficient hydrogen production and delivery infrastructure on a scale that can compete economically with current fuels. The challenge, however, is that hydrogen, being the lightest and smallest of gases with a lower viscosity and density than natural gas, readily migrates through small spaces and is difficult to compresses efficiently. While efficient and cost effective compression technology is crucial to effective pipeline delivery of hydrogen, the compression methods used currently rely on oil lubricated positive displacement (PD) machines. PD compression technology is very costly, has poor reliability and durability, especially for components subjected to wear (e.g., valves, rider bands and piston rings) and contaminates hydrogen with lubricating fluid. Even so called "oil-free" machines use oil lubricants that migrate into and contaminate the gas path. Due to the poor reliability of PD compressors, current hydrogen producers often install duplicate units in order to maintain on-line times of 98-99%. Such machine redundancy adds substantially to system capital costs. As such, DOE deemed that low capital cost, reliable, efficient and oil-free advanced compressor technologies are needed.

MiTi's solution is a completely oil-free, multi-stage, high-speed, centrifugal compressor designed for flow capacity of 500,000 kg/day with a discharge pressure of 1200 psig. The design employs oil-free compliant foil bearings and seals to allow for very high operating speeds, totally contamination free operation, long life and reliability. This design meets the DOE's performance targets and achieves an extremely aggressive, specific power metric of 0.48 kW-hr/kg and provides significant improvements in reliability/durability, energy efficiency, sealing and freedom from contamination. The multi-stage compressor system concept has been validated through full scale performance testing of a single stage with helium similitude gas at full speed in accordance with ASME PTC-10. The experimental results indicated that aerodynamic performance, with respect to compressor discharge pressure, flow, power and efficiency exceeded theoretical prediction. Dynamic testing of a simulated multi-stage centrifugal compressor was also completed under a parallel program to validate the integrity and viability of the system concept. The results give strong confidence in the feasibility of the multi-stage design for use in hydrogen gas transportation and delivery from production locations to point of use.

Mohawk Innovative Technology®, Inc.
1037 Watervliet-Shaker Road, Albany, NY 12205
URL: www.miti.cc
Phone: (518) 862-4290, FAX: (518) 862-4291

2.0 Acknowledgements

MiTi is grateful for the support from the DOE Hydrogen and Fuel Cells Program and, in particular, Sarah Dillich, Erika Sutherland, Katie Randolph, Monterey Gardiner and Mark Paster, for their sustained interest in our technology.

This has truly been a team effort. In addition to Dr. Hooshang Heshmat, who served as the PI on this project, almost all technical and non-technical staff at MiTi provided assistance. The MiTi Team included Dr. Jose Cordova, Andrew Z. Hunsberger, Dr. Said Jahanmir, Michael J. Tomaszewski, James F. Walton II, and many others. The exemplary assistance of Ms. Tiffany Truong, the Business Office Manager, is gratefully acknowledged.

The MHI team included Mr. Satoshi Hata, Mr. Daisuke Hirata and Mr. Masayuki Kita. MiTi is also grateful to expert advice received from our collaborators regarding the selection of appropriate materials for hydrogen service, particularly, Professor Petros Sofronis – U of Illinois, Dr. Brian Somerday – Sandia, and Dr. Rick Ricker – NIST.

Mohawk Innovative Technology®, Inc. URL: www.miti.cc
1037 Watervliet-Shaker Road, Albany, NY 12205 Phone: (518) 862-4290, FAX: (518) 862-4291

Table of Contents

Mohawk Innovative Technology®, Inc.
1037 Watervliet-Shaker Road, Albany, NY 12205
URL: www.miti.cc
Phone: (518) 862-4290, FAX: (518) 862-4291

Mohawk Innovative Technology®, Inc.
1037 Watervliet-Shaker Road, Albany, NY 12205
URL: www.miti.cc
Phone: (518) 862-4290, FAX: (518) 862-4291

3.0 List of Figures

Mohawk Innovative Technology®, Inc. URL: www.miti.cc
1037 Watervliet-Shaker Road, Albany, NY 12205 Phone: (518) 862-4290, FAX: (518) 862-4291

Mohawk Innovative Technology®, Inc.
1037 Watervliet-Shaker Road, Albany, NY 12205
URL: www.miti.cc
Phone: (518) 862-4290, FAX: (518) 862-4291

Mohawk Innovative Technology®, Inc. URL: www.miti.cc
1037 Watervliet-Shaker Road, Albany, NY 12205 Phone: (518) 862-4290, FAX: (518) 862-4291

Mohawk Innovative Technology®, Inc.
1037 Watervliet-Shaker Road, Albany, NY 12205
URL: www.miti.cc
Phone: (518) 862-4290, FAX: (518) 862-4291

4.0 List of Tables

Mohawk Innovative Technology®, Inc.
1037 Watervliet-Shaker Road, Albany, NY 12205
URL: www.miti.cc
Phone: (518) 862-4290, FAX: (518) 862-4291

5.0 Introduction

To meet the transmission and delivery compression needs of the DOE, novel and advanced high-speed, oil-free centrifugal compressor system technology is needed. MiTi has shown that three multi-stage centrifugal compressor frames, operating in series at speeds of 56,000, are both necessary and feasible. These high operating speeds, which exceed the highest current pipeline compressor speeds by a factor of 3-times, are needed because of the low molecular weight of hydrogen. In earlier SBIR efforts, MiTi demonstrated that centrifugal compressor stages employing advanced 3-D aerodynamic designs, combined with oil-free compliant foil bearings and close clearance compliant seals, make up the most critical components for the hydrogen transportation and delivery systems. Under this program, the compressor blade tip speeds of 1600 ft/sec (seen in advanced gas turbine engine components) and bearing DNs greater than 3 Million (where D is diameter in mm and N is speed in rpm), and exceed the capabilities of state-of-art (SOA) oil-lubricated bearings by a factor of 2 or more[1], are demonstrated. The double entry, multi-frame design was chosen to minimize thrust loads, machine complexity and power loss. This multi-frame system concept also offers a high degree of modularity to account for differing inlet conditions and requirements. For example, if inlet pressure conditions are lower than our reference inlet condition of 500 psig, then it would be possible to use more frames and or more stages per frame, as needed, to achieve the desired output conditions. This concept also incorporates an intercooler between frames for improved efficiency and packaging because the proposed compressor is approximately 20 times smaller in volume than SOA compressors.

MiTi has identified that SOA natural gas pipeline centrifugal compressors are unsuitable for economic transportation of hydrogen due to the use of moderate tip speed shrouded wheels; large clearances between the rotating components and stationary seals; and the emphasis on reliability over performance. A high compressor blade tip speed is important, as noted in the Euler turbomachinery equation: $W_x = U_2 C_{\theta 2} - U_1 C_{\theta 1}$, which relates the work delivered to the flow per unit mass to the change in exit velocities. Knowing the work delivered to the gas, the pressure ratio $pr_{Total} = \left(1 + \left(\eta / \left(C_p T_0\right)\right)\left(U_2 C_{\theta 2} - U_1 C_{\theta 1}\right)\right)^{k/(k-1)}$ may be determined where U = blade speed and C = absolute velocity, $k=C_p/C_v$, η = efficiency and T_0 = temperature. Given that pressure rise is a function of the velocity squared[23], the selected compressor design needs to impart a very high velocity and, hence, kinetic energy to the hydrogen since it is the smallest and lightest of elements. The shrouded centrifugal compressor design, having moderate tip speeds, will not permit the needed hydrogen pressure rise without a substantial increase in the number of stages or increases in tip speed. However, the needed speed increase is not possible in a shrouded wheel because the stresses at the shroud/blade interface will exceed material strength limits. Increasing the number of stages results in insurmountable rotordynamic challenges and increased radial and axial motions that will further increase seal clearances and, hence, leakage. The solution is, therefore, MiTi®'s unshrouded/open centrifugal compressor impeller system. Open impeller designs are commonly used in SOA helicopter gas turbine engines and turbochargers. While these compressors can achieve efficiencies at or above 80%, they need to operate at or near optimum speed and must maintain very small axial and radial clearances. By designing fewer stages per frame, it is easier to maintain small tip clearances; therefore; the design approach of using three independent frames, each operating at near optimum speeds for several stages, was chosen. Given the requirements for high tip speed and an open impeller design with

Mohawk Innovative Technology®, Inc.
1037 Watervliet-Shaker Road, Albany, NY 12205
URL: www.miti.cc
Phone: (518) 862-4290, FAX: (518) 862-4291

its stringent tip clearance requirements, it is easy to see why existing natural gas pipelines centrifugal compressors are unsuitable for hydrogen compression.

6.0 Technical Objectives

The overall objective of this effort was to demonstrate the integration of key technologies, needed to develop reliable and cost effective high-speed, oil-free centrifugal compressors, capable of meeting the DOE hydrogen transportation and delivery goals of 100,000 to 1,000,000 kg/day and at pressures to 1200 psig in a pipeline distribution system. Assuming an inlet pressure condition of 500 psi, this constitutes a pressure ratio of 2.4.

The MiTi team has met the program objectives by conducting an iterative design technique to converge of the most feasible solution. This design technique consisted of component level analysis of the compressor aerodynamics, stress analysis, material selection and rotor-bearing system dynamics. Following design, fabrication of the selected centrifugal compressor stage, and the corresponding oil-free bearings and seals was completed. Finally, testing of a single stage, high-speed, full-scale centrifugal compressor and oil-free compliant foil bearings was performed under realistic conditions using a similitude gas (helium) to verify aerodynamic performance.

The specific tasks of this program included: (1) Preliminary oil-free, multi-stage high-speed centrifugal compressor system design; (2) Detailed design of a full-scale centrifugal compressor stage; (3) Mechanical component detailed design of the oil-free bearings, seals and shaft system needed to test the compressor stage; (4) Test hardware fabrication; (5) Dynamic test; (6) Compressor performance test; (7) System design refinement; and (8) Program management and reporting.

6.1 Preliminary Design

A series of tradeoff studies was performed to demonstrate the feasibility of the proposed compressor concept, including identifying operating conditions and technologies critical to successful system development. These trade studies provided the information needed to define requirements for the key subsystem components, such as oil-free bearings, seals, material compatibility and aerodynamic components. Two compressor configurations were considered: a double-entry flow configuration to inherently balance thrust versus a single entry flow compressor for easier control of blade clearance. Following the trade-off study, a single compressor stage was selected for more detailed design and subsequent experimental validation.

6.2 Detailed Compressor Design

Following a preliminary design concept, a single compressor stage in detail and sufficient to fabricate the stage for testing in a realistic environment, was completed. Using the results of the preliminary design, the detailed design of the selected stage was prepared. The complete stage design included the inlet flow path, compressor impeller, diffuser and return channel. A volute was also designed for use. Three-Dimensional Computational Fluid Dynamic (CFD) aerodynamic software was used to evaluate and refine the compressor stage flow path design. Input data for the CFD analysis included impeller exit width and blade angle, impeller tip and hub radii, and the leading edge blade angle, as determined from flow velocity triangles.

Mohawk Innovative Technology®, Inc. URL: www.miti.cc
1037 Watervliet-Shaker Road, Albany, NY 12205 Phone: (518) 862-4290, FAX: (518) 862-4291

Using the established input parameters in the CFD model, an iterative aerodynamic design was completed to finalize blade angle, impeller width and blade exit angle and establish the impeller blade passage profiles to minimize internal flow turbulence. Impeller tip clearance was also evaluated. Following the CFD analysis, 3-D FEA was completed to ensure that stresses remained below critical threshold for the selected material, especially given the hydrogen environment. Materials known to be compatible with hydrogen and not susceptible to embrittlement, were reviewed and selected. When the compressor stage design was completed, the necessary fabrication design drawings were prepared for use in the hardware fabrication task. For single stage compressor testing a volute was used rather than a return channel which is only necessary in multi-stage compressors. The volute design was completed and drawings were created for fabrication.

6.3 Detailed Mechanical Component Designs

Given the expected high operating speed for the compressor stage, the criticality of maintaining blade tip clearances, and the importance of the bearing and seal losses to the overall system efficiency, it was imperative that the bearings and seals were properly designed and integrated with the test compressor stage. Therefore, the purpose and outcome of this task was the design of the oil-free bearings and non-contacting seals, needed to support the compressor rotors in a hydrogen environment.

Using the compressor sizing, blade tip clearance criteria and rotordynamic analysis, the foil bearings and seals were designed. Using coupled elasto-hydrodynamic design analysis for compressible fluid films and compliant elastic bearing surfaces, iterative design solutions were evaluated. Design studies were conducted to determine the detailed bearing and seal designs capable of meeting stiffness, load and differential pressure requirements of the compressor rotor system. Key design criteria included limiting rotor axial motion so that blade tip clearances were maintained, minimization of bearing/seal power loss and minimization of seal leakage.

6.4 Hardware Fabrication

Following a detailed mechanical design, the full-scale hardware needed to complete testing of a single compressor stage with a similitude gas (helium) was fabricated. Once the compressor, bearing design and critical design review were all completed, all necessary hardware was fabricated for testing. Compliant foil seals were not required in the single stage test configuration, as the system was hermetically sealed and no inter-stage sealing was required. The test compressor stage hardware fabricated included the inlet passage, impeller, diffuser and volute. Journal and thrust compliant foil bearings were fabricated to support the single stage compressor test. All fabricated hardware was inspected to ensure compliance with the manufacturing drawings produced under Task 3.

6.5 Performance Testing

The purpose and outcome of this task was to validate the compressor aerodynamic and the rotor-bearing-seal system designs through full-scale tests. Following bearing and seal mechanical component validation testing, the compressor was installed in appropriate compressor stage testing facilities. The compressor test facility included all key elements of the designed compressor stage and was instrumented to record inlet mass flow, temperature and pressure, as

Mohawk Innovative Technology®, Inc. URL: www.miti.cc
1037 Watervliet-Shaker Road, Albany, NY 12205 Phone: (518) 862-4290, FAX: (518) 862-4291

well as pressures and temperatures throughout the flow path and exit. For these tests, the industry standard ASME PTC-10 code for testing and validating compressor designs was followed. Tests were conducted at different inlet conditions to demonstrate stability and performance under varying conditions, simulating both lower and higher inlet pressures than the reference. Aerodynamic performance was validated through testing with a similitude gas (helium) using standard methods for Type 2 tests in accordance with PTC-10. While these tests adequately confirm mechanical performance of the single-stage compressor, material compatibility issues related specifically to hydrogen embrittlement with the selected titanium alloys were also studied and testing performed on representative titanium samples. A thorough literature survey was conducted and the most appropriate materials were determined for different components of the compressor, including shafting, foil bearings and compatibility of coatings. Due to a limited amount of experimental testing found in the literature, especially in high pressure hydrogen environments, it was decided to perform fracture testing in high pressure hydrogen. These tests were performed at Sandia National Laboratories with the objective to identify the effects of hydrogen on fatigue crack growth. The tests were conducted on compact tension specimens, according to ASTM standards, in both air and hydrogen environments at 1200 psig.

6.6 Design Refinement

Based upon the data acquired from both component and compressor stage testing, the hydrogen centrifugal compressor design concept was refined to account for the differences identified between test and analysis. This stage design was then used as the reference for subsequent scaling and streamline trimming, as needed to configure the full multi-frame, multi-stage modular compressor system concept. Using the reference design, compressor system performance, intercooler heat load and total driving power required per frame was estimated. Finally, having identified the total system configuration, estimates of capital costs were made and compared to the established DOE capital cost milestone.

6.7 Project Management and Reporting

MiTi has managed the program technical activities, schedule and costs to accomplish program objectives. Program management functions included preparation and delivery of required technical, schedule and financial reports. Reports and other deliverables were provided in accordance with the Federal Assistance Reporting Checklist, following the instructions included therein. The MiTi Program Manager was the primary technical focal point between the Contracting Office Technical Representative and the project team.

7.0 Results: Compressor Design

The overall design of the oil-free centrifugal hydrogen compressor followed a multidimensional iterative process consisting of aerodynamic analysis, design of foil bearings and seals, finite element stress analysis, rotordynamic stability analysis, provisions for manufacturing and economic analysis, single stage compressor design, and manufacturing and installation of the compressor station. This design methodology is illustrated in Figure 1. Although each set of analysis are presented in this report as separate sequential sections, it should be noted that many iterations were performed during the design and analysis effort.

Mohawk Innovative Technology®, Inc.
1037 Watervliet-Shaker Road, Albany, NY 12205
URL: www.miti.cc
Phone: (518) 862-4290, FAX: (518) 862-4291

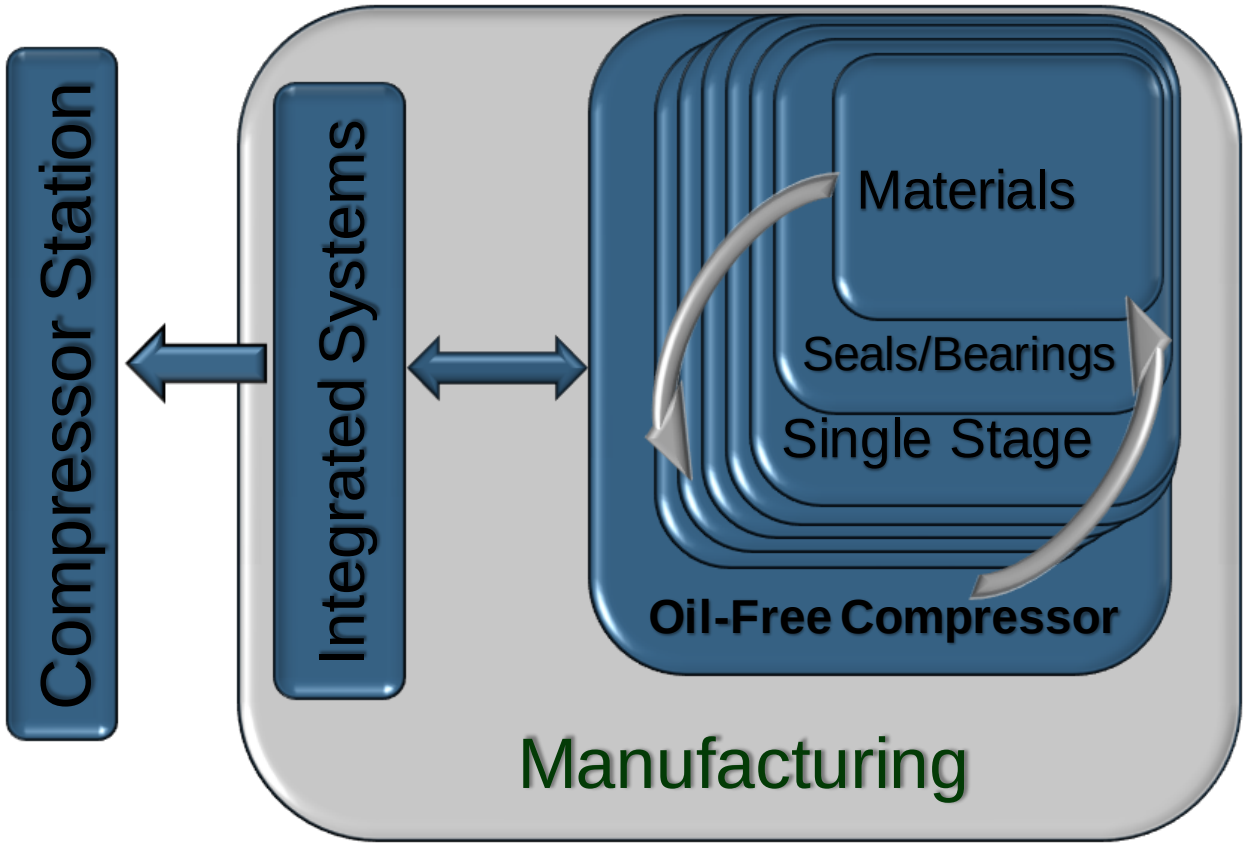

Figure 1. Conceptual integrated systems approach to compressor design

7.1 Preliminary Aerodynamic Design (Task 1)

In order to determine the approximate diameter and operating speed of the proposed compressor system, a preliminary sizing study was performed. This was accomplished using MiTi's proprietary, in-house software tools and also referencing commercial aerodynamic performance computer code. The preliminary design study began with an analysis of the first compression stage that will later form the basis for the multi-stage frames. The proposed pipeline compressor will employ a double entry configuration whereby the flow entering the compressor will be split in half, feeding each impeller stage with 250,000 kg/day, or half of the total projected flow. The justification for this design strategy is discussed in further detail in later sections. Sizing of the first compression stage began with review of non-dimensional performance data in literature, such as the curve presented in Figure 2. The non-dimensional performance curve presented is based on a collection of empirical data and provides reasonable approximation of expected performance from a centrifugal stage. The adiabatic efficiency of a single stage is shown to be highly dependent on the compressor's flow coefficient (Φ), a dimensional measure of the volume of flow that passes though a stage relative to the stage size and surface speed. Flow coefficient is defined as:

Mohawk Innovative Technology®, Inc.
1037 Watervliet-Shaker Road, Albany, NY 12205
URL: www.miti.cc
Phone: (518) 862-4290, FAX: (518) 862-4291

$$\Phi = \frac{\dot{m}}{\rho_{in}\pi r^2 U_2} \qquad \text{Eq. (1)}$$

where $\dot{m}$ is the mass flow, ρ_{in} is fluid density at the stage inlet, r is the compressor wheel radius and U_2 is the tip speed of the compressor wheel. The data presented is empirical and some deviation about this trend is possible; however, in order to develop the most efficient centrifugal compressor stage to meet the DOE's projected targets, it is crucial for the proposed compressor to have a flow coefficient at or near a value of 0.1.

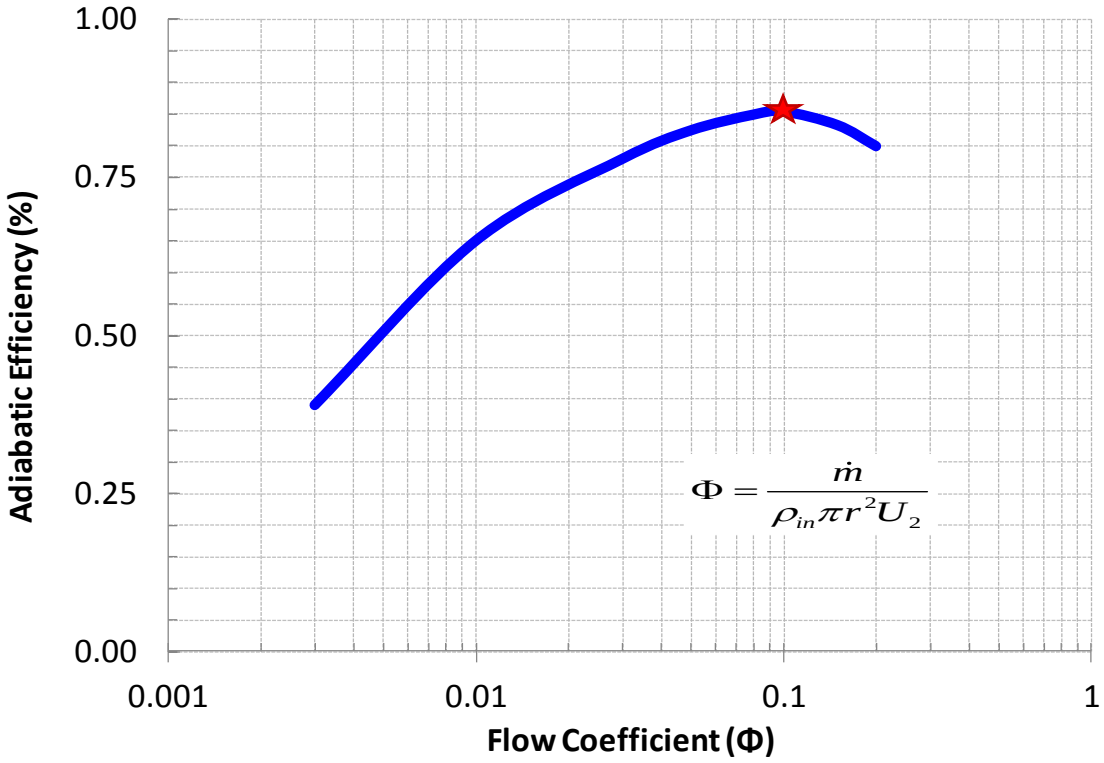

Figure 2. Expected stage adiabatic efficiency as a function of non-dimensional flow coefficient.[adapted from Aungier, R., "Centrifugal Compressors", ASME, 2000]

As a starting point for the preliminary design analysis, the flow coefficient was assumed to be held constant at 0.1. Both the mass flow and inlet pressure were fixed inputs to this design problem. As a reasonable assumption, the inlet gas temperature was assumed to be 100 ^{o}F so that gas density could be determined. This leaves only two remaining variables from equation (1) undefined: compressor diameter and tip speed.

The flow coefficient has been fixed to assure that this design study will yield a compressor concept capable of achieving the DOE's target for adiabatic efficiency. The second critical design requirement is to design a compact compressor system with the fewest number of stages, which is crucial for a concept that will also meet the DOE's targets for capital cost and footprint.

Mohawk Innovative Technology®, Inc.
1037 Watervliet-Shaker Road, Albany, NY 12205
URL: www.miti.cc
Phone: (518) 862-4290, FAX: (518) 862-4291

To achieve the objective 1200 psi discharge pressure in the fewest number of stages possible, maximum pressure ratio per stage is desired. The principle of operation of a centrifugal compressor is the conversion of kinetic energy from a rotating shaft to potential energy (pressure) in the working fluid. This kinetic energy is imparted on the gas through the high tip speeds of the compressor; however, centrifugal stresses present in the impeller and rotor provide a practical limit for the maximum achievable tip speeds for any realistic application. In addition, the potential for hydrogen embrittlement in this application may warrant increased safety margin with respect to the ultimate yield strength of the shaft materials. Therefore, a design trade-off must be considered, where some reduction in aerodynamic performance should be incurred in order to produce a robust machine with longer life and reduced risk.

An aerodynamic performance trade-off study was conducted using commercially available software to determine the maximum pressure ratio to expect from one centrifugal compressor stage. Performance was predicted at tip speeds of 1,000-2,000 ft/s. For this tradeoff, a stage flow coefficient of 0.1 was assumed for all cases. Each tradeoff design point evaluated represents a separately designed compressor stage, which was optimized for the imposed tip speed and geometry conditions. Each stage consisted of the impeller, crossover and return channel. In Figure 3, the results indicate that a pressure ratio of 1.16 to 1.18 was predicted at surface speeds of 1,800 ft/s to 2,000 ft/s. With a pressure ratio of 1.16 or greater, it can be seen that, to reach the desired 2.4 pressure ratio, 6 or less total stages would be required. While the relatively low stage count would be attractive and produce a smaller machine footprint and high power density, the centrifugal stresses on the rotating components will be high due to tip speeds. In the presence of high pressure hydrogen in this application, operation at high tip speeds is even riskier due to material complexities that arise due to embrittlement. These factors would inevitably result in higher cost materials and manufacturing requirements for the rotating components. The high surface speeds would require higher cost static components for safety and containment needs. Therefore, in order to achieve the performance requirement yield of a low cost design strategy, MiTi decided to maintain tip speeds at or below 1,800 ft/s. At 1,800 ft/s, we expect that a single stage compressor will achieve a pressure ratio of approximately 1.14 per stage and will achieve the necessary total pressure ratio of 2.4 with 6 stages. A more conservative and inevitably lower cost design would be to select 1,600 ft/s, which requires 8 stages to achieve 2.4. However, due to small pressure loss between frames, through intercoolers and to account for some performance degradation due to increasing temperature in subsequent stages, an additional stage will be likely be required.

Mohawk Innovative Technology®, Inc.
1037 Watervliet-Shaker Road, Albany, NY 12205
URL: www.miti.cc
Phone: (518) 862-4290, FAX: (518) 862-4291

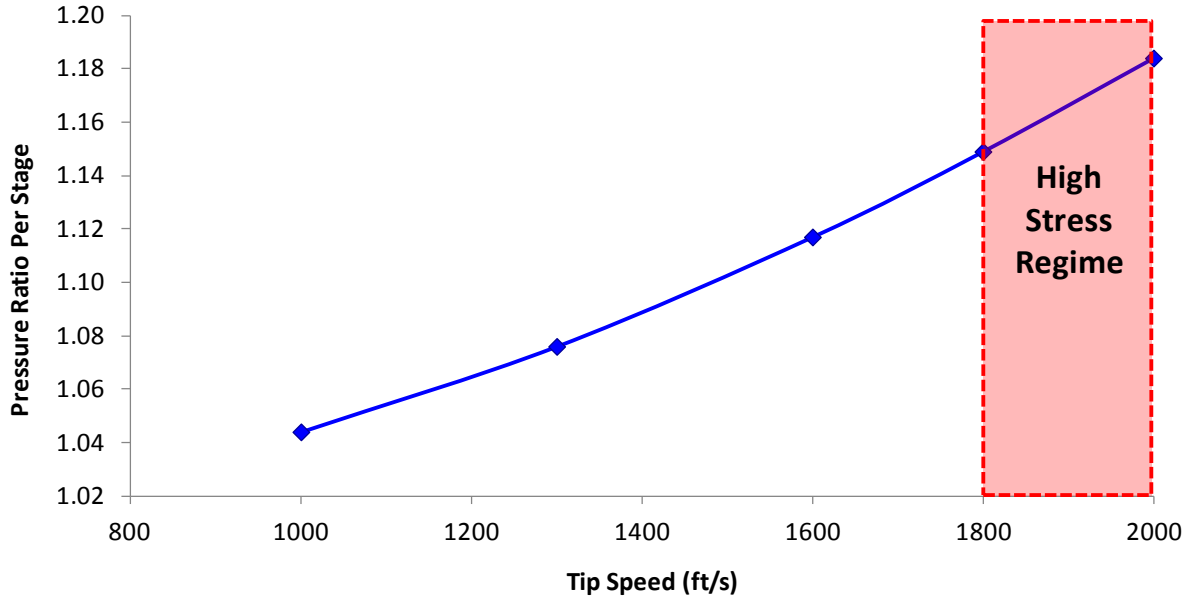

Figure 3. Predicted pressure ratio achieved in a single stage as a function of tip speed. Flow coefficient of 0.1 held constant for all design points.

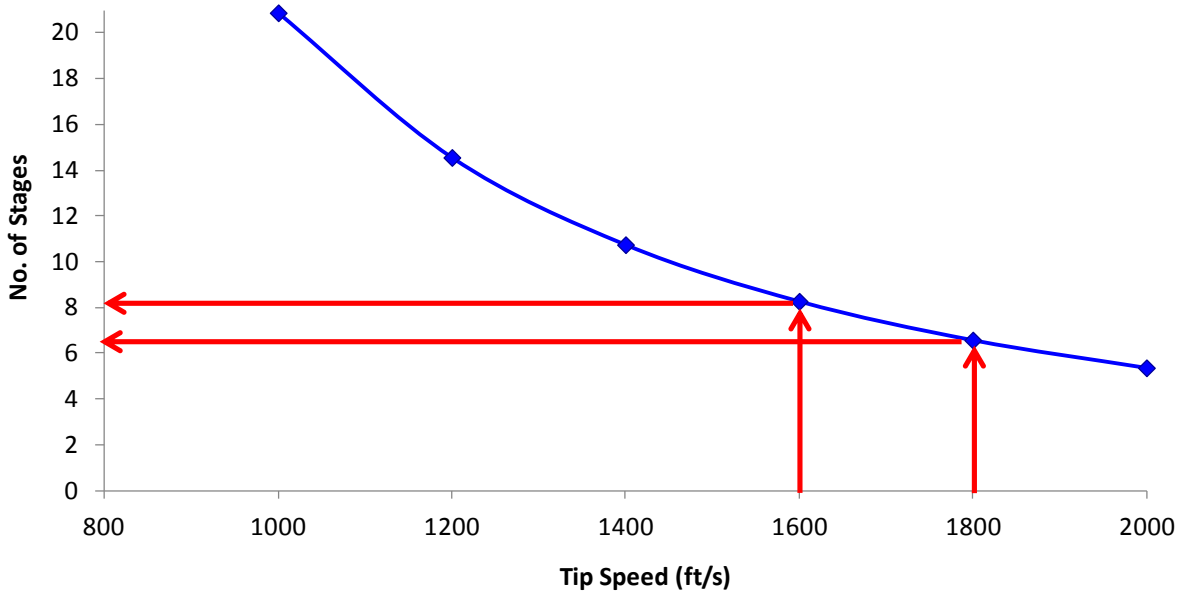

Figure 4. Effect of compressor tip speed of number of stages required to meet the required 2.4 pressure ratio.

The multi-stage system will consist of modular compressor frames each with a single rotating shaft. Each rotating shaft will consist of a maximum of 3 compression stages operating in series. Each shaft will be directly driven at the same speed without use of a gearbox. The justification for using no more than 3 compressor stages is due to resonant frequency limitations; further details are presented in Section 10.0. The use of three identical frames, each containing a single shaft, will also providing opportunity for gas inter-cooling and allow for design modularity should performance requirements vary in the future. Again using CompAero software, the

Mohawk Innovative Technology®, Inc.
1037 Watervliet-Shaker Road, Albany, NY 12205
URL: www.miti.cc
Phone: (518) 862-4290, FAX: (518) 862-4291

performance of the multi-stage frame was investigated in further detail. In Figure 5 the performance of combined multi-stage compressor system is plotted at several operating speeds. Intercoolers were assumed between each frame with a maximum of three stages per frame. The solid lines indicate discharge pressure and required power from the "full speed" condition (1,800 ft/s). The 95% speed and 90% speed conditions refer to tip speeds of 1,700 and 1,600 ft/s, respectively. Despite the small pressure drop experienced with intercoolers, the reduced power requirement more than justifies their inclusion in the system. It was also observed that the use of intercoolers would make it easier to match performance between stages and, thus, contribute to higher overall system performance. The results indicate that the full-speed condition would require seven stages to achieve the 1,200 psig discharge pressure, while the under-speed conditions would require eight and nine stages, respectively.

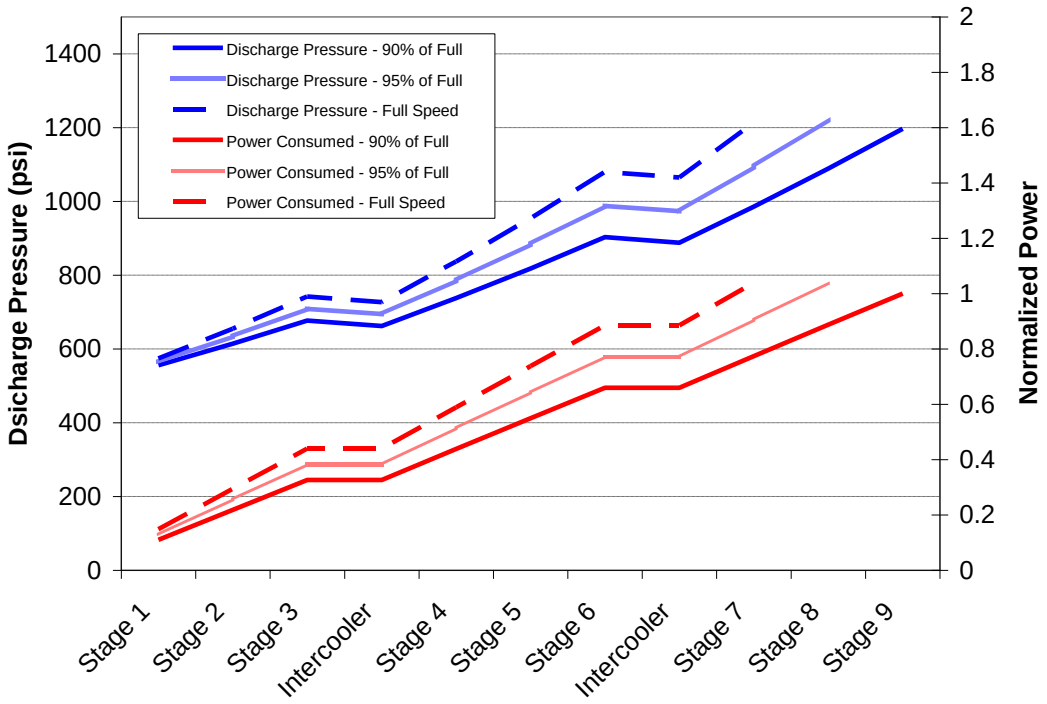

Figure 5. Multi-stage performance prediction at three operating speeds

Based upon the results presented thus far in this section, as well as results from more detailed analysis in later sections, it was concluded that the reduction in capital cost, increased safety and greater reliability afforded by the lower risk 1,600 ft/s design case would outweigh the performance gain with the higher risk 1,800 ft/s design speed. Therefore, an operating speed of 1,600 ft/s was selected for further design analysis in this study. Rotating machinery operating at or above 2,000 ft/s is, typically, reserved for exotic applications where peak performance outweighs any requirement for long-life, low cost or reliability. It is MiTi's opinion that the reduction in risk for this application outweighs the performance benefits gained (two fewer stages) by designing for the at 1,800-2,000 ft/s. Should the phenomenon of hydrogen

Mohawk Innovative Technology®, Inc.
1037 Watervliet-Shaker Road, Albany, NY 12205
URL: www.miti.cc
Phone: (518) 862-4290, FAX: (518) 862-4291

embrittlement become better understood in the future, such higher operating speeds can be considered.

With a tip speed of 1,600 ft/s and a flow coefficient of 0.1, the compressor diameter can be determined through evaluation of equation 1. The proposed centrifugal compressor will have a diameter of 6.5" and operate at a speed of 56,414 rpm. Given preliminary blade angles and heights, a 3D solid model was generated (Figure 6) to aid in design of the multi-stage system for performance of stress analysis and to build an FEA model for rotordyanamics.

Figure 6. Preliminary geometry of the proposed single stage centrifugal compressor

Other preliminary design techniques were also investigated through the course of this program to enhance performance without exceeding the maximum allowable tip velocity. The two most common approaches used in compressor design to increase performance (i.e., increase discharge pressure per stage) are employing forward-swept blade angle and employing vaned diffusers. A single compression stage was analyzed to determine the performance gain of forward-sweep and vaned diffusing. The results of each analysis are shown in Figure 7.

Mohawk Innovative Technology®, Inc.
1037 Watervliet-Shaker Road, Albany, NY 12205
URL: www.miti.cc
Phone: (518) 862-4290, FAX: (518) 862-4291

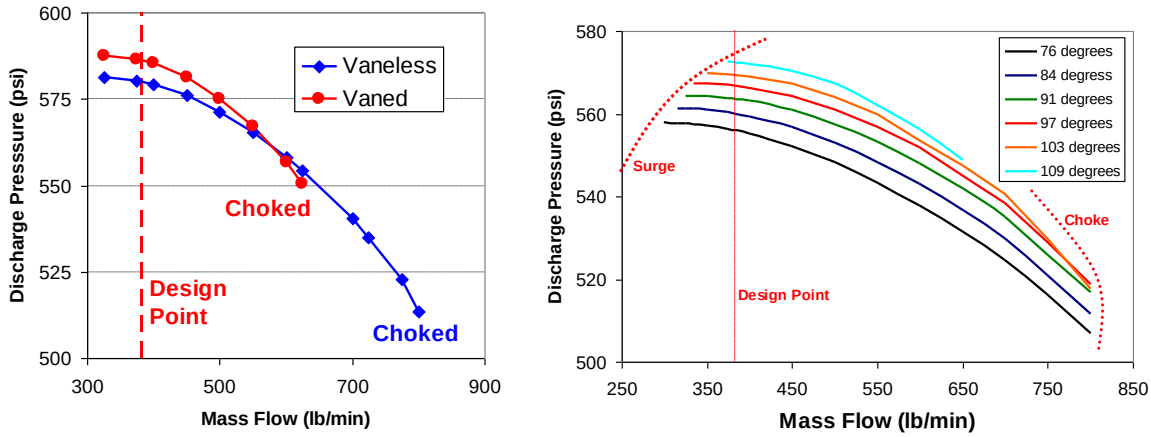

Figure 7. Alternative design approaches investigated of a single compressor stage

As expected, discharge pressure is found to increase in both cases. The costs of these approaches, however, are increased power requirement, increased manufacturing costs and decreased surge-choke margin. In the multi-stage analysis, both a vaned diffuser and a forward-swept blade resulted in about 8% differential pressure improvements. The power penalty was much greater with the forward-swept blade (15%) compared to only 2% from the vaned diffuser. If we are to consider multi-stage compressor performance at off-design conditions, the forward-swept blade approach greatly increase the likelihood of system instability. MiTi realizes that operating conditions could vary greatly in the application, including off-design flow conditions. For this reason, the most versatile, stable and cost-effective design is a three-frame design with back-swept impeller blades. However, the use of a vaned diffuser, given the improved pressure ratio and efficiency, is preferred for this application.

Based on the preliminary results described above, a complete system layout was drawn (Figure 8). The system contains three frames (nine stage total) coupled to a single rotating shaft. Also shown, intercoolers are located beneath each compressor frame, drive system and transmission. The design includes three frames for the hydrogen compressor capable of 500,000 kg/day with a pressure ratio of approximately 2.4. The rotors in all three frames operate at the same speed of 56,000 rpm with tip velocities kept to 1,600 ft/s to assure a structurally and economically feasible design. Each frame is a double entry design consisting of three back-to-back compression stages (Figure 9). The design includes vaned diffusers and a return channel. The final stage of each frame discharges to a volute.

Mohawk Innovative Technology®, Inc.
1037 Watervliet-Shaker Road, Albany, NY 12205
URL: www.miti.cc
Phone: (518) 862-4290, FAX: (518) 862-4291

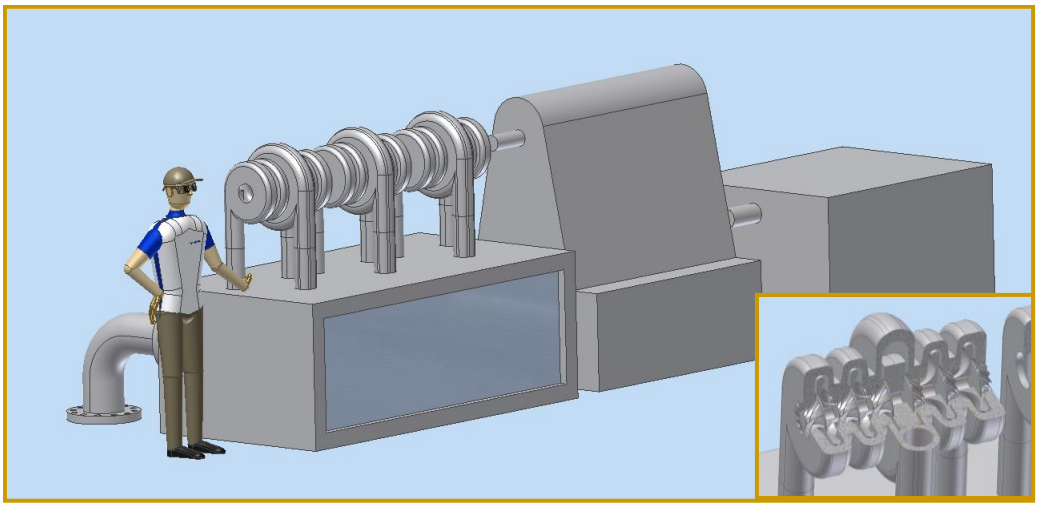

Figure 8. Full system layout shown with three-frame compressor, intercoolers, and drive system. A cut-away of a single frame (lower-right)

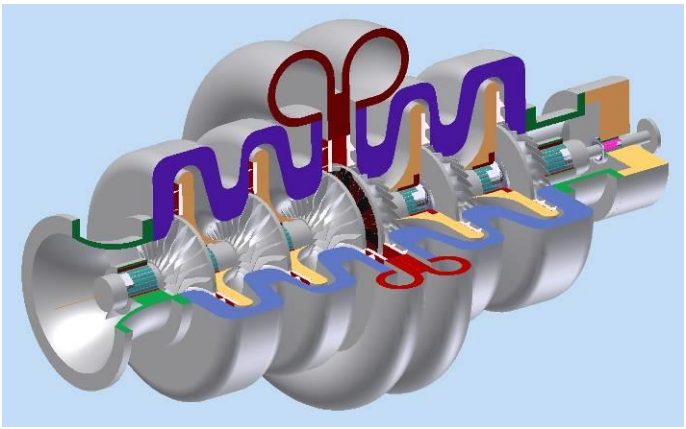

Figure 9. Three-quarter cut-away view of a single frame of the MiTi® hydrogen compressor design

The next step in the design process included several iterations between aerodynamic performance prediction, and structural and rotordynamic analysis. In the early stages of design, identical stage geometries were assumed as a cost effective measure. However, that approach produced marginal stability and minimal surge margin. Rather than using truly identical stages throughout, frames 2 and 3 have been designed with alternate shroud contours. The technique of reprofiling the impeller and diffuser dramatically improves stability without the added cost of designing and manufacturing unique compressor stages. A comparison of the identical stage solution to the reprofiled stage solution is shown in Figure 10. The additional pressure margin achieved in the reprofiled design is due primarily to the addition of the vaned diffuser. The use of a vaned diffuser in the identical stage design was not practical because it would only add instability to an already unstable design.

Mohawk Innovative Technology®, Inc.
1037 Watervliet-Shaker Road, Albany, NY 12205
URL: www.miti.cc
Phone: (518) 862-4290, FAX: (518) 862-4291

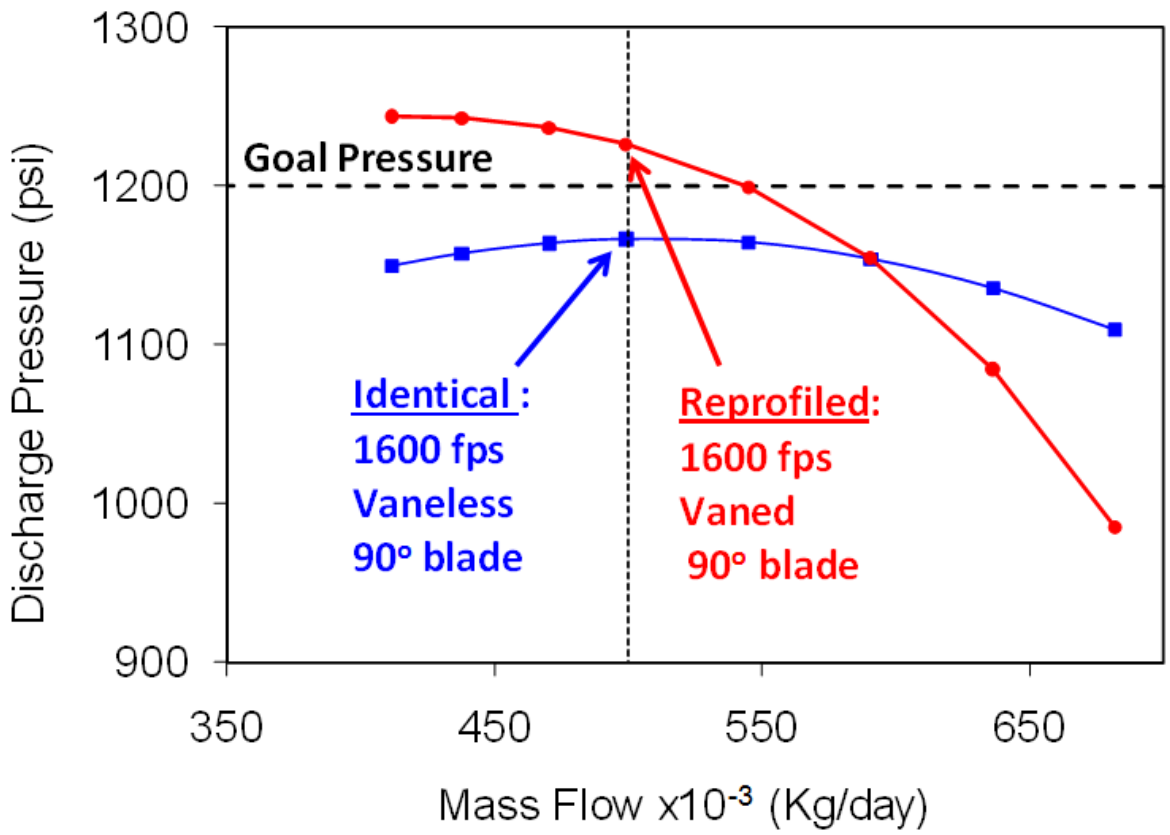

Figure 10. Predicted performance of the 9-stage hydrogen compressor

7.2 Single and Double Entry Compressor Concepts

During the course of the design effort, collaboration between MiTi and MHI was conducted regularly. This collaboration was conducted via phone conversations, emails and a personal visit to MHI facilities in Hiroshima, Japan by the program principle investigator (PI). During the visit, details regarding the MHI compressor design and future plans for testing were discussed. Two distinct design concepts were proposed as a result of this collaboration. A summary of the two design approaches investigated are provided in Table 1. The primary difference between the MiTi and MHI approach is related to the inlet flow. The MiTi design uses a double-entry technique, which splits mass flow evenly between two inlets at either end of the shaft. The benefit of this approach is inherently balanced thrust forces. The MHI design uses a single-entry approach that requires a balance piston to resolve excessive thrust loads. The advantage of this approach is that it allows for easy manipulation of axial clearance at all compressor impellers. A single frame (3 stages) of each approach is shown in Figure 11.

Mohawk Innovative Technology®, Inc.
1037 Watervliet-Shaker Road, Albany, NY 12205
URL: www.miti.cc
Phone: (518) 862-4290, FAX: (518) 862-4291

Table 1. Comparison between MiTi and MHI designs

Design Strategy	Mohawk Innovative Technology, Inc.®	MHI
Compressor Type	Double-Entry	Single-Entry
Number of Stages	6 and 9	7 and 9
Number of Frames	2 and 3	2 and 3
Flow Capacity (Kg H_2/day)	240,000 – 500,000	
Total Pressure Ratio	2.4 - 3.33	
Total Power Input (HP)	7,800-12,000	8,300 – 12,000
Max Tip Speed (1000 ft/s)	1.6 – 1.8	1.8 - 2.0
Compressor Footprint (ft^2)	145 - 160	150 - 175

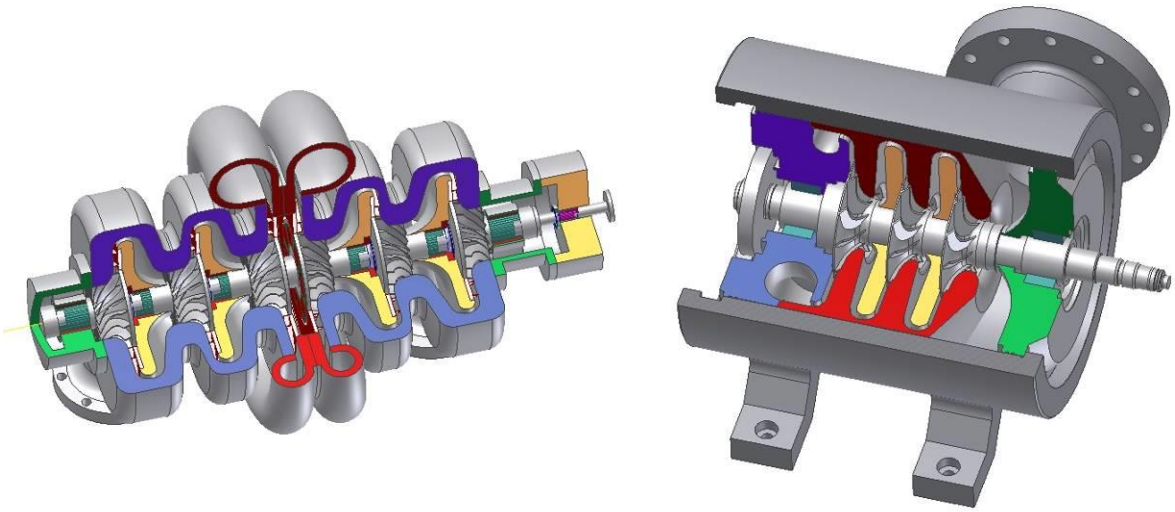

Figure 11. 3D model of the MiTi double-entry compressor (left) and the MHI single-entry compressor frame (right).

Despite the differences in design approaches, the overall performance of the two systems will be very similar. In Figure 12, independent results from MiTi and MHI are presented. The number of stages required to reach a particular pressure ratio are presented as a function of tip speed. Despite the use of double and single entry compressor designs, the results from MiTi and MHI

Mohawk Innovative Technology®, Inc.
1037 Watervliet-Shaker Road, Albany, NY 12205
URL: www.miti.cc
Phone: (518) 862-4290, FAX: (518) 862-4291

correlate well, especially at higher tip speeds within the expected operating range. This is because the inlet conditions, fluid properties and design point used for each concept were identical. MHI and MiTi both assumed similar conditions and both employ highly sophisticated but different software design tools. A close correlation between each design was encouraging.

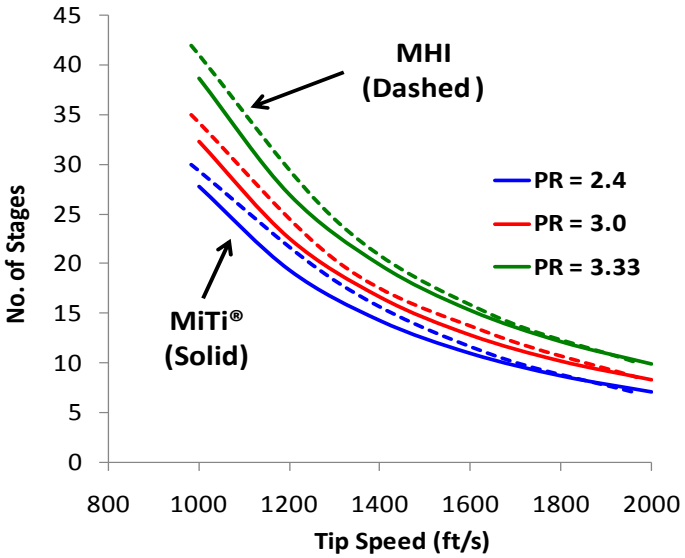

Figure 12. Estimation of stage numbers required as a function of tip speed and pressure ratio (PR).

At the initiation of the project, it was planned to pursue two design approaches for the hydrogen compressor: a double-entry design by MiTi and a single-entry design by MHI. During the design process, both companies held frequent conference calls and several site visits to exchange design information and coordinate the design process. The single stage compressor based on MiTi's double-entry compressor design was designed and assembled for testing, as described above. During the design process, an aerodynamic compressor design software, computational flow dynamics (CFD), finite element analysis (FEA) and rotordynamic analysis were performed to assure that the design met all the performance and safety requirements. The single-entry compressor design by MHI also followed the same comprehensive analyses but used different software packages available at MHI. During the design process, both MiTi and MHI checked each other's analyses to ensure accuracy of the different software. Both designs meet the performance criteria for the hydrogen pipeline compressor.

Comparing the two designs with respect to performance, safety and economics, however, indicates that the double-entry design is superior for the hydrogen pipeline compressor. As outlined in Table 2, the safety margin for the single-entry design is less due to larger tip speeds required. Also the analyses indicate that the single-entry compressor could be more costly due to the need for a balance piston and thrust bearings. Therefore, it was decided to pursue the MiTi double-entry design instead of the MHI single-entry compressor for performance verification testing.

Mohawk Innovative Technology®, Inc.
1037 Watervliet-Shaker Road, Albany, NY 12205
URL: www.miti.cc
Phone: (518) 862-4290, FAX: (518) 862-4291

Table 2. Pros and cons of single and double entry compressor designs.

	Pros	Cons
MiTi Design *Double Entry*	Internally Balanced Thrust Forces	Higher Parts Count
	All Stages Derived from Common Wheel Design – Economies of Scale	Control of Axial Clearance Requires Close Attention
	Modest Tip Velocities for Hydrogen Environment (25% Lower than MHI)	Careful Design of Double Inlet/Discharge Piping Required
	High Stress Safety Margin	
MHI Design *Single Entry*	Balance Piston For Thrust Loads	High Thrust Loads Requires Balance Piston Plus Thrust Bearing
	Control of Axial Clearance	High Tip Speeds Required
	Fewer Parts	Larger Diameter Wheels Used
	Simple Inlet Piping	Unique Impellers in each Frame
		Reduced Stress Safety Margin

7.3 Detailed Aerodynamic Design Study

Following the preliminary design study, the double-entry compressor concept was selected as the most feasible concept to achieve the DOE's performance target and meet the needs of hydrogen pipeline needs. Therefore, a more detailed aerodynamic design of the impeller and other components was conducted for MiTi's double-entry concept. Using a quasi-three dimensional inviscid internal flow analysis with well-known, commercially available compressor design software, the complex profile of the compressor blades were refined to meet performance requirements. The quasi-three dimensional flow field analysis is a cost effective design tool to quickly iterate between aerodynamic performance and the detailed flow field behavior. The flow field was carefully analyzed for areas of excessive diffusion, sudden velocity gradients and flow separation. The design was optimized through minor changes in impeller blade geometry. Once a design was found to have satisfactory flow field characteristics, structural and rotordynamic evaluation was performed. Using the final stage geometry, compressor performance was evaluated at five different operating conditions, including the design point of 500,000 kg/day. Solutions were obtained between 70% up to 120% of the design point condition. The velocity vector solutions of the final geometry operating at the design point are shown in Figure 13. Solutions obtained of the final stage geometry reveal good overall flow behavior with no regions of significant turbulence, stagnation or flow separation.

Mohawk Innovative Technology®, Inc.
1037 Watervliet-Shaker Road, Albany, NY 12205
URL: www.miti.cc
Phone: (518) 862-4290, FAX: (518) 862-4291

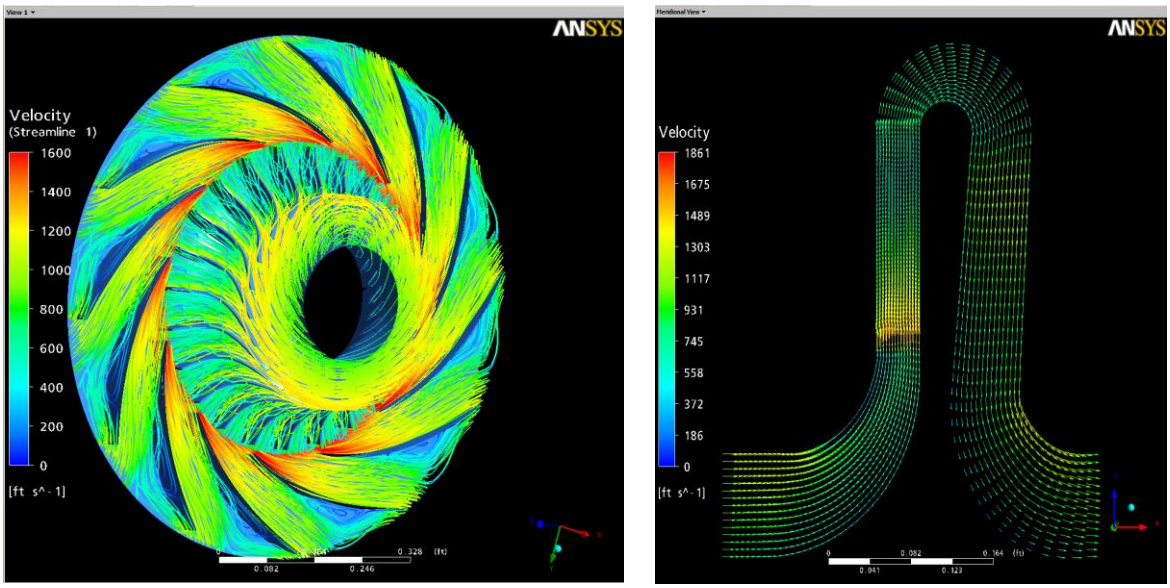

Figure 13. 3D Flow field solutions of the first stage impeller and diffuser (left) and 2D velocity vector solutions of the entire first stage, from inlet to return channel

In addition to providing detailed analysis of the flow patterns within the first stage of compression, the CFD analysis also served as in independent validation of the mean-line analysis that was used to develop the multi-stage hydrogen compressor system. A comparison of performance predictions with mean-line analysis and CFD at the design point are shown in Table 3 and Table 4. The results have shown very good agreement between the two numerical methods. At both the exit of the impeller and at the exit of the entire stage, better than 98% agreement was achieved.

Table 3. Comparison of CFD and mean-line analysis at the impeller exit

Impeller Exit	Units	Mean-Line	CFD	DEVIATION
Pressure	psia	568.15	569.28	0.20%
Temperature	F	239.09	239.06	-0.01%
Work	ft lbf/lbm	72662	72587	-0.10%
Polytropic Head	ft lbf/lbm	67048	68089	1.53%
Polytropic Efficiency		0.932	0.938	0.64%

Mohawk Innovative Technology®, Inc.
1037 Watervliet-Shaker Road, Albany, NY 12205
URL: www.miti.cc
Phone: (518) 862-4290, FAX: (518) 862-4291

Table 4. Comparison of CFD and mean-line analysis at the stage exit

Stage Exit	Units	Mean-Line	CFD	DEVIATION
Pressure	psia	560.23	559.15	-0.19%
Temperature	F	239.09	239.06	-0.01%
Work	ft lbf/lbm	72662	72587	-0.10%
Polytropic Head	ft lbf/lbm	59681	58667	-1.73%
Polytropic Efficiency		0.821	0.808	-1.61%

The two numerical methods were also evaluated at operating conditions above and below the design point. The results in Figure 14 and Figure 15 show good correlation between the two methods across a wide operating range. The average discrepancy between CFD analysis and mean-line analysis was less than 2% for operating conditions between 70% - 120% of the design point. These results provide independent validation of the mean-line analysis methods used and provide increased confidence in the performance predictions of the complete 9-stage MiTi® hydrogen compressor.

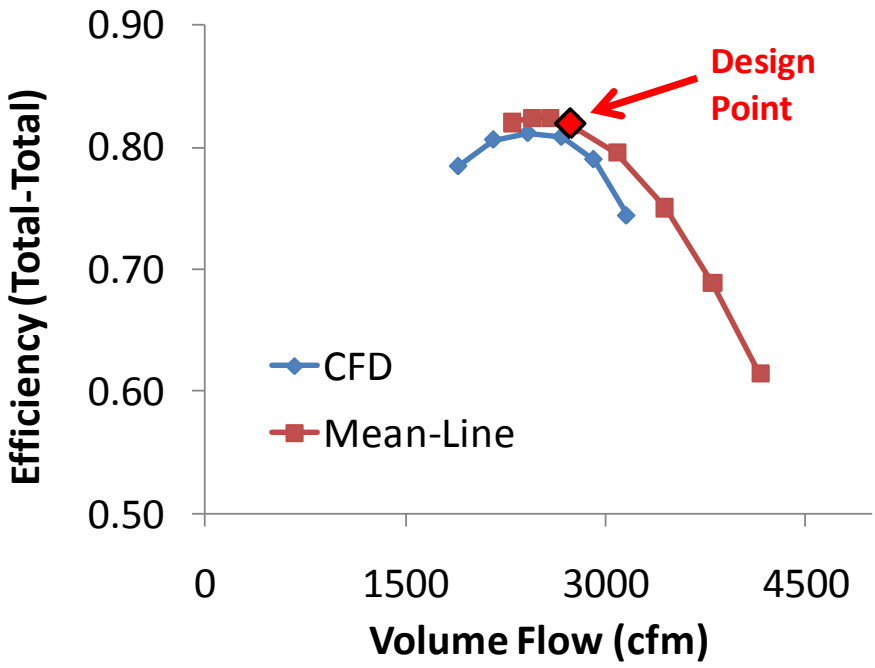

Figure 14. A comparison of results from CFD and mean-line analysis for total-total efficiency at the exit of stage 1

Mohawk Innovative Technology®, Inc.
1037 Watervliet-Shaker Road, Albany, NY 12205
URL: www.miti.cc
Phone: (518) 862-4290, FAX: (518) 862-4291

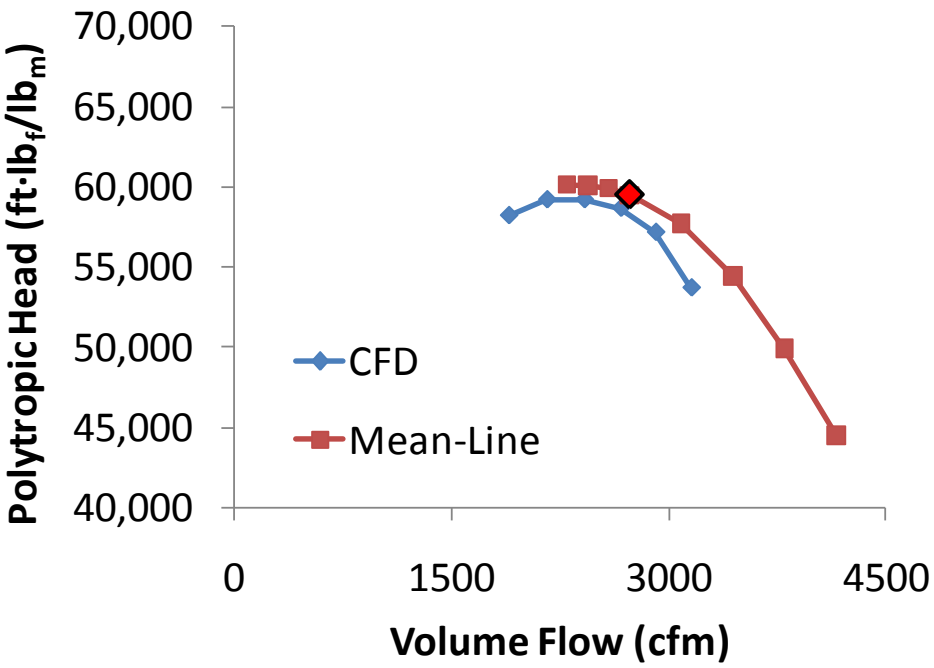

Figure 15. A comparison of results from CFD and mean-line analysis for total-total head at the exit of stage 1

The results of CFD analysis independently confirm the aerodynamic performance prediction used to design the detailed compressor stage. The subcontractor's complete report describing the CFD analysis can be found in Appendix B. Following the aerodynamic design, a full scale mock-up was constructed to visually check the design and identify any areas that require modification. The full-scale mock-up of a single frame of the MiTi® H_2 compressor was completed, as shown in Figure 16.

Mohawk Innovative Technology®, Inc.
1037 Watervliet-Shaker Road, Albany, NY 12205
URL: www.miti.cc
Phone: (518) 862-4290, FAX: (518) 862-4291

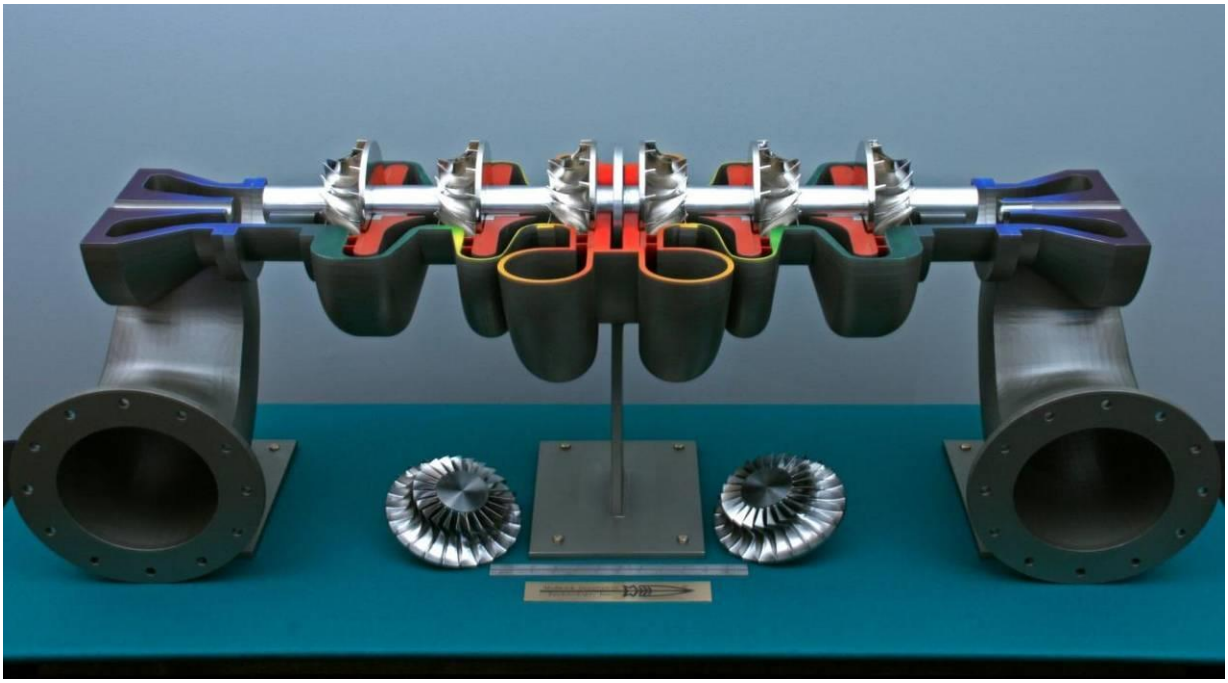

Figure 16. Full-scale, multistage compressor mock-up

7.4 Finite Element Stress Analysis

To further assess the mechanical feasibility of the proposed compressor concept, FEA was used to evaluate the stress distribution of the rotor design selected for the compressor. Stress analysis was conducted with a bladeless, multi-stage shaft (Figure 17) to investigate the bulk effects on the full shaft system. Stress analysis was performed using a Nastran solver (MSC Corp., Santa Ana, CA). Results were computed following mesh generation and assigning appropriate boundary conditions. First, one end of the shaft was assumed to be fixed and the rotational speed of 60,000 rpm was applied to the entire body as an internal load. Therefore, only centrifugal stress was considered. The analysis was used predominately in earlier design iterations so that a maximum speed envelope could be determined to aid in aerodynamic results and determining the number of stages required. From there, a more detailed stress analysis was also conducted on an individual compressor stage with detailed blade geometries. The results of the multi-stage shaft without compressor blades were conducted with high strength steel. Results indicate stresses on the order of 120-130 ksi for speeds of 60,000 rpm. While these results indicate a relatively conservative safety factor of more than 2x, common for in state-of-the-art compressor designs, the impact of hydrogen embrittlement warrants careful consideration in stress analysis.

More detailed stress analysis was continued with the bladed wheel following aerodynamic design. The analysis confirmed that the stress concentration on the backside of the disk could be greatly improved by modifying the transition radius. These results aided the final design geometry of the refined multi-stage system layout.

Mohawk Innovative Technology®, Inc.
1037 Watervliet-Shaker Road, Albany, NY 12205
URL: www.miti.cc
Phone: (518) 862-4290, FAX: (518) 862-4291

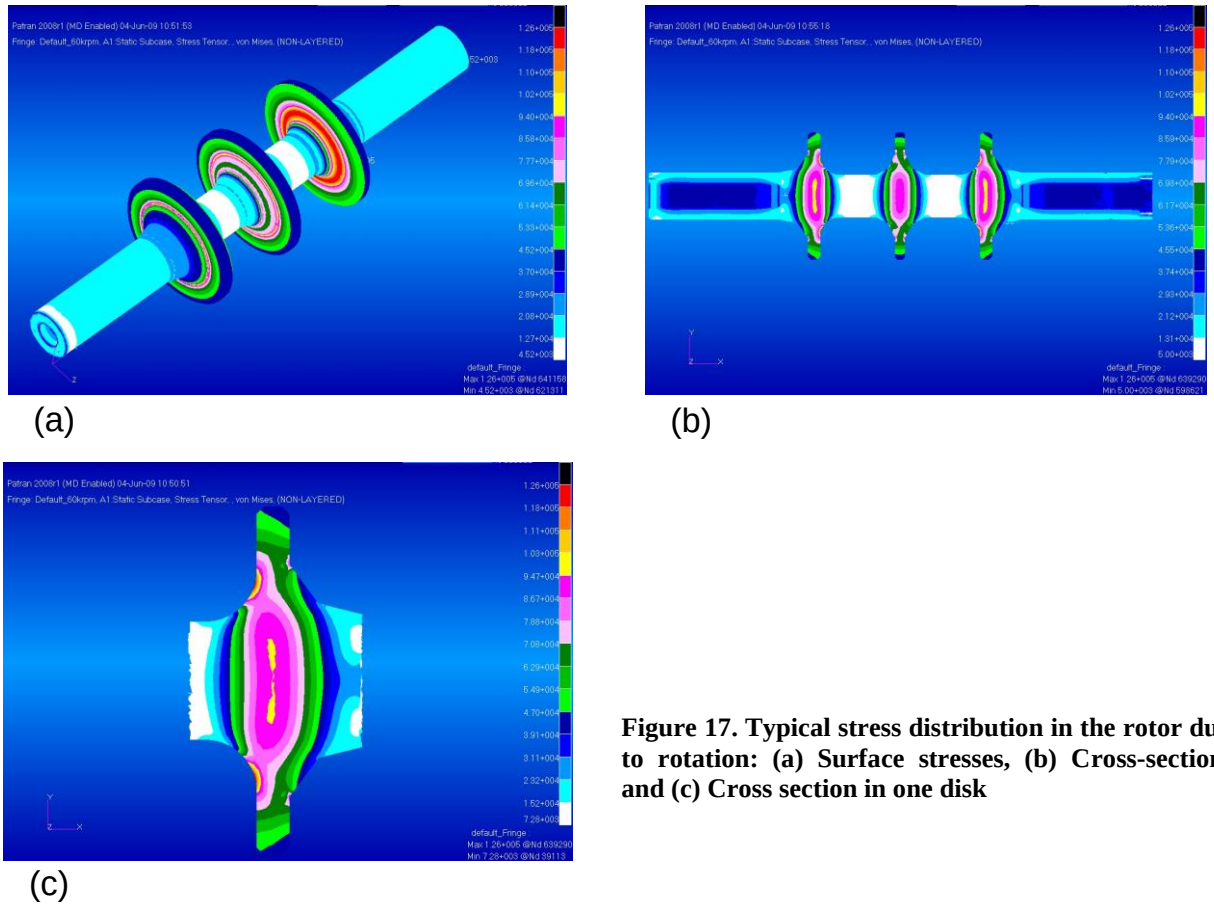

Figure 17. Typical stress distribution in the rotor due to rotation: (a) Surface stresses, (b) Cross-section, and (c) Cross section in one disk

The analysis included an investigation of the impact of blade thickness, taper and filets. Compressor wheel designs created from aerodynamic analysis were evaluated for structural integrity focused on the rotor, impeller hub and impeller blades. Three materials were investigated in the structural design analysis: aluminum alloy; titanium alloy and high-strength steel. Four different materials with a wide range of elastic properties and strength were selected and evaluated in this analysis. In addition, certain aspects of the design were varied in the analysis to evaluate the effects of geometric design on the stress distribution.

The results indicate significant safety margin for all three selected materials. Results from the high-strength steel impeller are shown in detail in Figure 18. The analyses performed for stress distribution in pure rotation was extended by the addition of a rotational torque. In addition to the rotational speed of 60,000 rpm, a torque corresponding to 5,500 hp at 60,000 rpm was applied to the free end of the rotor. In this analysis, both the centrifugal and torsional stresses were analyzed. The stress distribution, however, remained about the same as those without the torque. A summary of results for each material is given in Table 5.

The first design analyzed assumed thin blade profiles and yielded high stresses at the root of the impeller blade. A second iteration was investigated where the blade thickness was increased. The use of thicker blades yielded a 50% decrease in peak stress and only less than 0.5% decrease in predicted discharge pressure. The very large response in stress and small effect on

Mohawk Innovative Technology®, Inc.
1037 Watervliet-Shaker Road, Albany, NY 12205
URL: www.miti.cc
Phone: (518) 862-4290, FAX: (518) 862-4291

aerodynamic performance show that the stresses will be manageable without greatly affecting compressor performance.

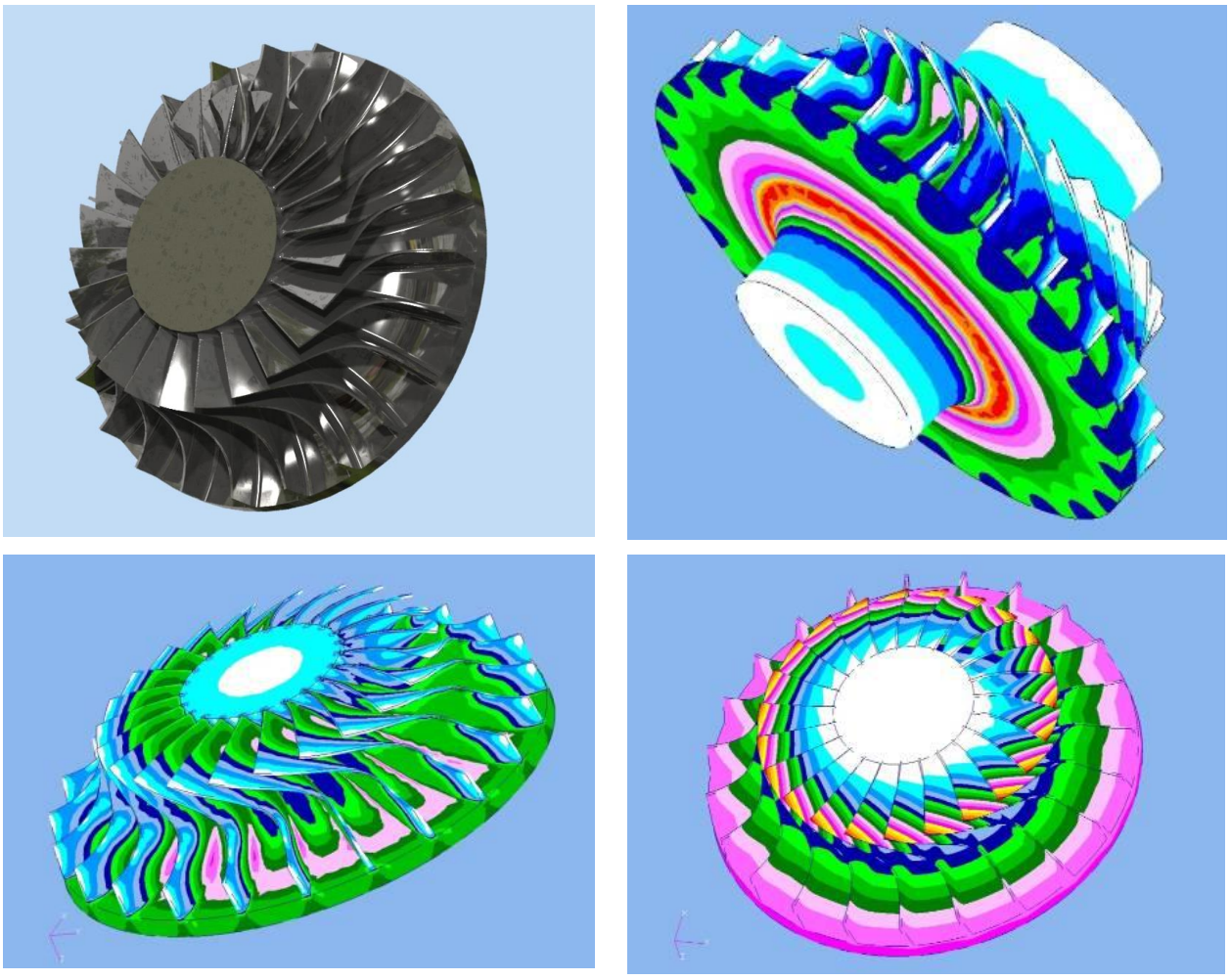

Figure 18. 3D solid model of the compressor impeller (upper left), von Mises stress predictions in the impell right and lower left) and predicted blade deflections due to centrifugal forces (lower right).

The results confirmed low stress in the impeller blades. Peak stress in the impeller is on the backface of the hub; however, stress magnitudes are well below the yield strength of the material. While all three materials appear to be acceptable with respect to the maximum stresses, the low fatigue limit of the aluminum alloy is of major concern. In fact, the blade stress is three times larger than the fatigue limit of this high strength aluminum alloy. However, both the steel and titanium alloy provide safe margins of 44% and 38% against low cycle fatigue in the blades. Three tip speeds were also considered in order to evaluate over-speed safety factor (1600, 1800 and 2000 fps). The results indicate significant safety margin, even at the tip speed of 2000 fps for all three selected materials. The blade stress magnitude is significantly lower than the peak stress and the peak deflection occurs at the tip of the blade towards the hub. Based upon these results, the use of aluminum alloy is not recommended, particularly due to its low safety margin with regard to high-cycle fatigue. Both high strength steel and titanium allow appear to be good

Mohawk Innovative Technology®, Inc.
1037 Watervliet-Shaker Road, Albany, NY 12205
URL: www.miti.cc
Phone: (518) 862-4290, FAX: (518) 862-4291

choices in terms of stress analysis only. However when taking hydrogen compatibility into consideration, high-strength steel does present greater risk.

Table 5. FEA results for various compressor tip speeds and materials.

Tip Speed	fps	1600		1800		2000	
Material	Ultimate Strength (ksi)	Max Stress (ksi)	Safety Factor	Max Stress (ksi)	Safety Factor	Max Stress (ksi)	Safety Factor
Aluminum Alloy	84	39.5	2.1	50.1	1.7	61.7	1.4
Titanium Alloy	170	64	2.7	81.1	2.1	100	1.7
High-Strength Steel	290	110	2.6	139	2.1	172	1.7

8.0 Material Selection

Hydrogen compressors operating at high pressures (about 300 psi) and often at high temperatures (about 200^{o}C) require high strength materials that can be used safely in the hydrogen environment. Besides the rotating group, materials are needed for the housing and the bearings/seals. The material used for the rotating group (i.e., shaft and impellers) must have high strength (particularly, high strength to weight ratio) and toughness as well as a high fatigue endurance limit to survive the high stresses imposed on the impeller during high speed rotation. The strength requirement for the housing is not as stringent as that of the rotating group, yet the material must possess a high durability and toughness under internal pressure. Materials used for the foil bearings/seals must have a high elastic modulus, high toughness and fatigue resistance. The strength must be sufficiently high to prevent plastic deformation under the imposed bearing loads. The foil bearings also require low friction, wear resistant coatings to allow smooth start/stop operations. The coatings must also have sufficient thermal and electrical properties to allow heat dissipation and conduction of electrical current due to static charge build up. Given the above requirements, different materials should be selected for different components.

8.1 Overview of Hydrogen Embrittlement

Hydrogen, the smallest and lightest of the elements, diffuses readily in most metallic alloys. Once inside the alloy, hydrogen can reduce the strength and decrease the toughness of the material. While the specific mechanisms can be quite complex and, in most cases, not well understood, the following simple explanation offers some insight into the process. Hydrogen atoms can react with certain metals forming brittle hydrides, while in others, hydrogen enhances the plastic deformation process. Hydrogen can segregate along grain boundaries, grain boundary phases and second phase constituents; further reducing strength by reaction with these constituents and/or formation of gas bubbles[4].

Past research and extensive testing have shown that most pure metals and alloys with strength below 1000 MPa are immune to hydrogen embrittlement,Table 6[5]. However, old data must be

Mohawk Innovative Technology®, Inc. URL: www.miti.cc
1037 Watervliet-Shaker Road, Albany, NY 12205 Phone: (518) 862-4290, FAX: (518) 862-4291

used with caution since, in some cases, the immunity is due to the natural oxides that protect against diffusion of hydrogen into the material rather than being inherently immune to hydrogen. In general, materials that are immune to hydrogen embrittlement include pure copper (OFHC), certain stainless steels and some titanium alloys[6]. Aluminum alloys are sometimes included in this list. However, there are uncertainties with respect to the inherent immunity of these alloys due the strongly attached aluminum oxide. Furthermore, the composition and microstructure play a critical role in the embrittlement process[7] and, for proper selection of materials for hydrogen environments, test data on each material must be carefully analyzed.

8.2 Housing Material

Stainless steel alloys usually have an excellent corrosion resistance but their strength is not sufficient for highly stressed components. There are various types of stainless steels, including ferritic, martensitic, austenitic, duplex and precipitation hardened. The austenitic stainless steels, and, particularly, type 316 and 316L, which are metastable alloys with molybdenum and nickel, are most resistant to hydrogen assisted fracture[8,9]. The strength and ductility as a function of test temperature are compared in air and for hydrogen pre-charged samples in Figure 19 and Figure 20. Testing under cyclic loading has also shown that the fatigue properties are also relatively unaffected by hydrogen exposure. Therefore, 316 series could be used as the housing for the hydrogen compressor.

Table 6. NASA Safety Standards for Hydrogen Systems (NSS 1740.16)

Material	Service			Remarks
	GH_2	LH_2	SLH_2	
Aluminum and its alloys	Yes	Yes	Yes	
Austenitic stainless steels with > 7% nickel (such as, 304, 304L, 308, 316, 321, 347)	Yes	Yes	Yes	Some make martensitic conversion if stressed above yield point at low temperature.
Carbon steels	Yes	No	No	Too brittle for cryogenic service.
Copper and its alloys (such as, brass, bronze, and copper-nickel)	Yes	Yes	Yes	
Gray, ductile, or cast iron	No	No	No	Not permitted for hydrogen service.
Low-allow steels	Yes	No	No	Too brittle for cryogenic service.
Nickel and its alloys (such as, Inconel® and Monel®)	No	Yes	Yes	Susceptible to hydrogen embrittlement
Nickel steels (such as, 2.25, 3.5, 5, and 9 % Ni)	No	No	No	Ductility lost at LH_2 and SLH_2 temperatures.
Titanium and its alloys	Yes	Yes	Yes	
Asbestos impregnated with Teflon®	Yes	Yes	Yes	Avoid use because of carcinogenic hazard.
Chloroprene rubber (Neoprene®)	Yes	No	No	Too brittle for cryogenic service.
Dacron®	Yes	No	No	Too brittle for cryogenic service.
Fluorocarbon rubber (Viton®)	Yes	No	No	Too brittle for cryogenic service.
Mylar®	Yes	No	No	Too brittle for cryogenic service.
Nitrile (Buna-N®)	Yes	No	No	Too brittle for cryogenic service.
Polyamides (Nylon®)	Yes	No	No	Too brittle for cryogenic service.
Polychlorotrifluorethylene (Kel-F®)	Yes	Yes	Yes	
Polytetrafluorethylene (Teflon®)	Yes	Yes	Yes	

Mohawk Innovative Technology®, Inc.
1037 Watervliet-Shaker Road, Albany, NY 12205
URL: www.miti.cc
Phone: (518) 862-4290, FAX: (518) 862-4291

Plain carbon steels are attractive structural materials, used in applications such as pipelines, because of their formability, weldability and adequate mechanical properties. C-Mn alloys are of particular interest and their mechanical properties in a hydrogen environment have been evaluated, particularly for plain carbon ferriritc steels[8]. While the yield strength of X42 alloy and X100 alloy with a higher Mn content is not affected by hydrogen exposure (360 MPa and 750 MPa), the ductility is reduced in hydrogen from 54% RA to 42% RA for X42 and from 75% RA to 38% RA for the X100. The toughness is still adequate for most applications, albeit some loss of ductility. However, the fatigue properties measured as crack propagation rate is degraded in hydrogen. Therefore, these materials could be used for the housing of the hydrogen compressor if cyclic fatigue is not an important issue.

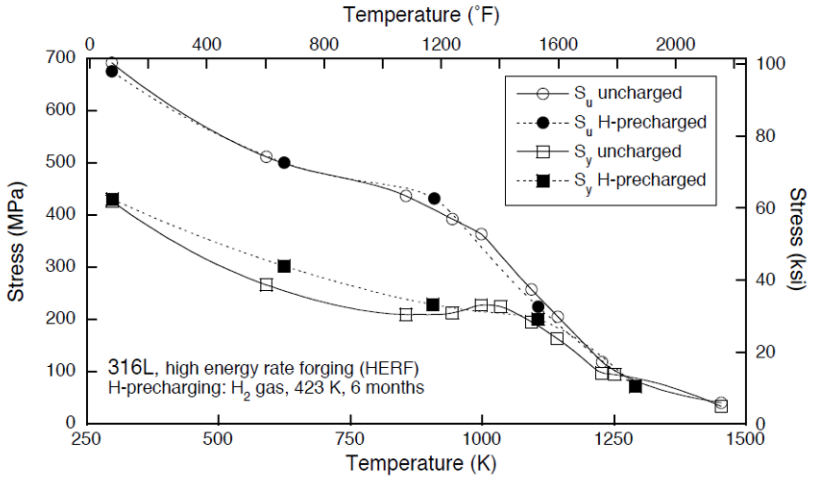

Figure 19. Tensile strength of 3416L stainless steel in air and thermally pre-charged in hydrogen gas8

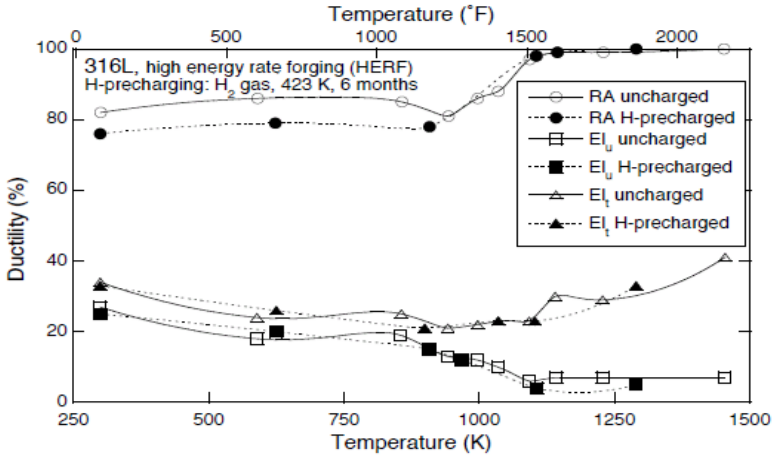

Figure 20. Ductility of 3416L stainless steel in air and thermally pre-charged in hydrogen gas8

Mohawk Innovative Technology®, Inc.
1037 Watervliet-Shaker Road, Albany, NY 12205
URL: www.miti.cc
Phone: (518) 862-4290, FAX: (518) 862-4291

8.3 Impeller Material

Titanium alloys have a high strength-to-weight ratio and, therefore, are suitable for the rotating group in the compressor. There are three forms of these alloys that include α, β, and α+β. Titanium alloys have been in wide usage in the aerospace industry for many years and all three types are in use today[10,11]. These alloys have high specific strengths; they are corrosion resistant and compatible with other materials. They are used as support structures, fastners, duct work, rotating components, compressor disks and blades, exhaust components, windshield frames, springs, landing gear, etc. Titanium alloys, however, can be susceptible to hydrogen embrittlement. It is well known that the alpha containing titanium alloys can be severely affected by hydrogen due to hydride formation. Therefore, commonly used alloys, such as Ti 6-4, are not suitable for use in the hydrogen environment[12]. However, β alloys are more immune to hydrogen embrittlement, although precipitation hardened beta alloys that contain α precipitates can be degraded by hydrogen. Precipitation of Ti3Al in alpha and alpha/beta, and hydrogen segregation at grain boundaries and slip planes in beta alloys, cause reduction of strength, ductility and fatigue life. Solution treated and aged beta alloys are most susceptible to degradation in hydrogen but solution treated, single phase beta alloys are immune (or less affected).

While many types of beta alloys have been developed, only four alloys are commercially available; these include Ti10V2Fe3Al (Ti 10-2-3), Ti3Al8V6Cr4Zr4Mo (Beta-C), Ti15Mo3Nb3Al0.2Si (Beta 21S or TIMETAL 21S) and Ti15V3Cr3Al3Sn (Ti 15-3). The first two are available only in bar and ingot forms, suitable for the rotating group of the hydrogen compressor, and the last two in only sheet form that could be used for foil bearings/seals.

Table 7 lists the range of mechanical properties that can be obtained through solution treatment and aging of the Ti 10-2-3 and Ti Beta-C[15]. The latter material, however, is susceptible to hydrogen embrittlement both in the solution treated[13] and in the aged condition[14]. Test data for Ti Beta-C with samples charged from the gas phase producing maximum hydrogen concentration of 8 at.%H have shown that strength increases (

Figure 21) but impact strength (Figure 22) and fatigue threshold (Figure 23) are reduced as the hydrogen concentration is increased. Hydride formation and interaction of hydrogen with dislocations are suggested as primary mechanisms for such changes. In contract with the Beta-C, strength of the Ti-10-2-3 is reduced (Figure 24), but impact strength (Figure 25) and fatigue threshold (Figure 26) increase for the hydrogen treated samples. It is suggested that, in this case, the beta phase is stabilized with hydrogen[13].

Table 7. Mechanical Properties of Beta Titanium alloys in air (International Titanium Association15); basic properties depend on heat treatment used during processing.

Beta TI Alloy	Ultimate Tensile ksi	0.2% Yield ksi	% Elongation
Ti-10-2-3	145-200	135-184	4-20
Ti Beta C	115-195	110-185	6-25

Mohawk Innovative Technology®, Inc.
1037 Watervliet-Shaker Road, Albany, NY 12205
URL: www.miti.cc
Phone: (518) 862-4290, FAX: (518) 862-4291

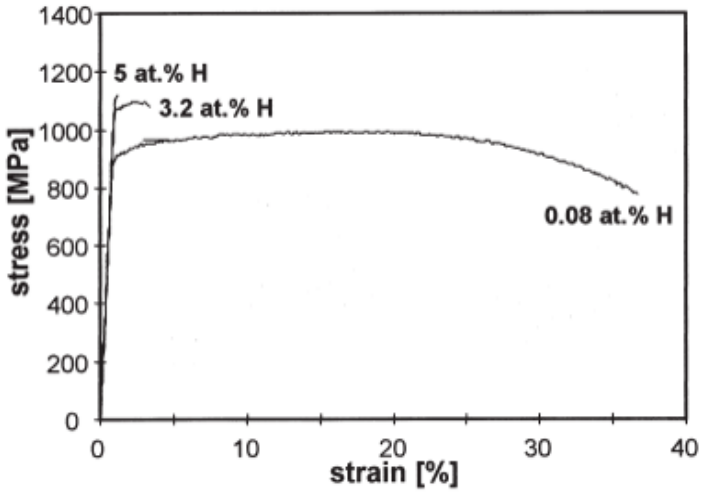

Figure 21. Yield stress of solution treated Ti Beta-C with different hydrogen content[13]

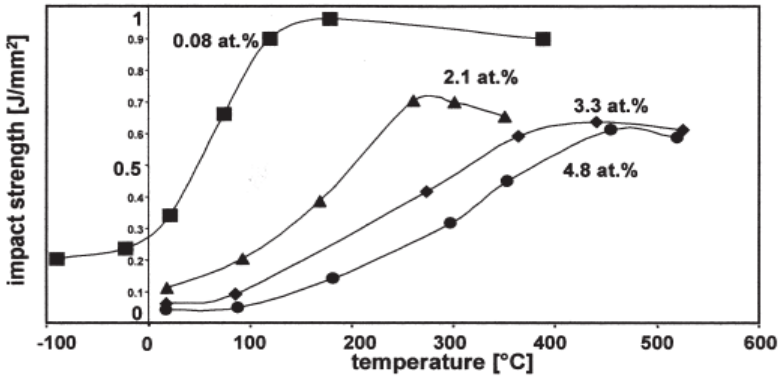

Figure 22. Impact strength of solution treated Ti Beta-C with different hydrogen content[13]

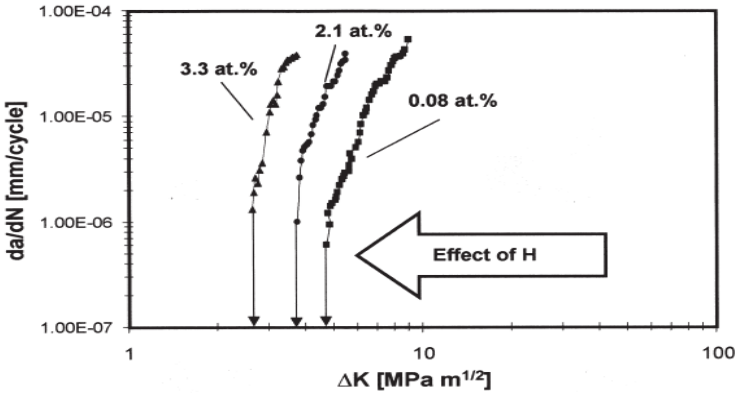

Figure 23. Fatigue crack growth rates of solution treated Ti Beta-C with different hydrogen content13

Mohawk Innovative Technology®, Inc.
1037 Watervliet-Shaker Road, Albany, NY 12205
URL: www.miti.cc
Phone: (518) 862-4290, FAX: (518) 862-4291

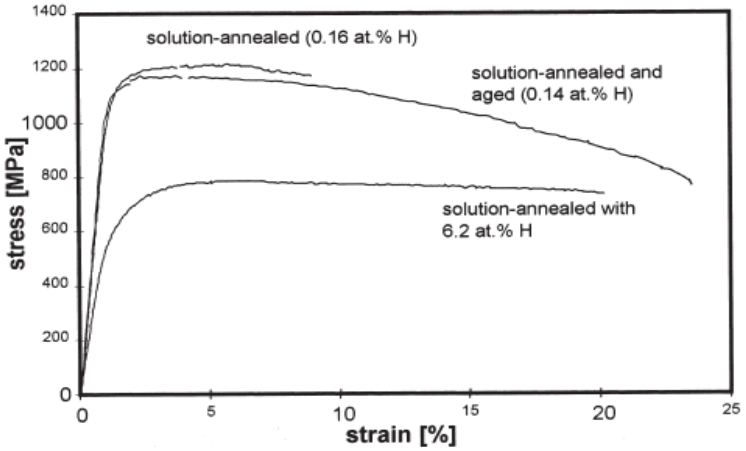

Figure 24. Yield stress of solution treated Ti 10-2-3 with different hydrogen content[13]

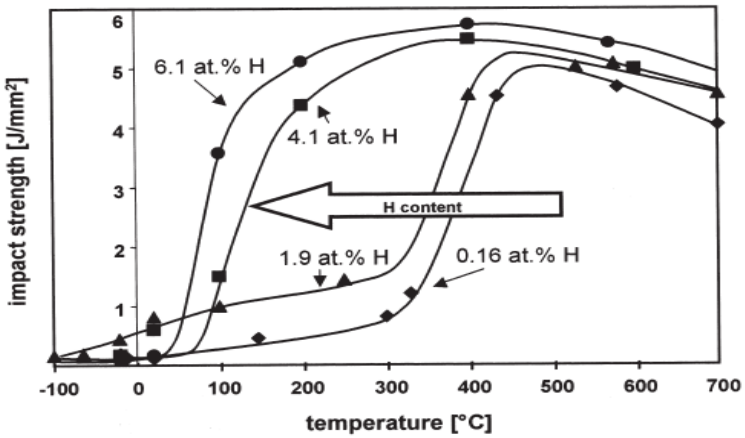

Figure 25. Impact strength of solution treated Ti 10-2-3 with different hydrogen content[13]

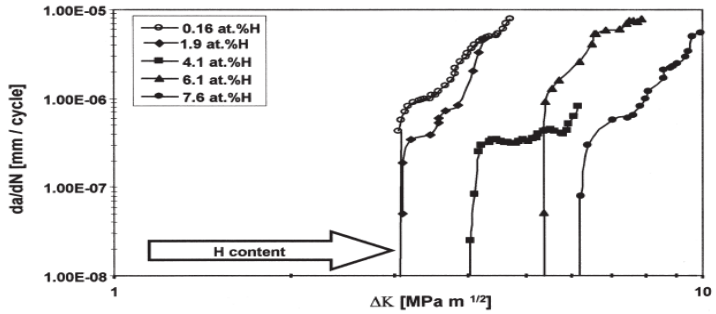

Figure 26. Fatigue crack growth rates for solution treated Ti 10-2-3 with different hydrogen content[13]

The effect of hydrogen treatment for these two beta alloys are summarized in Table 8. Given the high strength of the Ti 10-2-3, and the fact that toughness and fatigue strength are improved in

38

presence of hydrogen, it would be safer to use this alloy for the rotating group of the compressor rather than the Beta-C with reduced toughness and fatigue properties in hydrogen. Although solution treated and cold-worked single phase Beta-C is immune to embrittlement[16], the processing cost would increase.

Table 8. Mechanical property modifications as a result of hydrogen charging for solution annealed alloys.

Beta TI Alloy	Ultimate Tensile ksi	0.2% Yield ksi	% Elongation	Fatigue Threshold $MPam^{1/2}$	Comments
Ti-10-2-3	174 to116	160 to77	8 to 20	3 to 6	Gains ductility
Ti Beta C	145 to160	128 to162	37 to 3	5 to 2	Loses ductility

It should be noted that strength data are only available for low hydrogen concentrations or testing in hydrogen producing environments. Data in high pressure hydrogen are scarce or not available. At high hydrogen pressures (and high temperatures), beta Ti can hold a large amount of hydrogen in solid solution and hydride formation could occur, and deleterious intrinsic hydrogen effects can cause embrittlement[17]. However, hydrogen barrier coatings can be used as an effective measure in keeping the hydrogen concentrations sufficiently low[18]. Hydrogen barrier coatings are ineffective in alpha and alpha/beta alloys since very little hydrogen is needed for hydride formation. The most effective hydrogen barrier coatings are SiC, Aluminum Oxide, TiC/TiN, TiO2, Tungsten, CrN and TiC[19,20,21,22]. Also, direct oxidation of steel (i.e., Fe-Cr-Al mixed Oxides, Aluminizing {FeAl = AlO2}), are also effective[23]. It should be noted that a very thin coating of 1-10 nm is sufficient for protection against hydrogen diffusion.

Typical construction of a foil bearing consisting of a corrugated, or bump, foil and a smooth top foil is shown in Figure 27. The geometric features, such as the bump dimensions and spacing, foil thickness, etc. are designed for a specific foil material to impart the required stiffness, damping and elastic deflections. Some of the important properties to consider include the yield strength, ultimate strength, fatigue endurance limit, elastic modulus, thermal expansion coefficient, thermal conductivity, electrical conductivity and others. Table 9 compares some of the properties of a nickel alloy, which has been used successfully by MiTi for foil bearings of various sizes, with stainless steel 316L and two beta titanium alloys. In addition to the above mentioned properties, the foil material must have a good weldability and formability. The nickel alloy cannot be used in the hydrogen environment due to severe hydrogen embrittlement[24]. Stainless steel and beta alloys listed in the table are available in the thickness needed for the foil bearings and seal, and both materials can be used in the hydrogen environment. However, the strength of the stainless steel is not sufficient for highly loaded foil bearings, and the beta titanium alloys are superior in terms of strength and fatigue properties. In comparison to Ti 15-3, the Beta 21S is more susceptible to hydrogen embrittlement (Figure 28) due to grain boundary

Mohawk Innovative Technology®, Inc.
1037 Watervliet-Shaker Road, Albany, NY 12205
URL: www.miti.cc
Phone: (518) 862-4290, FAX: (518) 862-4291

precipitation[25] and by decohesion mechanism of hydrogen embrittlement[26]. While higher strengths are possible for both alloys through aging following solution treatment, aging treatment results in precipitation of alpha particles, which makes the material more prone to hydrogen embrittlement. Therefore, Ti 15-3 in the solution treated form is suitable for foil bearings and seals used in the hydrogen compressor.

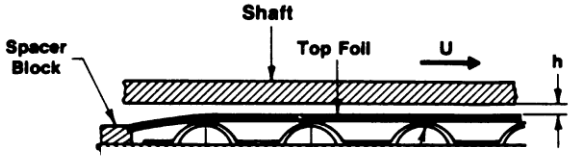

Basic Elements of Bearing

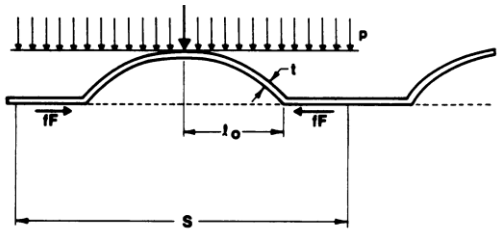

Bump Foil Configuration

Figure 27. Basic construction of a typical foil bearing

Table 9. Typical properties of several alloys in air as candidates for foil bearing fabrication

Material	UTS ksi	Hydrogen Embrittlement	Modulus ksix10^3	Fatigue Limit ksi	Thermal Expansion µin/in F	Electrical Resistivity µohm in
X-750 Ni	192	YES	31	80	7.8	48
316L SS	70	NO	28	37	8.6	30
Ti-15-3	200	NO	14.5	87	4.7	55
Ti Beta 21S	190	Yes	15	?	5.3	53

Beta titanium exhibits superior strength and fatigue life, particularly when exposed to hydrogen. Two of beta titanium considered for the rotating group are shown in

Table 10. Both Ti-10-2-3 and Ti Beta C are available in bar stock form and possess the necessary strength and fatigue properties. The mechanical properties listed in the Table are, however, measured in air and not hydrogen.

Mohawk Innovative Technology®, Inc.
1037 Watervliet-Shaker Road, Albany, NY 12205
URL: www.miti.cc
Phone: (518) 862-4290, FAX: (518) 862-4291

Table 10. Tensile properties of beta titanium alloys available in bar stock.

Beta TI Alloy	Ultimate Tensile ksi	0.2% Yield ksi	% Elongation
Ti-10-2-3	145-200	135-184	4-20
Ti Beta C	115-195	110-185	6-25

The effect of hydrogen on mechanical properties of these alloys is not well studied but limited data exist. MiTi has been able to locate one study, which compared Ti-10-2-3 and Ti Beta C both before and after exposure to low concentrations of hydrogen. The results are presented in Table 11. Despite the fact that both materials are beta titanium alloys, the effect of hydrogen exposure is very different. The particular Ti-10-2-3 evaluated in that study experiences a 45% drop in yield strength but gains ductility when exposed to hydrogen, while the effect on Ti beta C is nearly the opposite. For this application, the increase in ductility with Ti-10-2-3 is more critical than the improvement in yield strength exhibited with Ti beta C. Therefore, MiTi recommends the Ti-10-2-3 alloy for this application.

Table 11. Changes in tensile properties of Beta titanium after exposure to H2

Beta TI Alloy	Ultimate Tensile ksi	0.2% Yield ksi	% Elongation	Fatigue Threshold ksi.in$^{1/2}$	Comments
Ti-10-2-3	174 →116	165 → 90	8 → 20	2.7 → 5.5	Ductility Gain
Ti Beta C	145 →160	128 →162	37 → 3	4.5 → 1.8	Ductility Loss

Mechanical properties change as a result of hydrogen charging for solution annealed alloys [Christ et al 2003].

Mechanical properties of beta titanium alloys in air are highly dependent on the exact method of heat treatment, exposure time, temperature and hydrogen concentration in service. Further data are needed in order to make a final confident selection. In the meantime, MiTi recommends a coating such as TiN or CrN be applied to all surfaces exposed to hydrogen to further reduce the likelihood of embrittlement and degradation of mechanical properties.

While Ti-10-2-3 has been selected as the most appropriate material for the rotating group, this material is not available in thin foil form for the foil bearings. Therefore, following a similar material selection study, Ti-15-3 has been identified as an excellent candidate for the foil

Mohawk Innovative Technology®, Inc.
1037 Watervliet-Shaker Road, Albany, NY 12205
URL: www.miti.cc
Phone: (518) 862-4290, FAX: (518) 862-4291

bearings and seals. This material is available in thin stock and has demonstrated excellent properties in the hydrogen environment.

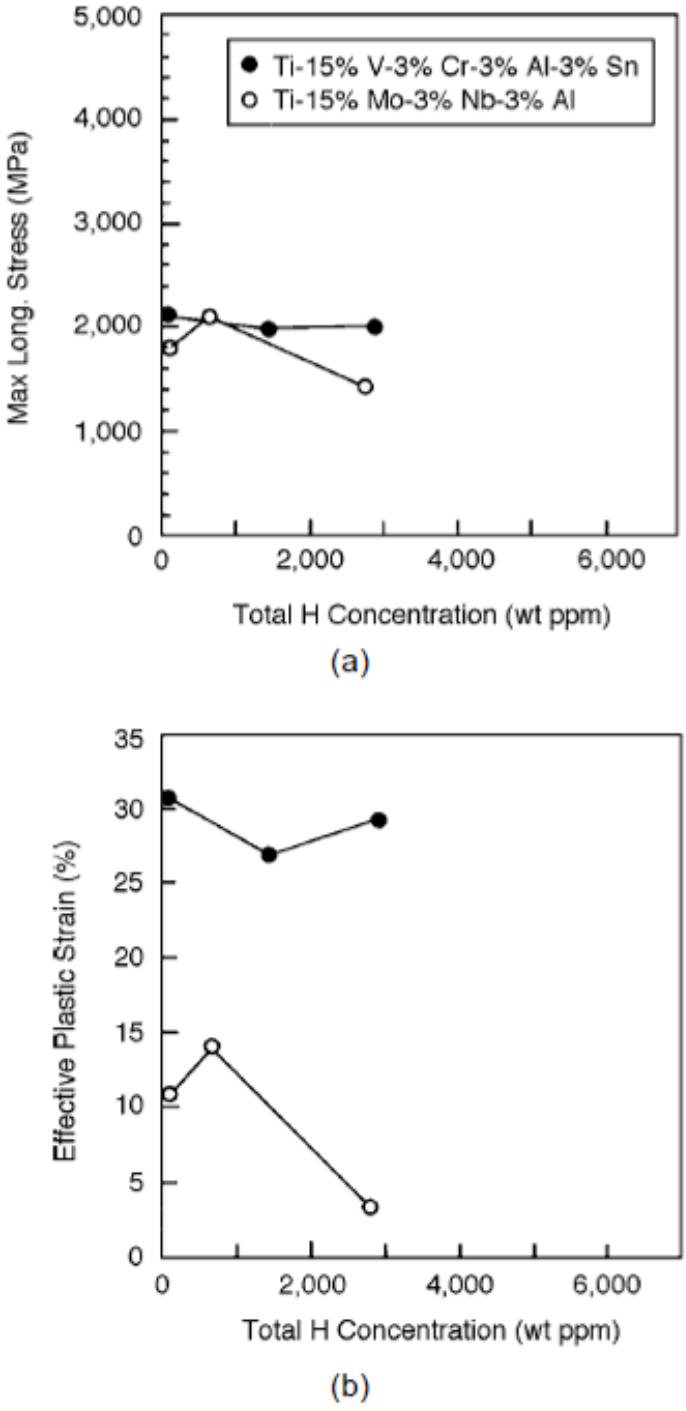

Figure 28. Strength and ductility of solution treated Ti 15-3 (solid symbols) and 21S25

Mohawk Innovative Technology®, Inc.
1037 Watervliet-Shaker Road, Albany, NY 12205
URL: www.miti.cc
Phone: (518) 862-4290, FAX: (518) 862-4291

8.4 Foil Bearing Coating

During normal operation of foil bearings and seals, surfaces are separated by a thin film of lubricating gas; in this case, hydrogen. However, during start and stop periods, the top foil makes contact with the rotating surface, i.e., the shaft, and therefore, there is need for a low friction, wear resistant coating system. Our experience has shown that a hard, wear-resistant coating should be placed on the rotating components and a relatively softer, low friction coating on the top foil surface. MiTi has developed a series of low friction coatings specifically for foil bearing applications that extend to temperatures above 800°C. These coatings, known as KOROLON®, have been successfully evaluated and implemented in various foil bearing and seal applications with a special chrome coating on the running surface. However, the Cr plating can be severely degraded in the hydrogen environment and the potential effect of hydrogen on KOROLON® coatings needs to be explored. Since our KOROLON® coatings contain some commonly used solid lubricants, it is instructive to review the effect of hydrogen on the tribological performance of various materials.

Extensive tribological studies have been conducted on various materials and coatings in air, inert atmospheres and also in vacuum[27]. However, studies in hydrogen gas are very rare and limited. While tribological properties of many materials are strongly affected by sliding in air due to oxidation, such phenomena would be absent in hydrogen. Early studies with chemisorbed gases on tungsten in vacuum have shown that, while any adsorbed gas including hydrogen can reduce the coefficient of friction, the most effective species is oxygen[27]. In one study, it was shown that hydrogen adsorption on an iron surface does not prevent the friction couples from "welding" but oxygen and some sulfur compounds reduce the tendency for welding and, therefore, reduce the coefficient of friction when testing is performed in high vacuum[28]. Hydrogen gas might reduce the natural oxide layer and protect against oxidation, thus, leading to high coefficients of friction and severe wear rates. The coefficient of friction of Ni alloys (X-750) and stainless steels (316) remain essentially unchanged in air, nitrogen, vacuum and hydrogen; that of Ti alloys (6 4) and Al alloys (6061) increases drastically in hydrogen[29]. Hydrogen can influence the friction of transition metals and other metals that react chemically with hydrogen, producing stable hydrides.[30,31] Studies have shown that the presence of water in hydrogen can have pronounced effects on the tribological properties of some metals, such as pure iron, Ni alloys, stainless steels and Co based alloys.[32,33]

Recent research has shown that commonly used solid lubricants, such as graphite, molybdenum disulphide, and tungsten disulphide, do not necessarily provide low friction in hydrogen. The friction of these lamellar solid lubricants that provide easy shear of their crystallographic planes depends on the environment. While shear of graphite layers requires moisture, the disulphides work best in the absence of adsorbed water vapor. Recent research has shown that molybdenum disulphide provides a fairly low coefficient of friction (0.1-0.2) in pure hydrogen gas as well as in nitrogen and in vacuum[29]. The lowest coefficient of friction (0.03-0.04) in hydrogen is observed for hydrogenated DLC. Excellent tribological behavior has been reported for molybdenum disulphide (0.03), PTFE (0.15) and DLC (0.15) in dry hydrogen[34]. However, the durability of the PVD disulphide coatings was limited to 10,000 sliding cycles.

An extensive study of fiber reinforced polymer composites (PEEK and PTFE) has shown that the coefficient of friction is much smaller in hydrogen (0.07-0.13) than in air (0.2-0.4) for the composites evaluated[34]. Similarly, lower friction was observed in liquid hydrogen than in air for

Mohawk Innovative Technology®, Inc. URL: www.miti.cc
1037 Watervliet-Shaker Road, Albany, NY 12205 Phone: (518) 862-4290, FAX: (518) 862-4291

the composites irrespective of the solid lubricant fillers used (graphite, molybdenum disulphide or bronze). The presence of humidity can also influence the friction and wear properties of polymers against steel. In one study, the wear rate of PTFE was reduced with an increase in environmental humidity in hydrogen. This effect was shown to be related to the formation of iron hydroxide on the 316 stainless steel counterface[35].

In another study, various polymers including PTFE, PEEK, PPS (polyphenylene sulfide), polyimide and Polyamide-imide were evaluated against steel[36]. The wear rates of PTFE, PEEK and Polyamide-imide were generally lower in hydrogen than in air, with the wear rate of the others about the same as in air and hydrogen. The coefficient of friction of PTFE (filled with 15% polyimide) was the lowest in hydrogen at about 0.4, the others had a coefficient of friction higher than 0.5 and nearly 1 for PPS. The use of a hydrogenated DLC on the steel surface reduced the coefficient of friction for Polyamide-imide (with 12%graphite and 3& PTFE) to 0.3.

Although the contact during stop/start operation is very brief (about 1 s), considerable damage can occur if the surfaces are not protected. The high sliding speed combined with the high load sets up various complicated tribological interactions that include chemical reactions, plasma formation, generation of static electricity and others. The coatings should be durable and stable under such conditions in the hydrogen gas. While research on tribological phenomena in hydrogen is still at its infancy, some useful information and data are emerging. While some metals can react to form hydrides, others can form oxides through a reaction pathway that includes formation of water[37,38]. Formation of both hydrides and oxides can, in fact, reduce the coefficient of friction. However, in the absence of reaction products, the native oxide can be reduced and the friction can increase. Among the materials that have been evaluated in hydrogen, PTFE and polyamide-imide have shown to provide acceptable tribological properties[39]. Furthermore, the addition of graphite to these coatings tends to improve the wear resistance[40,41].

The lowest reported coefficient of friction in hydrogen is for a hydrogenated DLC[42]. With the coefficient of friction less than 0.01 and often 0.003, this behavior is often referred to as "superlow friction". However, if only one surface is coated with the H-DLC film, a transfer film is required on the uncoated surface, which occurs after a short period of run-in. The superlow friction phenomenon is also observed for non-hydrogenated DLC in hydrogen[43]. It is believed that hydrogen saturation across the shearing plane through weak van der Waals interactions between the polymer-like hydrocarbon top layers contributes to the low friction phenomenon. Basically, repulsion of positively charged hydrogen terminated surfaces results in low attractions between the surfaces and reduces the coefficient of friction. It should be noted that H-DLC has a high hardness that provides both a low coefficient of friction and wear resistance.

Aside from solid lubricant coatings for the foil bearing pad, as stated earlier, a hard coating is needed on the rotating group where it makes contact with the foil bearing or foil seal. Due to uncertainties associated with the effect of hydrogen on mechanical properties and integrity of the rotating group, it is also beneficial to explore the use of hydrogen barrier coatings, especially those that could also provide wear resistance. Published literature on hydrogen barrier coatings indicate that metals with low hydrogen solubility and covalent, and ionic bonded materials, such as oxides and carbides, have low hydrogen permeability. Materials with lowest hydrogen permeability include aluminum oxide, tungsten, gold, glasses, tungsten and molybdenum silicides, molybdenum, nickel aluminide, copper, platinum and nickel[44]. Generally, a very thin film is needed as a hydrogen barrier coating.

Mohawk Innovative Technology®, Inc.
1037 Watervliet-Shaker Road, Albany, NY 12205
URL: www.miti.cc
Phone: (518) 862-4290, FAX: (518) 862-4291

Hydrogen barrier coatings can be used as an effective measure in keeping the hydrogen concentrations sufficiently low[45]. Hydrogen barrier coatings are ineffective in alpha and alpha/beta Ti alloys since very little hydrogen is needed for hydride formation. Effective hydrogen barrier coatings include SiC, Aluminum Oxide, TiC/TiN, TiO2, Tungsten, CrN and TiC[46,47,48,49]. Also, direct oxidation of steel, for example Fe-Cr-Al mixed Oxides, Aluminizing (FeAl = AlO2), are also effective[50]. It should be noted that a very thin coating of 1-10 nm is sufficient for protection against hydrogen diffusion. For example, a 50 nm coating of titanium dioxide is sufficient to retard the hydrogen embrittlement in a 15-5 PH stainless steel. Zirconium alloy coating on high strength steels can acts as diffusion barriers for hydrogen. In a sliding contact Zr and also Nb form hydrides and provide solid lubrication and lower friction as well.[37]

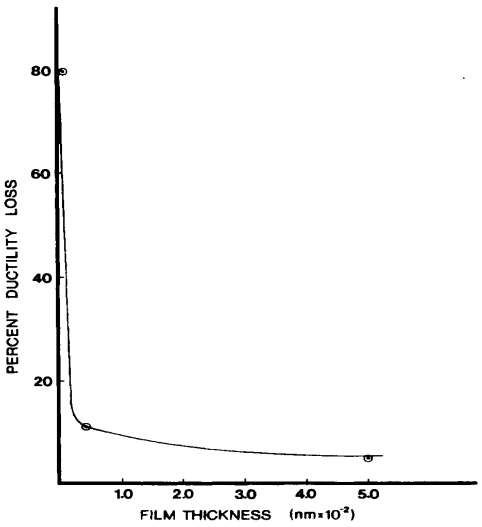

Figure 29. Effect of thin coatings on ductility of hydrogen charged 15-5PH stainless steel coated with TiO_2

While the above review suggests that H-DLC might be the best coating to obtain a low coefficient of friction and the required wear resistance, there are two issues that detract from selection of this coating for foil bearings and seals lubricated with hydrogen. First, the H-DLC is fully saturated with hydrogen and does not provide protection for hydrogen permeation into the counterface. Second, recent tests at our company have shown that, when H-DLC is used on the foil bearing and tested in air against a chrome plated disk or a disk coated with a proprietary tungsten disulfide coating (KOROLON 900), either the initial coefficient of friction was too high or the speed for lift-off was unacceptably high[51]. However, successful results were obtained when H-DLC was placed on the disk surface and the Korolong™ coating on the foil pad. However, the tribological behavior of this combination was similar to the results obtained with Korolon™ and chromium plate. When testing was performed at 300 C, the H-DLC coated disk, while providing a very low coefficient of friction during start, did not provide hydrodynamic lift[52]. While a different behavior might occur in hydrogen instead of air, hydrogen adsorption into the coating and substrate prevents this coating from use as both a hydrogen barrier and wear resistant coating.

Based on the above review, we propose the following approach for the foil bearing coatings. Hard coatings should be selected for the rotating group to inhibit hydrogen adsorption and also provide wear resistance. For example, TiC/TiN and TiN/CrN are all excellent wear resistant coatings and are commonly used in various applications. Therefore, these coatings are good candidates for coating on the rotating surfaces. Since our KOROLON 700 coating has been successfully used as a foil bearing coating for many diverse applications, and the polymeric constituents and the solid lubricant fillers have been successfully tested in hydrogen, it should be further evaluated for use on the top foil surfaces in the hydrogen compressor. In addition, PTFE filled with graphite could also be evaluated as an alternate foil coating material.

Mohawk Innovative Technology®, Inc.
1037 Watervliet-Shaker Road, Albany, NY 12205
URL: www.miti.cc
Phone: (518) 862-4290, FAX: (518) 862-4291

8.5 Material Testing in Hydrogen

The selection of beta titanium alloy was based on a comprehensive analysis of published data on performance of different types of titanium alloys in hydrogen. Titanium alloys possess excellent strength to density ratios, thus, they are ideal for applications requiring high strength and low weight. Ti-10V-2Fe-3Al, in particular, was chosen based on results that suggested this beta alloy would be safe in hydrogen service. Those results were obtained for testing of the alloy in air after hydrogen charging. Due to the uncertainty associated with such types of testing, it was decided to perform fracture testing in high pressure hydrogen. These tests were performed at Sandia National Laboratories with the objective to identify the effects of hydrogen on fatigue crack growth. The tests were conducted on compact tension specimens (Figure 30), according to ASTM standards, in both air and hydrogen environments (at 1200 psig). While the results confirmed no strength reduction when the specimen was exposed to hydrogen prior to testing in air, the results when loading in high pressure hydrogen were unacceptable (Figure 4). The particular heat treatment used, for the as received material, consisted of solution annealing (SA), which produces very small alpha regions in the material. Although the published results and those presented here both indicated that the presence of small alpha regions in this beta alloy does not produce an issue when the alloy is pretreated in hydrogen prior to testing in air, the alpha phase was suspected as the cause of poor performance in the hydrogen environment. The presence of titanium hydride (TiH_2) formed from the alpha phase was confirmed by XRD analysis (Figure 31). Thus, the heat treatment condition used and the resulting microstructure for this alloy are not appropriate for the proposed application. The next step in this effort is to heat treat the test specimens to assure a completely beta phase microstructure and repeat the tests in high pressure hydrogen.

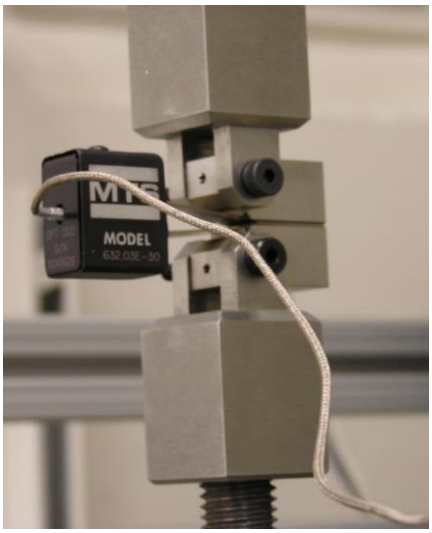

Figure 30. Ti alloy test specimen mounted for testing in air.

Mohawk Innovative Technology®, Inc.
1037 Watervliet-Shaker Road, Albany, NY 12205
URL: www.miti.cc
Phone: (518) 862-4290, FAX: (518) 862-4291

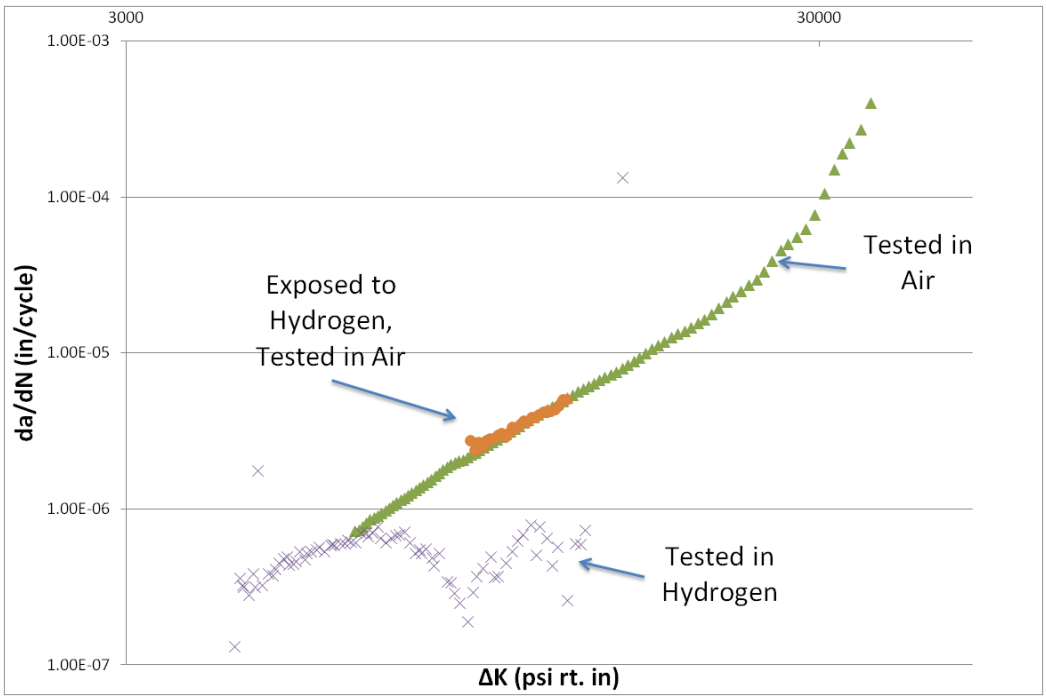

Figure 31. Preliminary test results in air and hydrogen gas, courtesy of Sandia National Laboratory

9.0 Oil-Free Foil Bearings and Seals

MiTi's 9-stage hydrogen compressor design consists of three double entry systems, each with three back-to-back compression stages. In each frame, a single shaft is supported by compliant foil bearings, allowing for 100% contaminant operation without the need for external lubricants. Two foil journal bearings are located towards either end of the shaft (Figure 32) and support the radial position of the shaft. While a dual inlet design was selected, in part, due to the inherently balanced thrust loads, some transient thrust should be expected. MiTi® foil thrust bearings have been designed to address these transient loads. Two thrust bearings will be located at the center of the shaft, as shown in Figure 33.

The design and development of these foil bearings for this application were fabricated and experimentally validated in a previous DOE funded SBIR program (DE-FG02-05ER84245). Under this prior effort, compliant foil bearings were built and tested on a simulator shaft and operated at full speed (56,000 rpm). A key technological accomplishment resulting from this prior SBIR effort was the demonstration of a multi-stage compressor shaft operating above the bending critical speed (ie. first resonance). Such super-critical operation at high-speed has only been demonstrated by MiTi[53,54] and provides significant benefit to the overall machine, which included reduced footprint, reduced parasitic losses and improved reliability through reduced complexity.

Mohawk Innovative Technology®, Inc.
1037 Watervliet-Shaker Road, Albany, NY 12205
URL: www.miti.cc
Phone: (518) 862-4290, FAX: (518) 862-4291

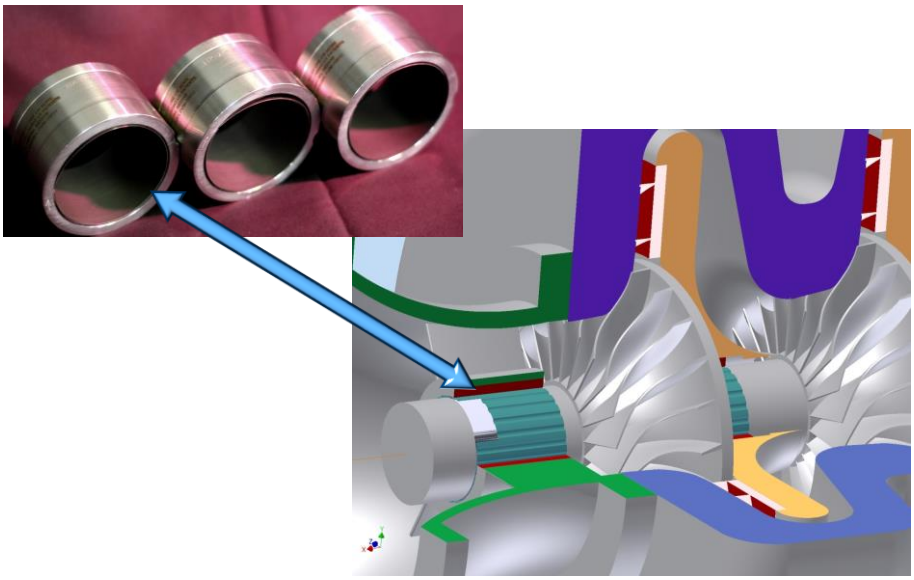

Figure 32. MiTi® foil journal bearings selected for use in the hydrogen compressor

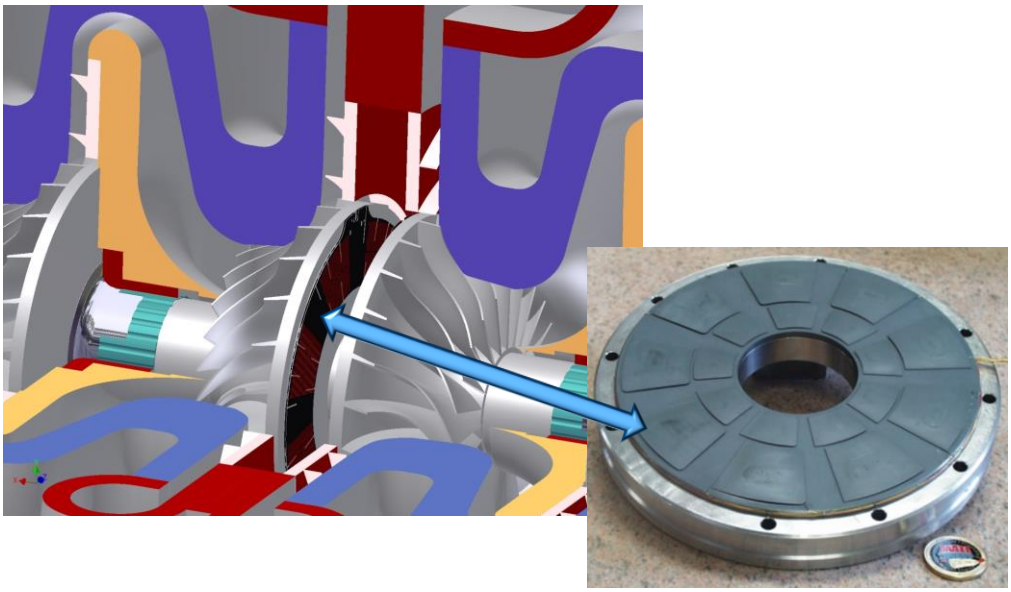

Figure 33. MiTi® foil thrust bearings selected for use in the hydrogen compressor

Mohawk Innovative Technology®, Inc.
1037 Watervliet-Shaker Road, Albany, NY 12205
URL: www.miti.cc
Phone: (518) 862-4290, FAX: (518) 862-4291

As a result of the preliminary and detailed aerodynamic design analysis conducted in this investigation, the multi-stage compressor system design has been revised. These changes have slightly changed the load and performance requirements of the compliant foil bearings from what was initially assumed during the previous SBIR bearing design efforts. In order to accommodate these updated system changes, the foil bearing design was revisited and any changes to bearing properties were recalculated since they will greatly impact other design analysis. For example, speed dependant bearing stiffness was determined and used as an input into the lateral vibration FE model for revised rotordynamic analysis. Coupled finite difference and finite element methods were used to analyze the foil thrust bearing. Results of the elasto-hydrodynamic analysis using the finite difference method and applied to the structural finite element model of the foil thrust bearing were used to determine the distributed pressure profile within the bearing. Typical results from the selected journal bearing design are shown in Figure 34 and a single pad from the selected thrust bearing design is shown in Figure 35. The dynamic behavior of the compliant foil seals and their impact on system performance are discussed further in the rotordynamic analysis.

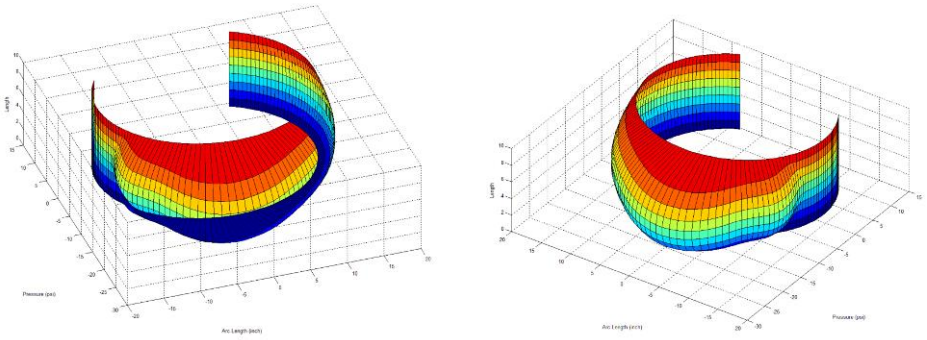

Figure 34. MiTi® foil journal bearing pressure profile developed at 56,000 rpm in the hydrogen compressor

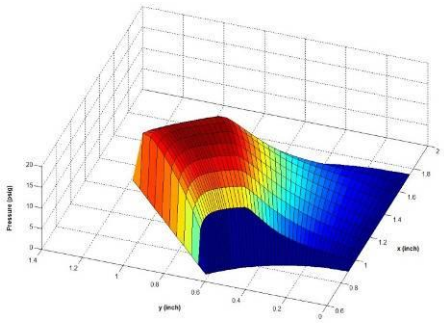

Figure 35. Single pad pressure profile for MiTi® foil thrust bearing from finite difference elastohydrodynamic analysis

The solid model of the compliant foil seal selected for this application is shown in Figure 36. Design and experimental performance testing of the complaint foil seals in hydrogen applications

Mohawk Innovative Technology®, Inc.
1037 Watervliet-Shaker Road, Albany, NY 12205
URL: www.miti.cc
Phone: (518) 862-4290, FAX: (518) 862-4291

was evaluated in a parallel DOE project (DOE Grant No. DE-FG02-07ER84779). Results indicated superior performance, and very low leakage in air and helium environments at 56,000 rpm, relative to other state-of-the-art seal technologies available. The compliant foil seal will be used between each compression stage to reduce inter-stage leakage which will allow for high adiabatic compression to be maintained throughout the system.

At total of four MiTi® compliant radial foil seals will be used for inter-stage sealing. As was done with the compliant foil bearings, the elastohydrodynamic FEM solution was computed for the selected compliant foil seal program using MiTi proprietary software tools. The resulting pressure profile is shown in Figure 37.

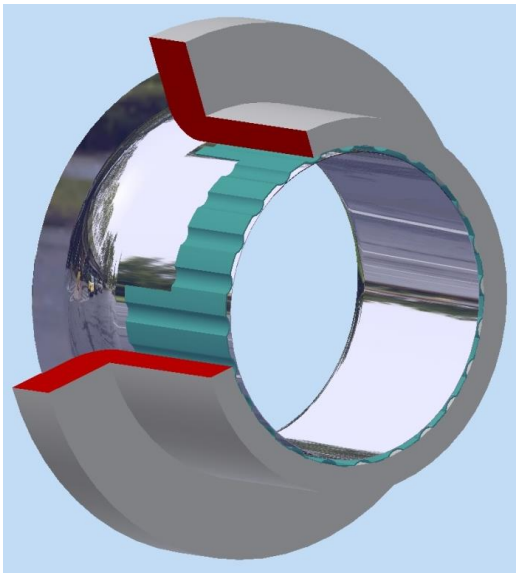

Figure 36. 3D solid model of the MiTi® complaint foil seal for inter-stage sealing needs

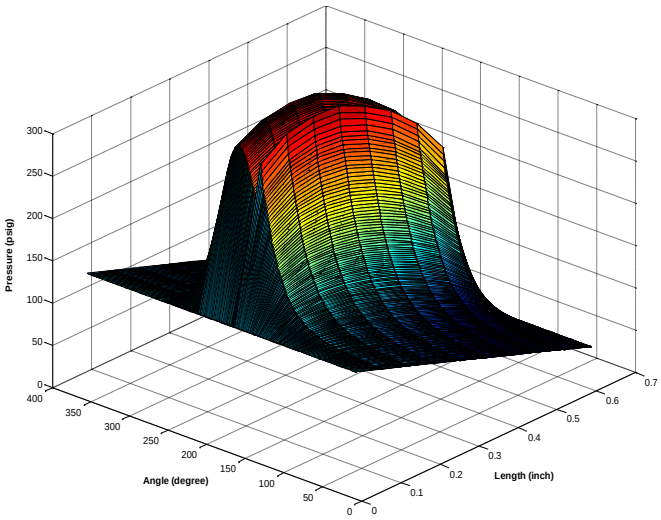

Figure 37. Elastohydrodynamic plus hydrostatic pressure for MiTi® radial foil seal from finite difference analysis

10.0 Rotordynamic Stability Analysis

10.1 Multi-Stage Rotor

The design and experimental validation of a multi-stage centrifugal compressor operating above the first bending critical speed has been previously demonstrated by MiTi in a previous DOE funded SBIR program (DE-FG02-05ER84245), as stated above. Based upon design modifications and refinements conducted in the above aerodynamic and bearing design sections of this investigation, the rotordynamic models were updated and analysis was repeated. Rotor dynamic analysis began using the rotor geometry, as defined in the earlier DOE SBIR, in order to validate new results and serve as a baseline. The model is shown in Figure 38 where the unbalance forces were included to match the rotor responses at two sensor locations, measured from previous experiments. The predicted rotor response at the sensor locations and the bending moments at the bearing locations are shown in Figure 39 for one of the analyses. The analysis predicted that, in this case, the first critical bend would occur at about 35,000 rpm. The finite element model was modified by adding two grounded springs attached to the shaft at each

Mohawk Innovative Technology®, Inc.
1037 Watervliet-Shaker Road, Albany, NY 12205
URL: www.miti.cc
Phone: (518) 862-4290, FAX: (518) 862-4291

bearing location to constrain the two perpendicular radial directions, instead of fixing the shaft at one end. Appropriate bearing stiffness values were assigned as the spring constants and the bending moments at the first bending critical speed from the rotor dynamic analysis were applied to the shaft at the two bearing locations. The analysis was performed for a rotational speed of 60,000 rpm. Therefore, in this analysis, both the centrifugal and bending stresses were included. The results indicated that the effect of adding the bending moment was insignificant and the stress values remained practically unchanged. Therefore, it is concluded that the torque and bending moments are carried by the core shaft only and have no effect on the disks, which mainly carry the centrifugal stress.

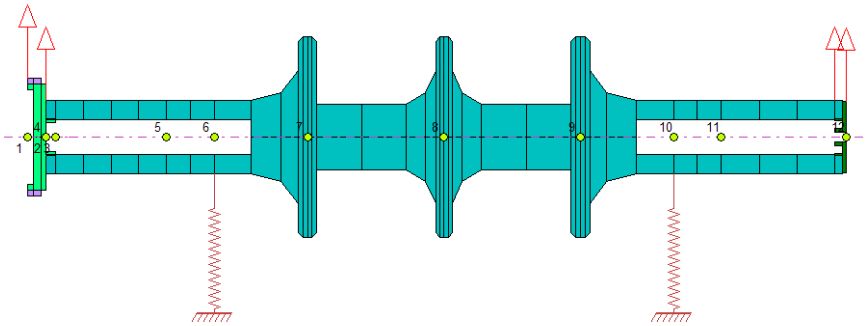

Figure 38. Model of the rotor for rotor dynamic analysis

The estimated stiffness and damping properties of the designed foil bearings were used for rotordynamic analysis of the compressor rotor. Rotor dynamic analysis model was then modified to include the full 3-stage configuration with dual-inlet, yielding six total compressor wheels in a single Frame 1 (Figure 40). Two foil journal bearings are located at both ends of the shaft. Based on preliminary aerodynamic analysis, an optimized shaft diameter between the compressor wheels was selected. Data presented below assumes a high-strength steel; however, similar analysis was performed with the titanium and aluminum alloys.

Mohawk Innovative Technology®, Inc.
1037 Watervliet-Shaker Road, Albany, NY 12205
URL: www.miti.cc
Phone: (518) 862-4290, FAX: (518) 862-4291

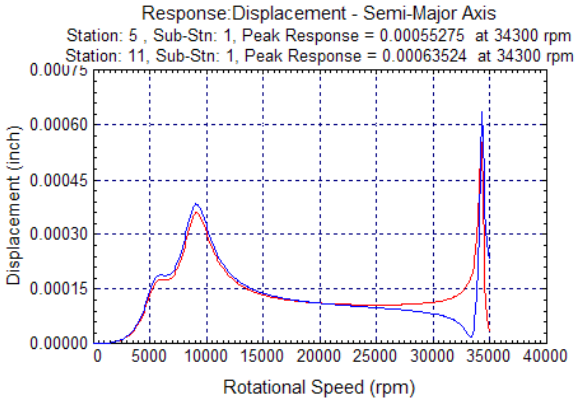

(a)

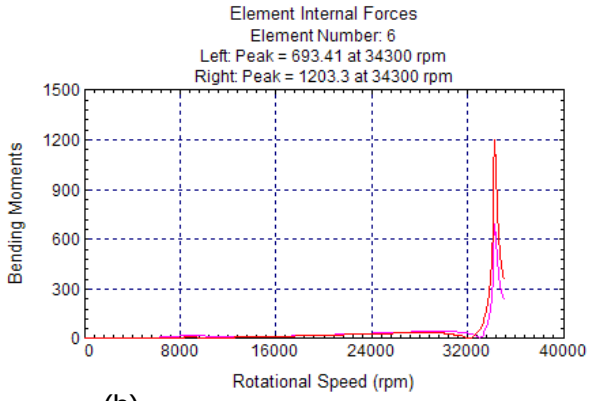

(b)

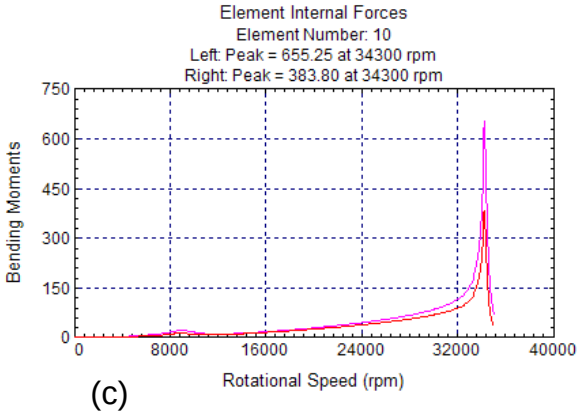

(c)

Figure 39. Predicted results from the rotor dynamic analysis: (a) Displacements, (b) Moments in one bearing location, and (c) Moments in the other bearing location

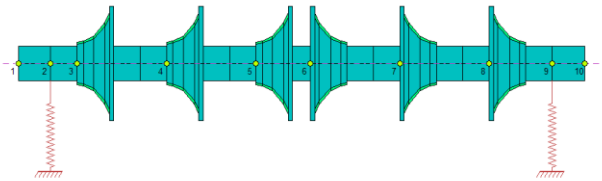

Figure 40. Finite element rotor dynamic model of three stage double entry centrifugal compressor system

The critical speed analysis results, shown in Figure 41, indicate that the first bending mode is 21,666 rpm and the second bending mode is 60,853 rpm. In this case, not only the first bending mode is within the operating speed range but the second bending mode is too close to the design speed of 56,300 rpm.

Mohawk Innovative Technology®, Inc.
1037 Watervliet-Shaker Road, Albany, NY 12205
URL: www.miti.cc
Phone: (518) 862-4290, FAX: (518) 862-4291

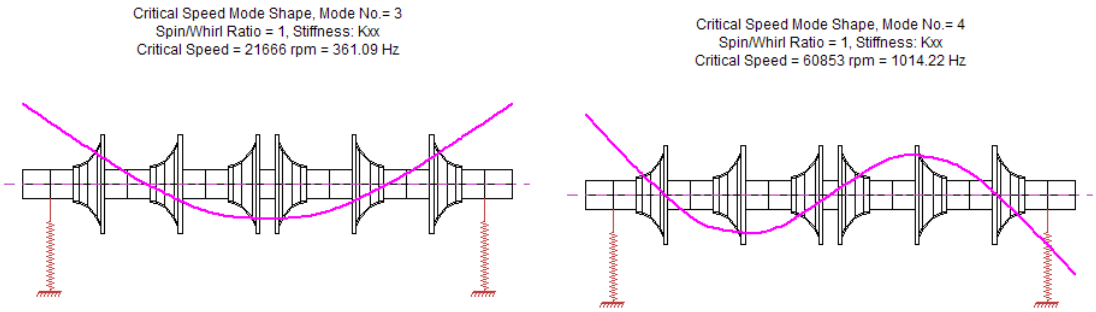

Figure 41. 1st and 2nd bending modes of three stage double entry compressor rotor

Operation near the second bending critical speed presents further design challenges and is preferred to avoid this scenario. In order to avoid operation near the second bend mode, the diameter of the shaft in between the compressor wheels was increased. The increase in shaft diameter resulted in an increase of the first bending mode to 27,700 rpm and the second bending mode of 76,321 rpm, as shown in Figure 42. The diameter increase has introduced a sufficient safety margin away from the second bending mode. Rotordynamic analysis was also performed with the titanium and aluminum alloys. As seen in Table 12, the selection of material type has little impact on the rotordynamic behavior.

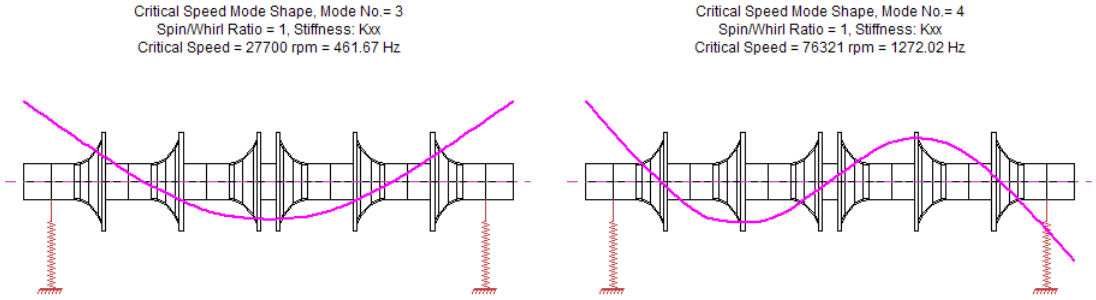

Figure 42. 1st and 2nd bending modes of three stage double entry compressor rotor with the larger diameter shaft

Table 12. Summary of various materials predicted bending critical speeds.

	1st Bend Critical (RPM)	2nd Bend Critical (RPM)
Aluminum Alloy	27,100	74,633
Titanium Alloy	26,092	72,044
High-Strength Steel	27,700	76,321

Mohawk Innovative Technology®, Inc.
1037 Watervliet-Shaker Road, Albany, NY 12205
URL: www.miti.cc
Phone: (518) 862-4290, FAX: (518) 862-4291

Next, a detailed rotordynamic evaluation was performed in which the shaft of the three stage double entry centrifugal compressor system was modified to include the thrust disk for the two foil thrust bearings at the center, two foil journal bearings located at both ends of the shaft and four journal foil seals used for inter-stage sealing. The speed-dependent stiffness coefficients were calculated and damping properties were estimated for the bearings and seals. Whirl speed and stability analysis were conducted using the finite element rotor dynamic model shown in Figure 43.

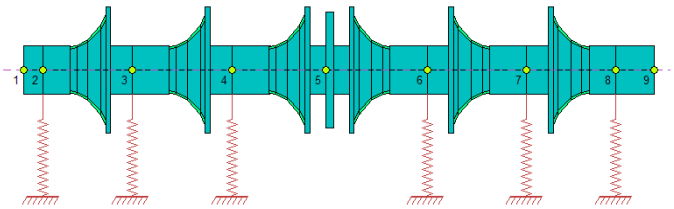

Figure 43. Finite element rotor dynamic model of three stage double entry centrifugal compressor system

The whirl speed map in Figure 44 shows the first four damped natural frequencies, including the cylindrical and conical rigid body modes as well as the 1st and 2nd bending modes, of the three stage double entry compressor rotor as a function of the rotational speed. Figure 45 shows the corresponding mode shapes at 70,000 rpm. In Figure 46, the logarithmic decrement values for these four modes are plotted as a function of speed. Excellent stability was achieved for all the four modes. In these analyses, nominal damping coefficient was used for the two foil bearings. All four modes were stable, but the 2nd bend was marginal. The data presented here assumes titanium alloy; however, similar analysis was also performed with high-strength steel.

Mohawk Innovative Technology®, Inc.
1037 Watervliet-Shaker Road, Albany, NY 12205
URL: www.miti.cc
Phone: (518) 862-4290, FAX: (518) 862-4291

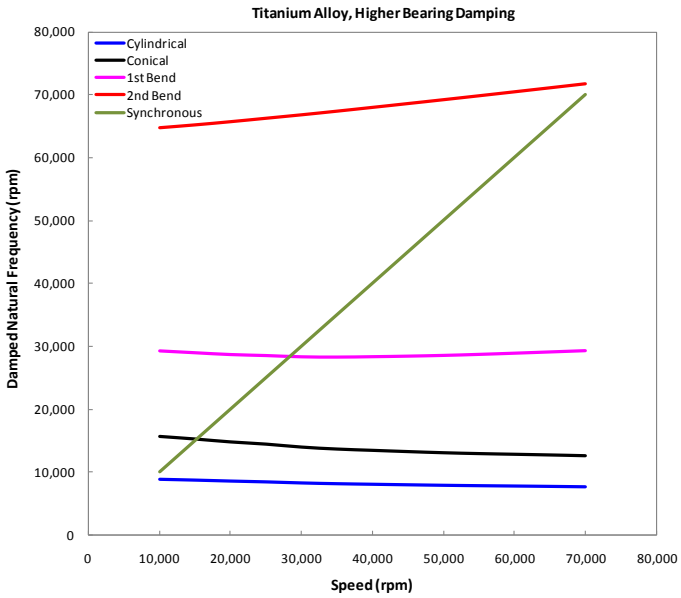

Figure 44. Whirl speed map of three stage double entry centrifugal compressor rotor of titanium alloy with nominal foil bearing damping

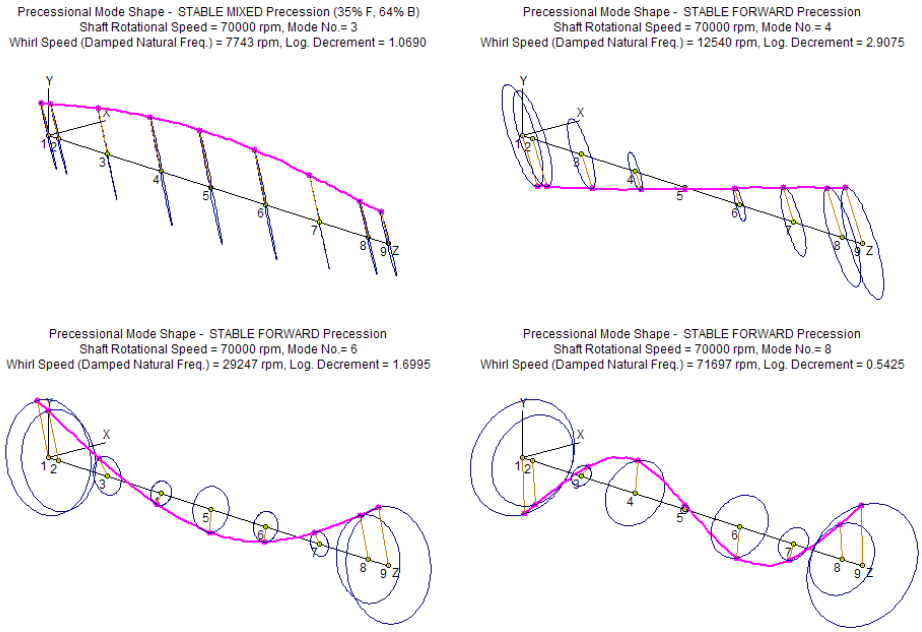

Figure 45. Cylindrical and conical rigid body modes, 1st and 2nd bending modes of three stage double entry compressor rotor of titanium alloy with nominal foil bearing damping

Mohawk Innovative Technology®, Inc.
1037 Watervliet-Shaker Road, Albany, NY 12205
URL: www.miti.cc
Phone: (518) 862-4290, FAX: (518) 862-4291

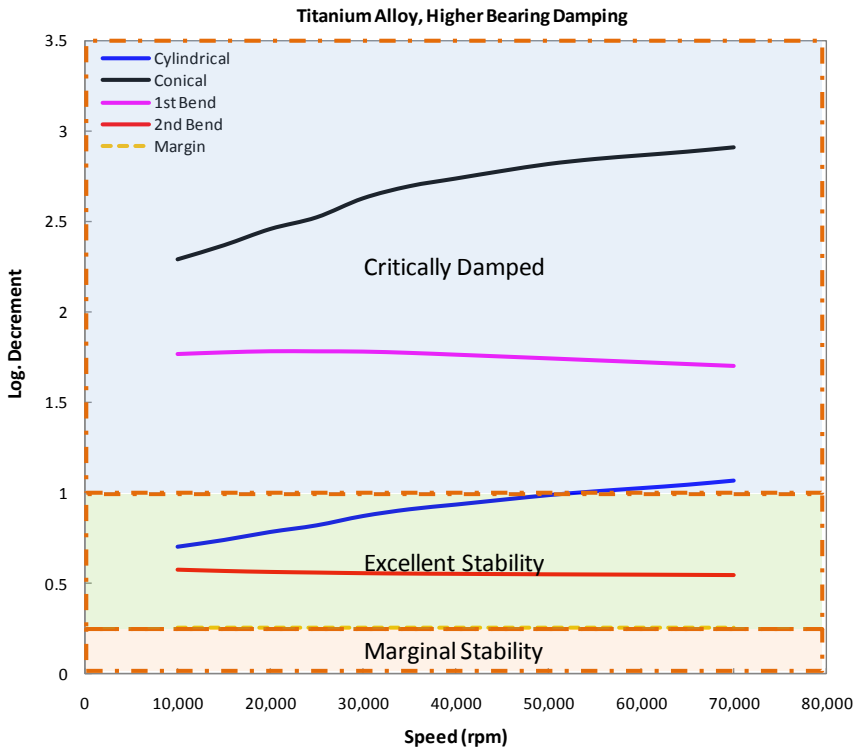

Figure 46. Stability map of three stage double entry centrifugal compressor rotor of titanium alloy with nominal foil bearing damping

10.2 Single Stage Test Rig

Assessment of the rotor/bearing system dynamics was also conducted for the 200 kW motor and single stage compressor wheel at the full speed of 1600 ft/s (56,414 rpm) to verify stable operation during PTC-10 tests. At the designed inlet pressure of the multi-stage compressor of 500 psia, more than 800 hp shaft power was required to reach full speed. By reducing inlet pressure to 20-50 psi and preserving the same volume flow rate, shaft power was reduced to less than 200 kW. No single, direct-drive 200 kW drive motor capable of operating at 56,000 rpm exists. MiTi has developed, at our own expense, the 60,000 rpm, 100 kW motor. Since the objective of this program is to demonstrate the thermodynamic performance of the compressor, MiTi has opted to couple two high speed, 100 kW motors together to provide the needed drive power rather than develop a single 200 kW, direct drive motor. The predicted power requirement of the single stage compressor operating with helium is shown in Figure 47. When operating with helium at 70% of full speed, or 39,200 rpm, the critical non-dimensional performance parameters, such as Reynolds number, mach number and flow coefficient, match those with hydrogen at 100% full speed. Therefore, this operating speed is the selected operating speed for the single-stage testing, conducting in accordance with ASME PTC-10 and described later this report.

Mohawk Innovative Technology®, Inc.
1037 Watervliet-Shaker Road, Albany, NY 12205
URL: www.miti.cc
Phone: (518) 862-4290, FAX: (518) 862-4291

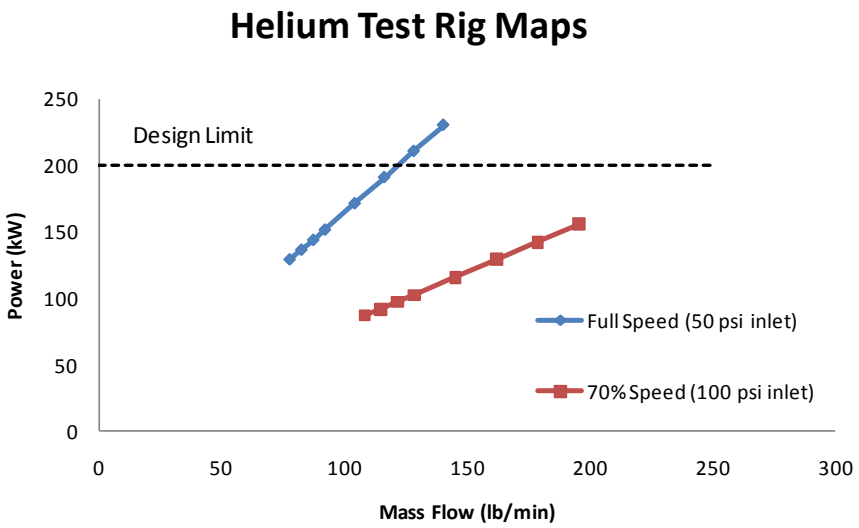

Figure 47: Performance curves for the helium compressor test rig at the full speed operating condition (blue) and the similitude test condition (red)

To assure stable operation of the proposed dual motor drive system for the single stage compressor, detailed rotordynamic analysis was performed. The finite element (FE) model of the coupled shaft system is shown in Figure 48. The compressor is rigidly attached to the shaft on the left. The two rigid shafts are connected by a flexible coupling, which is a proprietary technology developed by MiTi. Each individual shaft is supported on MiTi® compliant foil journal and thrust bearings.

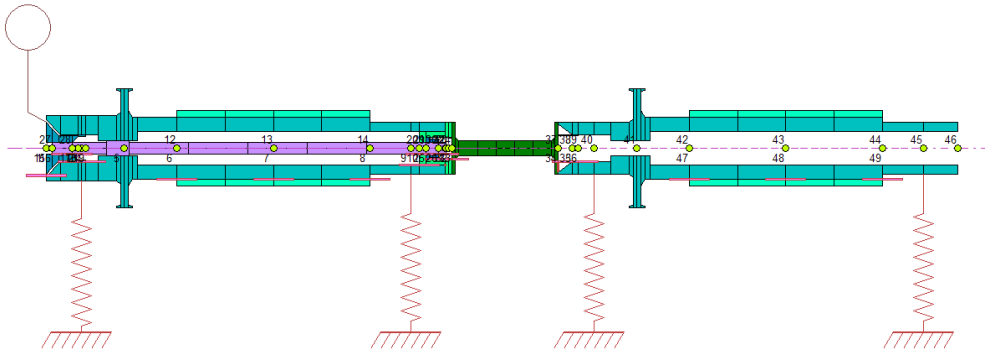

Figure 48: FE model of the compressor and dual drive system.

Appropriate stiffness and damping values for bearings were selected and rotordynamic analysis was conducted with DyRoBes© software (Eigen Technology Inc.). The analysis indicated that each individual shaft would be operating safely below its bending critical speed (Figure 49). All bending within the system would occur within the flexible coupling, as designed, and as has been demonstrated by MiTi in numerous other applications.

Mohawk Innovative Technology®, Inc.
1037 Watervliet-Shaker Road, Albany, NY 12205
URL: www.miti.cc
Phone: (518) 862-4290, FAX: (518) 862-4291

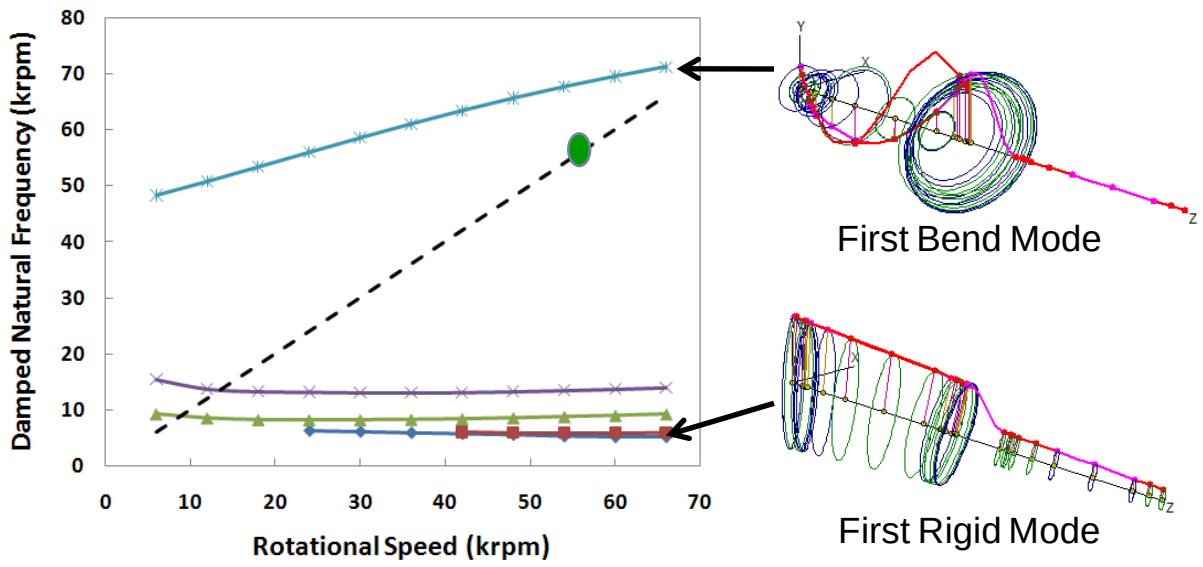

Figure 49: Rotordynamic analysis of the dual drive single stage test rig

11.0 Single Stage Compressor Design

In order to conduct thorough experimental validation of the proposed centrifugal hydrogen compressor, a single stage compressor test facility was developed. The facility included a secure test cell with reinforced walls, stainless-steel closed-loop piping and a oil-free centrifugal hydrogen compressor. A detailed model of the proposed single stage test rig is shown in Figure 50. The approximate locations of key instrumentation measurement points along the length of the rotating shaft are indicated. The impeller and volute of the single stage test rig are identical to that of a single stage within the first frame of the 9-stage system. The single stage compressor will be driven with two MiTi® electric motors, which will be coupled together to produce up to 200 kW of shaft power. The test rig will be totally oil-free using MiTi®'s foil bearings and foil seals.

Mohawk Innovative Technology®, Inc.
1037 Watervliet-Shaker Road, Albany, NY 12205
URL: www.miti.cc
Phone: (518) 862-4290, FAX: (518) 862-4291

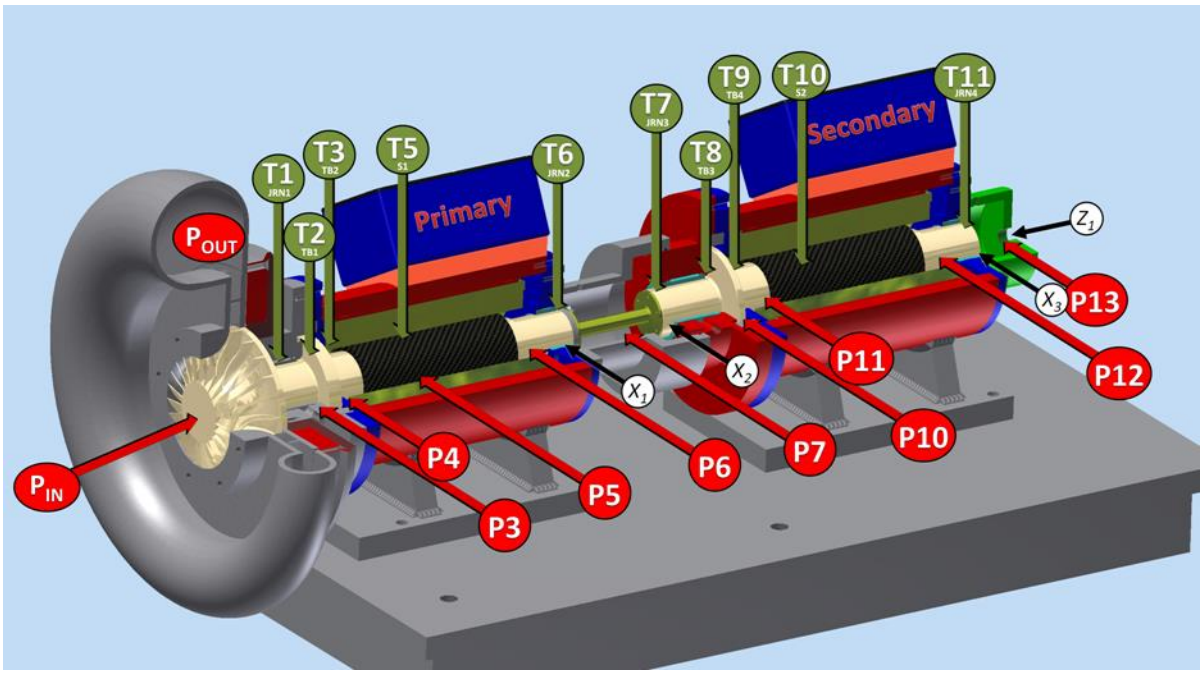

Figure 50. Single stage test rig with safety enclosure (left). Cross-section view of the single stage test rig with showing the titanium impeller, shaft and coupled drive (right).

The purpose of the single stage testing is to validate the thermodynamic performance of the centrifugal compressor design proposed, as well as the rotor/bearing system performance under realistic speed and stress conditions expected in the 9-stage system. In order to validate the performance predictions of the MiTi® oil-free hydrogen compressor concept, the single stage testing will be conducted per ASME performance test code 10 (PTC-10). This test code provides explicit test procedures to determine compressor thermodynamic performance with a high level of accuracy. There are two types of tests described within PTC-10; type 1 and type 2 tests. A type 1 test is one conducted with the design gas, at the design point. Under the scope of this program, testing with hydrogen is not feasible; therefore, a type 1 test will not be conducted. Since testing with all possible gases at all test conditions is often not feasible, ASME established the type 2 test based the standard design practice of compressor similitude. With this approach, key non-dimensional parameters are maintained constant in testing so that thermodynamic performance of a compressor stage in one gas would apply to other gases and at other test conditions. For this investigation, the best similitude gas is helium. Helium is an affordable and safe alternative to hydrogen with a similarly low molecular weight. It is critical that the first compressor stage performance testing not be complicated with the issues of hydrogen embrittlement. The issues of material compatibility and embrittlement are being addressed in a parallel effort in this program and these two issues should not be integrated at this time. The use of helium in these first compressor performance tests allows us to focus on aerodynamic and thermodynamic characterization. Helium testing will allow us to establish a performance baseline so that any performance effects due to embrittlement will be apparent at a later time. The operating conditions of the helium test rig that will allow non-dimensional similitude between the design point and the test rig operating conditions were determined:

Mohawk Innovative Technology®, Inc.
1037 Watervliet-Shaker Road, Albany, NY 12205
URL: www.miti.cc
Phone: (518) 862-4290, FAX: (518) 862-4291

- Speed: 39,323 rpm
- Inlet Pressure: 100 psi
- Inlet Temperature: 100 ^{o}F
- Power: 102 kW

At these operating conditions, the values of the critical non-dimensional parameters are within the permissible deviation of type 2 test (Table 13).

Table 13. Non-dimensional parameter values for the helium test rig and permissible type 2 deviations.

Quantity	Symbol	He Test Rig Performance	Type 2 Permissible Deviation
Specific Volume Ratio	v_i/v_d	1.052	1.018 – 1.126
Flow Coefficient	Φ	0.1253	0.120 - 0.130
Machine Mach No.	Mn	0.3266	0.141 - 0.532
Machine Reynolds No.	Re_m	3.33e5	1.55e5 – 1.55e7

The individual 100 kW motor elements of the single stage compressor drive system is shown in Figure 51. The fabrication and heat treatment of the drive shafts during various stages of assembly are shown in Figure 52. The final machining of these crucial dynamic elements of the rotating assembly was performed in-house. Static elements of the drive system were fabricated outside. The fabrication of the impeller was performed by a 5-axis CNC vendor. In order to assure the highest safety material standards, the raw material used to fabricate the compressor impeller was subjected to ultrasonic inspection per ASTM-2375. This material was subjected to the highest NDE inspection standard to assure that no internal voids or cracks were present. Such testing was necessary and is commonly used to avoid premature failure of the rotating group. The two shafts of the dual-drive system were fabricated and prepared for installation. Along with the shaft components, the fabrication steps of other static components of the dual-drive system are shown in Figure 53. The components shown below were assembled and prepared for the initial demonstration testing of the motor drive system. In addition to these components, MiTi® thrust and journal bearings were fabricated for assembly into the 100 kW motor. Each 100 kW motor contains two journal and two thrust bearings for a total of eight compliant foil bearings to support the entire rotating group. In parallel with fabrication, electric motor variable frequency drives (VFDs) were installed and the facilities were upgraded to accommodate the 400 amp, 480 volt requirements. The dual VFDs are shown in Figure 54 shortly after being received.

Mohawk Innovative Technology®, Inc.
1037 Watervliet-Shaker Road, Albany, NY 12205
URL: www.miti.cc
Phone: (518) 862-4290, FAX: (518) 862-4291

Figure 51. Pair of 100 kW motor elements for use in the dual drive single stage compressor

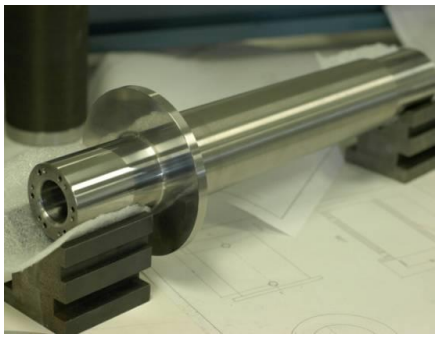

Figure 52. The two shafts of the dual-drive system of the single stage compressor. The rough shafts are shown following heat treatment (above). The shafts were then machined (above, right) and finally precision ground for a high-tolerance fit (right) with the motor assembly

Mohawk Innovative Technology®, Inc.
1037 Watervliet-Shaker Road, Albany, NY 12205
URL: www.miti.cc
Phone: (518) 862-4290, FAX: (518) 862-4291

Figure 53. Completed components of the dual-drive system of the single stage compressor test

Figure 54. Dual motor variable frequency drives (VFD) shown after being received at MiTi

Initial dynamic testing of the motor and VFDs was performed prior to compressor performance testing. A single 100kW electric motor was assembled for testing of the shaft and rotor only, as shown in Figure 55. Data from this initial dynamic testing of the motor are shown in Figure 56. The motor was first successfully tested up to 25,000 rpm and stable operation was observed. Testing was performed for each motor individually up to 60,000 rpm to demonstrate stable performance.

Mohawk Innovative Technology®, Inc.
1037 Watervliet-Shaker Road, Albany, NY 12205
URL: www.miti.cc
Phone: (518) 862-4290, FAX: (518) 862-4291

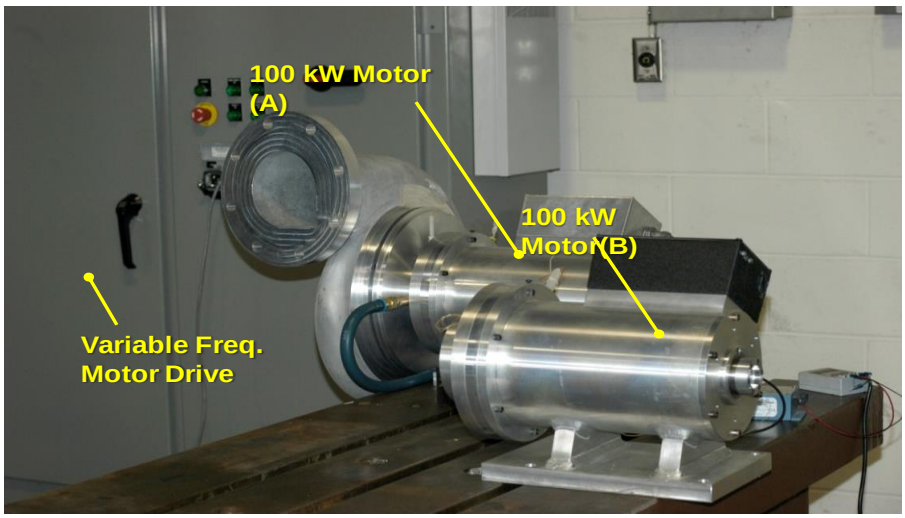

Figure 55. 100 kW motor and VFD assembled and ready for testing.

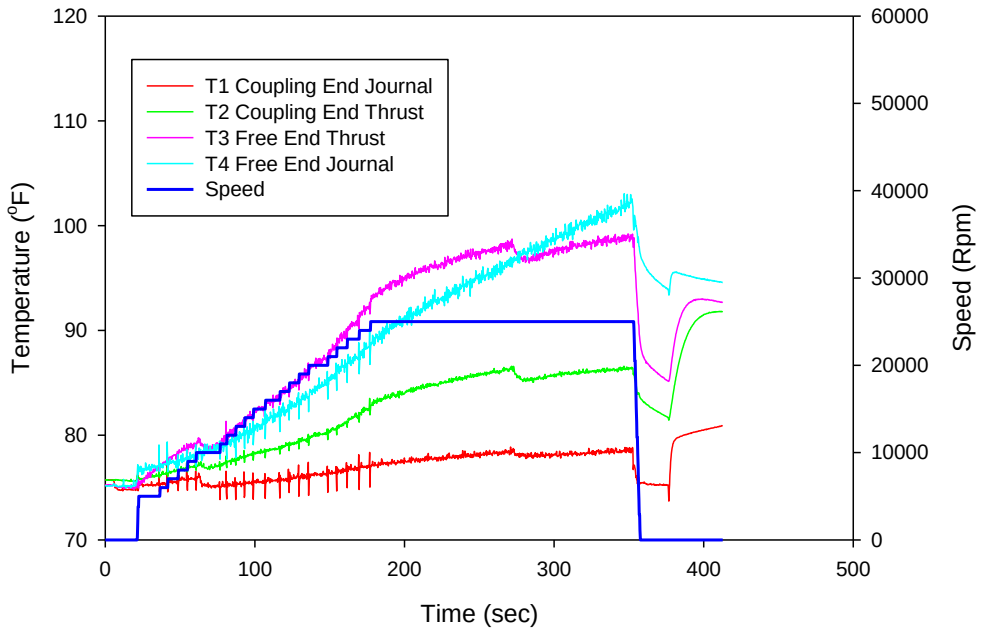

Figure 56. Data from initial dynamic testing of the 100 kW motor to 25,000 rpm, demonstrating stable operation

The next phase of testing will be to couple the two motors and demonstrate full speed operation without the impeller and, secondly, with the bladeless impeller.

Each 100 kW motor was tested to 60,000 rpm. Test data for Motor (A) are provided in Figure 57. Testing was conducted at speeds ranging from 10,000 rpm to 60,000 rpm and stable motor speed control was demonstrated. Foil bearing temperatures were carefully monitored during testing and stable bearing performance was observed during operation. Bearing temperatures were less than 150°F at full speed. During testing, cooling air was supplied externally at a rate of 15 scfm;

Mohawk Innovative Technology®, Inc.
1037 Watervliet-Shaker Road, Albany, NY 12205
URL: www.miti.cc
Phone: (518) 862-4290, FAX: (518) 862-4291

however, in the single stage compressor, bearing cooling gas was taken from the compressor bleed rather than externally provided. Rotor vibrations were recorded during full speed testing using fiber-optic proximity probes. The maximum rotor motions measured at full speed were 0.0002" (see Figure 58). This represents extremely low vibrations as it is approximately equivalent to the mechanical run-out of the rotor.

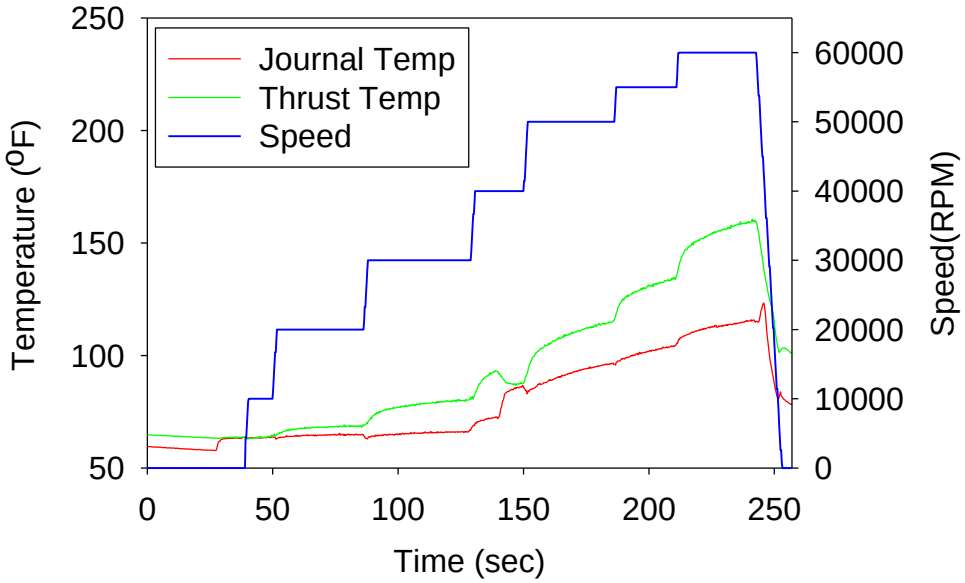

Figure 57. Testing of the individual 100 kW motor up to 60,000 rpm

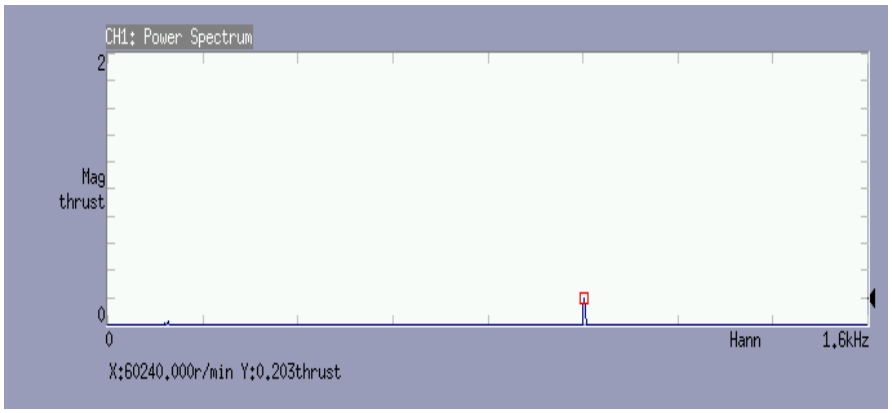

Figure 58. Rotor motion measurement recorded during testing (60,240 rpm) was found to be 0.0002". This value is equivalent to the mechanical run-out

Following successful testing of the individual motors, a bladeless compressor wheel was attached to Motor "A". The bladeless wheel (Figure 59-left) was designed to have the same mass, center of gravity and inertial properties as the bladed compressor wheel. Bladeless wheel testing was a cost effective method to demonstrate rotordynamics and system stability before testing with more delicate and costly components, such as bladed compressor wheels. Test data with the bladeless wheel are presented in Figure 59-right. The bladeless wheel testing was successful and the compressor performed as predicted. Stable operation and low foil bearing temperature were observed. Testing with the bladeless wheel was limited to 40,000 rpm for

Mohawk Innovative Technology®, Inc.
1037 Watervliet-Shaker Road, Albany, NY 12205
URL: www.miti.cc
Phone: (518) 862-4290, FAX: (518) 862-4291

safety reasons. Testing beyond 40,000 rpm with a compressor wheel was not conducted until the construction of the dedicated test cell, with proper safety provisions, was completed.

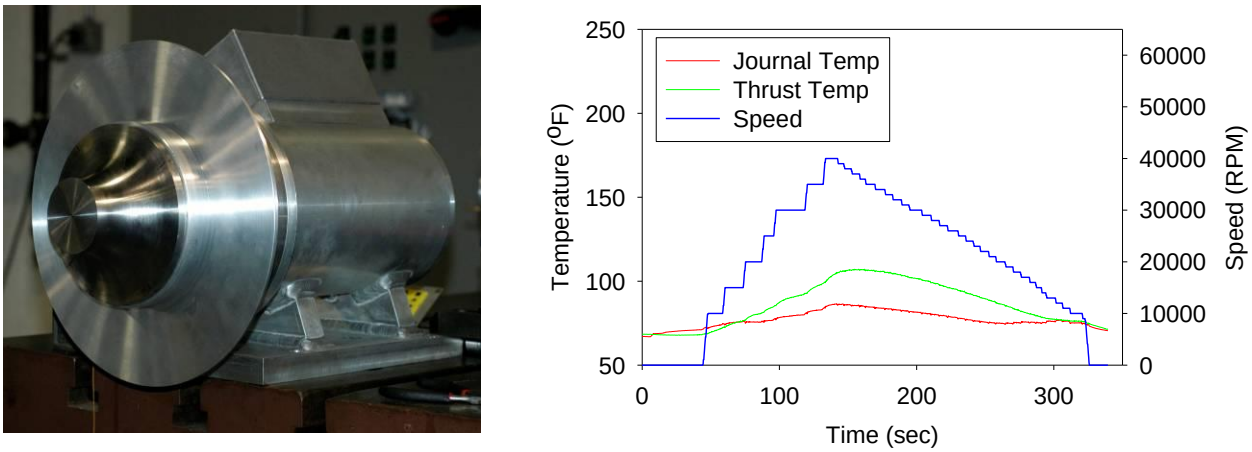

Figure 59. The 100 kW motor drive with a bladeless compressor wheel (left) and stable test data from operation up to 30,000 rpm

After testing with the bladeless wheel, the bladed compressor wheel and volute were installed and tested (Figure 60). Bearing temperatures were found to be lower in the bladed wheel due to additional cooling flows, which were provided by the compressor bleed air that was not available with the bladeless wheel. Testing with the bladed wheel was limited to 15,000 rpm for safety reasons. Results are shown in Figure 61.

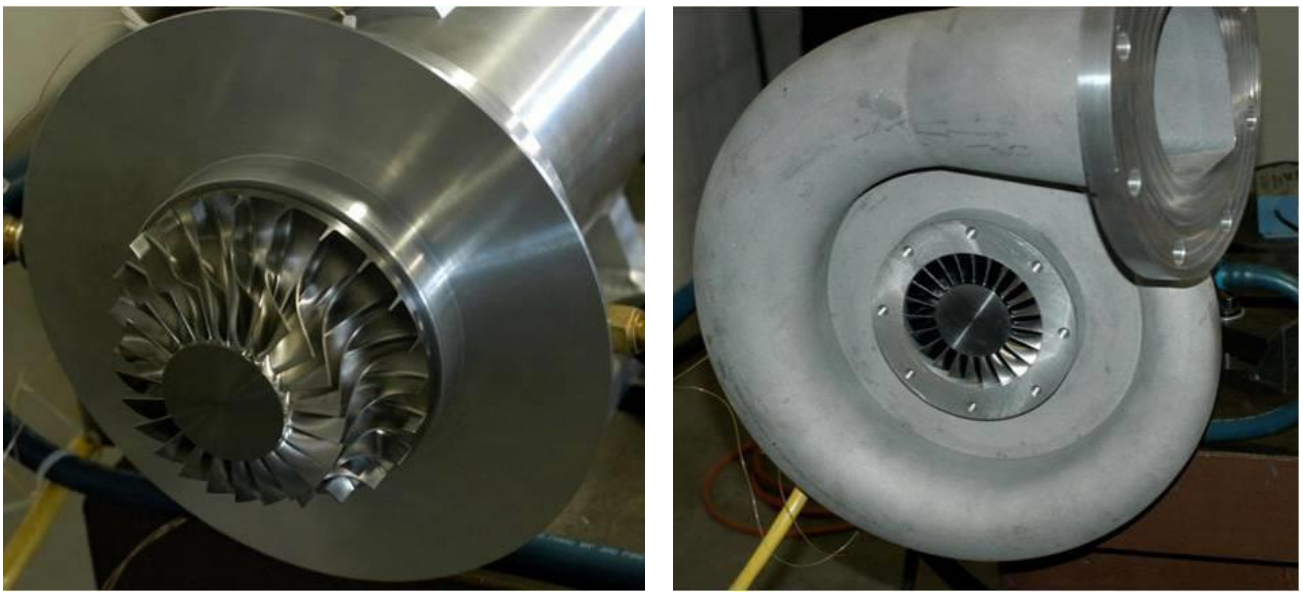

Figure 60. The bladed compressor wheel (left) and volute (right) attached to the 100 kW motor for performance testing.

Mohawk Innovative Technology®, Inc.
1037 Watervliet-Shaker Road, Albany, NY 12205
URL: www.miti.cc
Phone: (518) 862-4290, FAX: (518) 862-4291

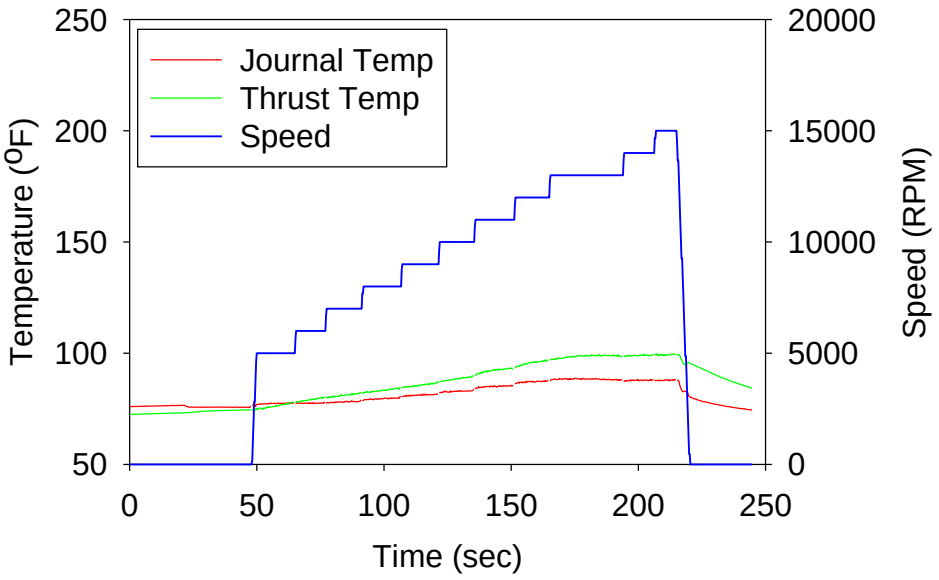

Figure 61. Performance testing of the 100 kW motor with bladed compressor wheel and volute.

After stable operation on the individual 100 kW motors was demonstrated at low speed (<15,000 rpm), dynamic "check-out" testing of the coupled dual-drive system was performed. In this test, the two 100 kW motor drives were mechanically coupled to one another to produce the necessary 200 kW needed for the single stage helium testing. Again, without a dedicated test cell at the time, testing was limited to 15,000 rpm. Testing was successful and low vibration was observed. The FFT data presented in Figure 62 show no sign of sub-synchronous vibrations. Full speed testing and aerodynamic evaluation were completed once the dedicated test cell was completed.

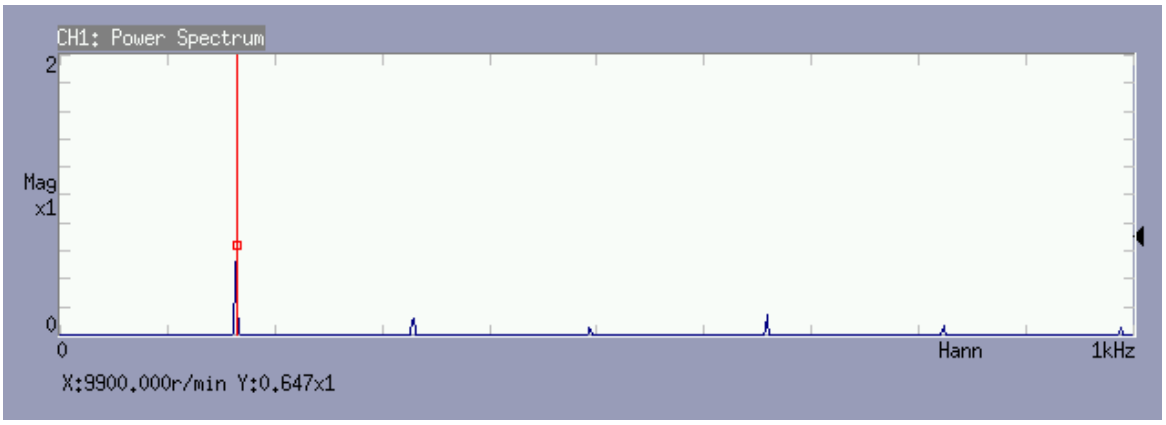

Figure 62. Vibration data during coupled motor testing

Mohawk Innovative Technology®, Inc.
1037 Watervliet-Shaker Road, Albany, NY 12205
URL: www.miti.cc
Phone: (518) 862-4290, FAX: (518) 862-4291

12.0 Single Stage Compressor Testing

In order to test the single stage compressor system to the design speed of 56,000 rpm and fully evaluate the aerodynamics, a dedicated test cell was designed and constructed. The test cell houses the 200 kW single stage compressor system for testing according to the guidelines published in ASME PCT-10. The test cell was designed with reinforced walls and ceiling to protect against catastrophic failure. Design of the proposed test cell, with necessary safety measures for high-speed rotor testing, is shown in Figure 63.

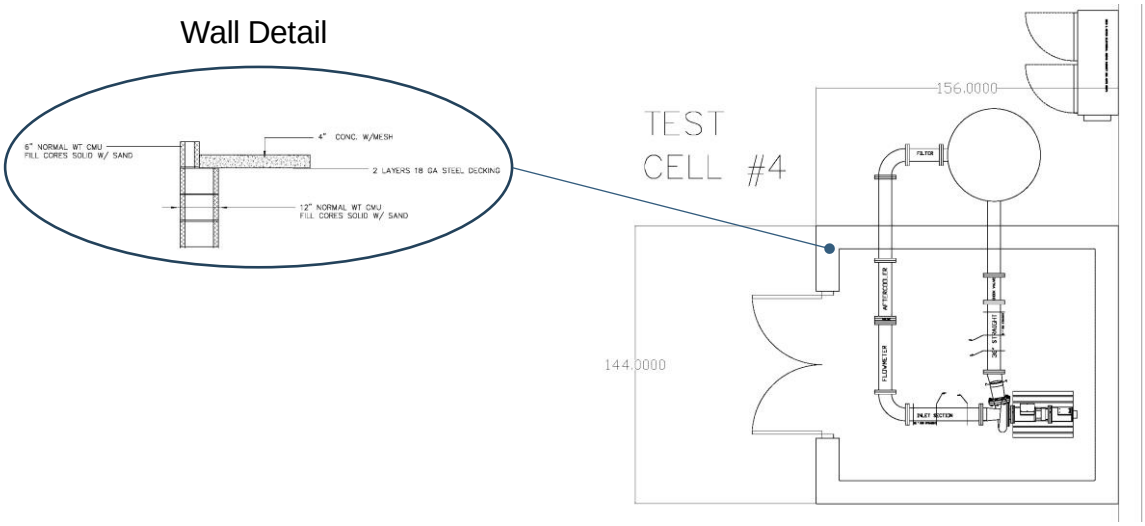

Figure 63. Test cell layout

An independent review of ASME PTC-10 conformance for the single stage testing was performed by McHale & Associates Inc., an outside consultant, to verify the proposed single stage testing as well as verify the dedicated test cell had sufficient space for all the required plumbing and instrumentation. McHale is an established expert in the field of compressor testing and auditing, and will provide valuable insight and assure compliance with PTC-10. The first task performed by McHale was an overall review of the test instrumentation and test loop hardware, including review of the requirement for anti-surge hardware. McHale performed calculations to determine surge volume required. McHale also reviewed the test loop component capacity and sizing, and provided conclusions in a letter report. Finally, a review of the test instrument selection and accuracy based on ASME PTC-10 requirements was performed.

The primary objectives of McHale's work included test rig component sizing, loop configuration, valve sizing, surge prevention verification, and instrumentation and uncertainty estimation. McHale concluded that MiTi's test plan conforms with ASME PTC-10 and that the test loop components and configuration are appropriate. Several helpful suggestions were made and recommendations regarding specific selection of critical components were given. For example, a control valve was selected with a flow coefficient (C_V) of 130-270 within the operating range of 20 - 80% compressor flow. This specification is critical in avoiding unstable flow behavior that

Mohawk Innovative Technology®, Inc.
1037 Watervliet-Shaker Road, Albany, NY 12205
URL: www.miti.cc
Phone: (518) 862-4290, FAX: (518) 862-4291

could result in surge. Given the promising results of the independent review by McHale, MiTi moved ahead with fabrication and assembly of the closed-loop system for testing the compressor with helium. The complete report provide by McHale can be found in Appendix A.

Photographs documenting different phases of test cell construction are shown in Figure 64. A 3D rendering of the test cell with the closed flow loop and major components is shown in Figure 66. The system includes a holding tank, filter, control valve, after cooler and flow meter prior to intake at the compressor. A return flex line is also shown. Note that the 3D model does not show the reinforced ceiling and door. MiTi selected a local small business with extensive experience in high pressure plumbing to complete the construction of the closed loop stainless steel flow system.

Mohawk Innovative Technology®, Inc.
1037 Watervliet-Shaker Road, Albany, NY 12205
URL: www.miti.cc
Phone: (518) 862-4290, FAX: (518) 862-4291

Figure 64. Photographs of different stages of test cell construction

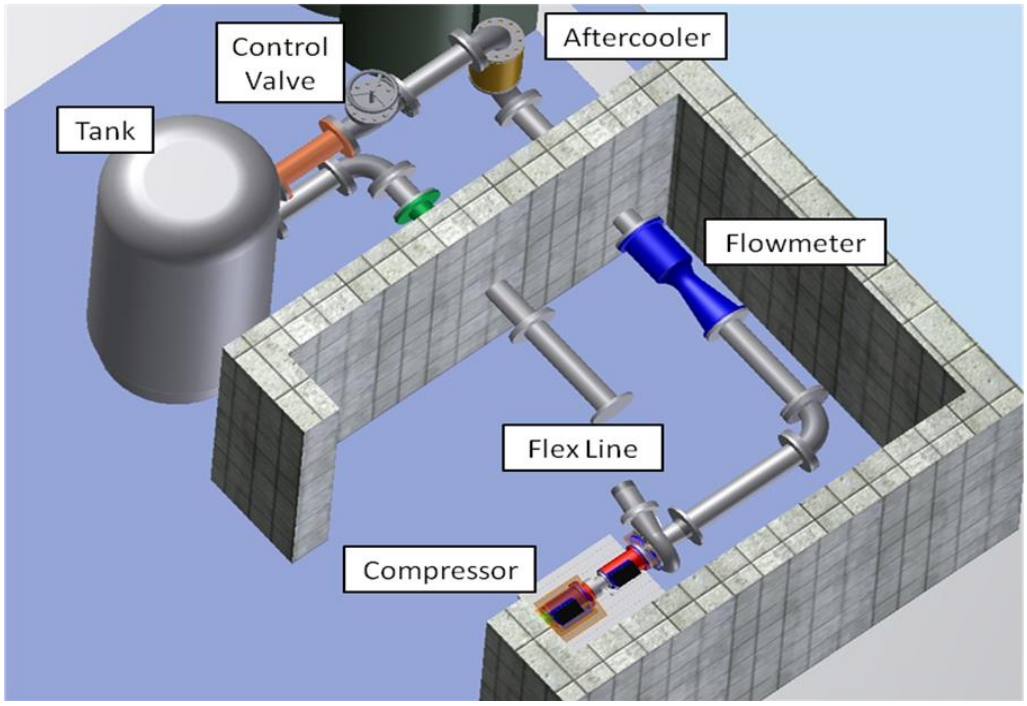

Figure 65. Top view of the 3D rendering of the completed single stage test cell with closed loop stainless steel plumbing

Mohawk Innovative Technology®, Inc.
1037 Watervliet-Shaker Road, Albany, NY 12205
URL: www.miti.cc
Phone: (518) 862-4290, FAX: (518) 862-4291

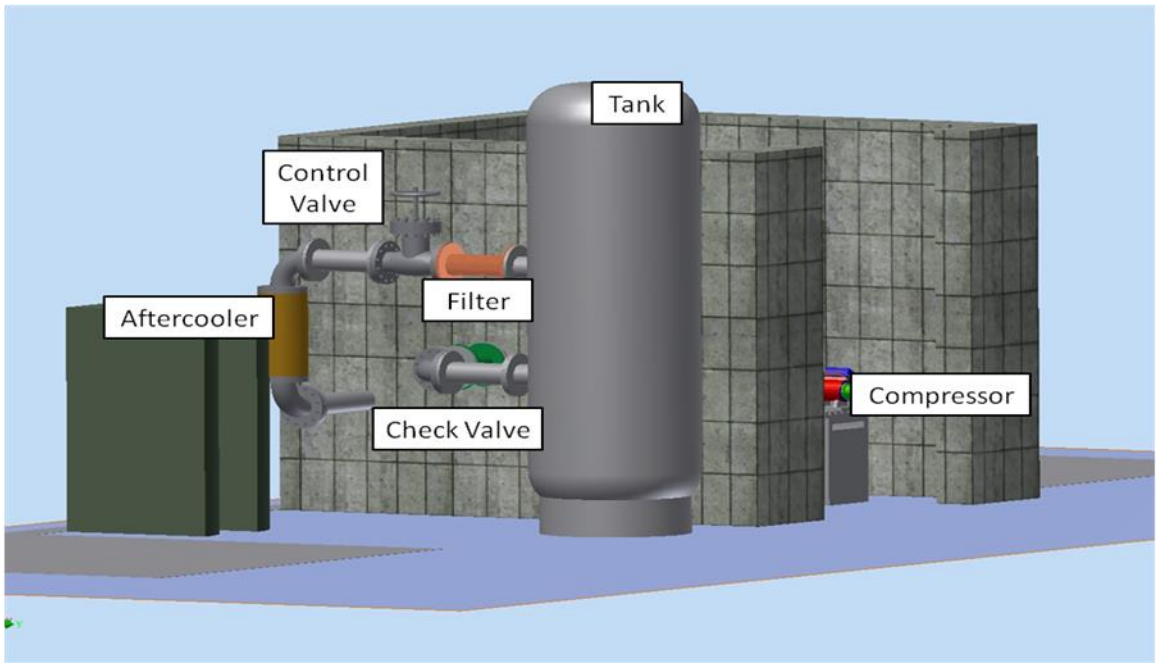

Figure 66. Side view of the 3D rendering of the completed single stage test cell with closed loop stainless steel plumbing

The stainless steel volutes were received by MiTi from an outside casting vendor. The newly fabricated stainless steel volutes are shown in Figure 67 and were used for compressor tests with system pressures of 25-100 psia.

Mohawk Innovative Technology®, Inc.
1037 Watervliet-Shaker Road, Albany, NY 12205
URL: www.miti.cc
Phone: (518) 862-4290, FAX: (518) 862-4291

Figure 67. Stainless steel volutes for high pressure testing

After receiving the volutes from the casting vendor, final machining of the compressor shroud profile was performed by MiTi to assure reliable blade clearance during high speed operation. Once complete, a volute was installed on the single-stage compressor and fit was verified (Figure 68).

Mohawk Innovative Technology®, Inc.
1037 Watervliet-Shaker Road, Albany, NY 12205
URL: www.miti.cc
Phone: (518) 862-4290, FAX: (518) 862-4291

Figure 68. Fitting and installation of the stainless steel volute on the single-stage compressor

All instrumentations and controls were placed outside the cell to protect the expensive instrumentations and personnel. The completed test cell is shown in Figure 69. MiTi subcontracted a local small business with extensive experience in high pressure plumbing to fit and weld the closed loop stainless steel flow system, fabricate the tank to ASME specifications, and align and install other key components of the system.

Other features of the test facility include a high resolution video camera for remote monitoring and video recording. A custom command console has been completed for the monitoring of all system data and simultaneous monitoring of the drive motor. A custom GUI has been developed using Labview software (National Instruments). The new GUI allows for direct command of motor speed control, monitoring of all pressure and temperature data, as well as high frequency spectral analysis of up to four proximity probes for vibration measurement. Finally, the command console has remote access capabilities to allow the operator to control all test compressor and drive functions from a safe distance away from the cell.

Mohawk Innovative Technology®, Inc.
1037 Watervliet-Shaker Road, Albany, NY 12205
URL: www.miti.cc
Phone: (518) 862-4290, FAX: (518) 862-4291

Figure 69. The instrumented single-stage compressor showing the test cell, the compressor, motor drive unit and command console

Another addition to the test facility that was completed was a closed loop liquid cooling system for the motor drives. The cooling system consisted of a ¾ HP electric motor, solid particulate filter and liquid-to-air radiator. The system was capable of removing greater than 50 kW of heat load, if necessary. We anticipated a heat load of 10-20 kW for this application and, therefore, the cooling system was well sized for this application.

A thermal mass flow meter (Sage Metering Inc., Monterey CA) was recently received and has been installed (Figure 70). The flow meter, in conjunction with measurement of inlet and discharge gas pressure and temperature, allowed the compressor performance to be fully mapped and verified. The completed single stage compressor with helium flow-loop and 200 kW drive motors is shown in Figure 71.

Mohawk Innovative Technology®, Inc.
1037 Watervliet-Shaker Road, Albany, NY 12205
URL: www.miti.cc
Phone: (518) 862-4290, FAX: (518) 862-4291

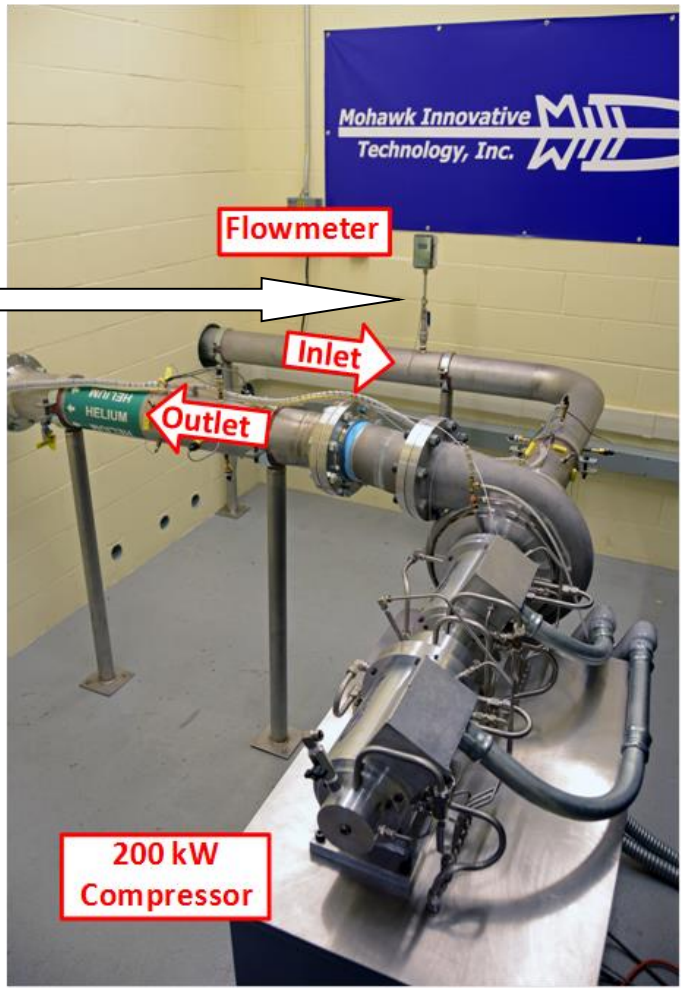

Figure 70. The recently installed thermal mass flow meter (above). Closed loop helium compressor test facility with the recently added flow meter (right)

Mohawk Innovative Technology®, Inc.
1037 Watervliet-Shaker Road, Albany, NY 12205
URL: www.miti.cc
Phone: (518) 862-4290, FAX: (518) 862-4291

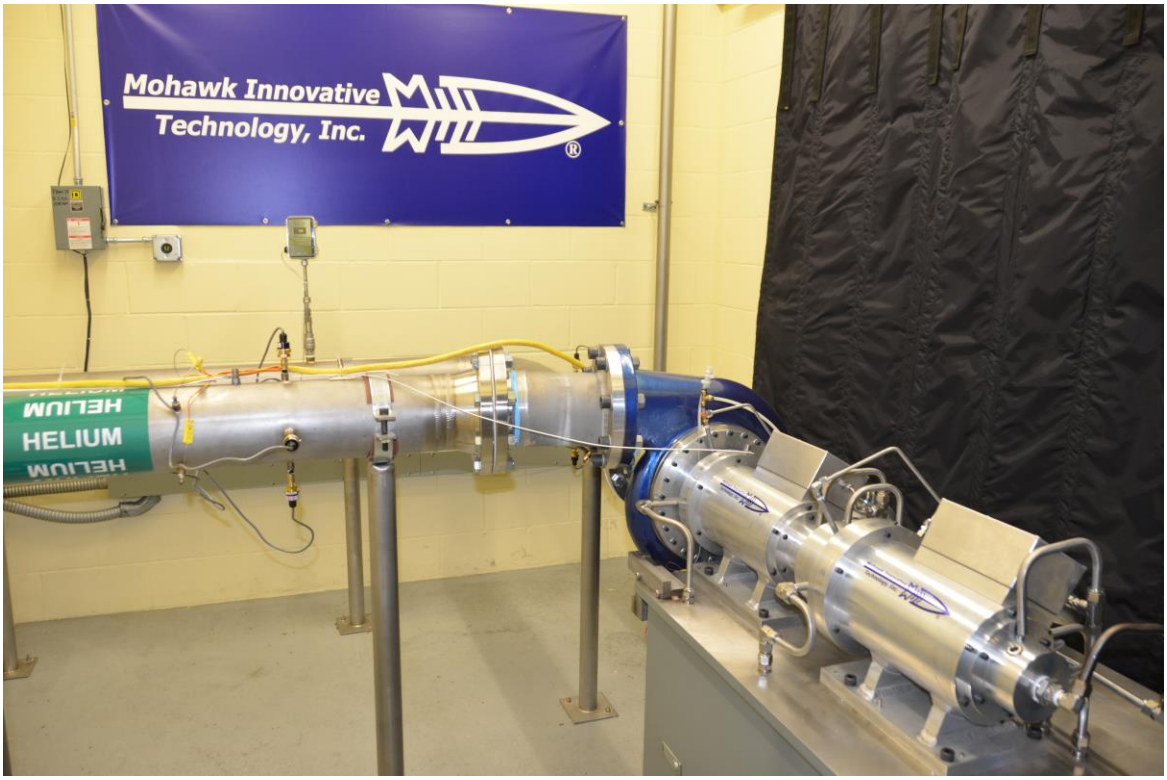

Figure 71. Single stage compressor with newly fitted stainless steel volute (blue in color) for higher ambient pressure testing

The first series of performance tests were conducted at rotational speeds of 20 krpm, 30 krpm and 40 krpm. Since the single-stage compressor was a closed-loop system, the helium gas was recycled and gas temperature continued to rise during operation until a steady state condition was reached. The temperature differential between compressor discharge and inlet (T_{out}-T_{in}) is plotted in Figure 72 for 40 krpm; the data (in blue) show that steady state behavior was achieved after approximately 500 seconds. At that point, the slope of the compressor differential temperature was less than 0.1 ^{o}F/min. The differential pressure ($P_{out} - P_{in}$) is also plotted in the same figure (in red). A fairly steady pressure differential, i.e., pressure rise of about 2.4 psi, was obtained under the tested condition.

Several testing cycles were conducted with conditions specifically selected to satisfy the ASME PTC-10 requirements of a Type 2 test to validate the aerodynamics of the compressor system. The full-scale H_2 compressor has a design speed of 56 krpm with a flow rate of 2770 CFM per compressor wheel. In Table 14, the non-dimensional performance estimates of the H_2 full-scale design point are listed. In order to match these estimates under a Type 2 test with a similitude gas, the single-stage compressor testing was conducted at 40 kprm and a helium flow rate of 2,000 CFM. The experimentally achieved performance parameters are summarized in the right-hand column of Table 14. It can be seen that the helium testing conducted had successfully satisfied all four non-dimensional requirements for similitude necessary for the ASME PTC-10 type 2 test.

Mohawk Innovative Technology®, Inc.
1037 Watervliet-Shaker Road, Albany, NY 12205
URL: www.miti.cc
Phone: (518) 862-4290, FAX: (518) 862-4291

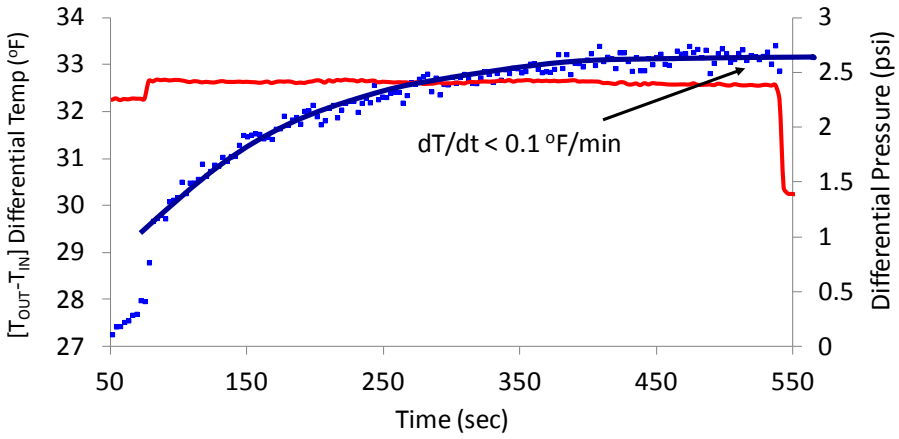

Figure 72. Single-stage compressor pressure and temperature data in helium at 40 krpm for 8 mins to achieve steady state conditions

Table 14. Summary of operating conditions to meet ASME PTC-10 type 2 test

Quantity	H_2 Design Point	ASME Acceptable Test Variation	Experimental Results
Specific Volume Ratio	1.072	1.018 – 1.126	1.095
Flow Coefficient	0.1253	0.120 - 0.130	0.126
Machine Mach No.	0.3266	0.141 - 0.532	0.322
Machine Reynolds No.	6.6e5	6.6e4 – 6.6e6	8.0e4

In addition to aerodynamic performance verification at a single operating point, the compressor was operated at a variety of speeds. At each fixed speed operating point, the control valve position was slowly adjusted between 100% open, down to 20% open to obtain a complete compressor performance map. These data are presented in Figure 73 - Figure 76, where critical aerodynamic performance data of the single-stage compressor are shown at three operating speeds. On each plot, the design point of similitude for ASME PTC-10 is shown with a star. Theoretical performance predictions obtained from CENCOM commercial software are shown as solid lines. Experimentally measured data are presented as data points. Close agreements with theoretical calculation were observed, providing confidence in the proposed H_2 compressor performance estimates on the multi-stage design concept. The experimentally measured head and efficiency were higher than theoretical predictions. In order to verify that higher than predicted compressor discharge head was not a result of the air impurities within the flow loop, careful measurement of oxygen within the system was monitored before testing. The concentration of oxygen, as measured from the bottom of the 1,000 gallon recirculation tank, was kept between 0.5 - 0.9% O_2 by volume. Since the concentration of air at the bottom of the recirculation tank was highest at this location, the purity of helium within the

Mohawk Innovative Technology®, Inc.
1037 Watervliet-Shaker Road, Albany, NY 12205
URL: www.miti.cc
Phone: (518) 862-4290, FAX: (518) 862-4291

entire closed-loop system was conservatively estimated to be between better than 99%. The predicted compressor head curves generated from the CENCOM computer software were then repeated with 1% air impurities. The predicted increase in compressor discharge head from this small impurity was not significant.

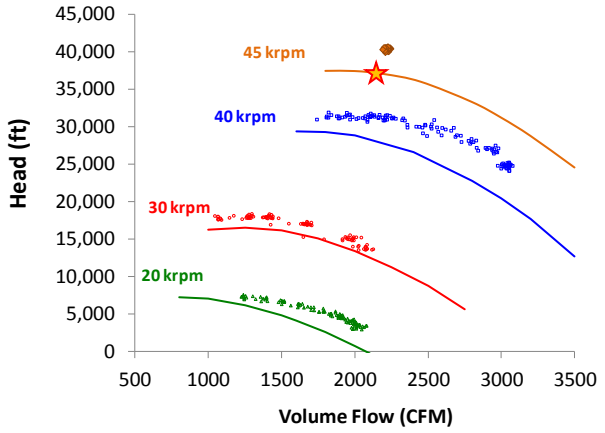

Figure 73. Comparison of theoretical and experimental compressor discharge head

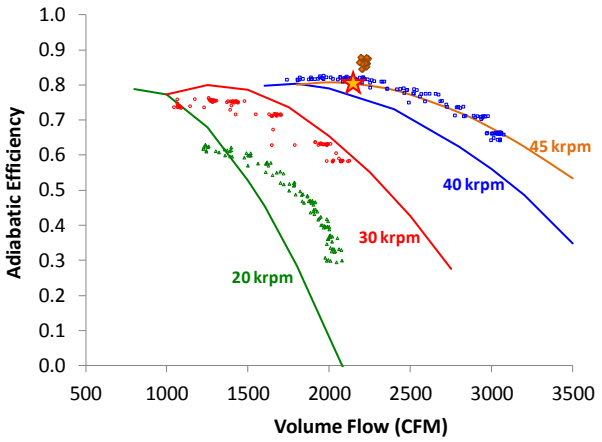

Figure 74. Comparison of theoretical and experimental adiabatic efficiency

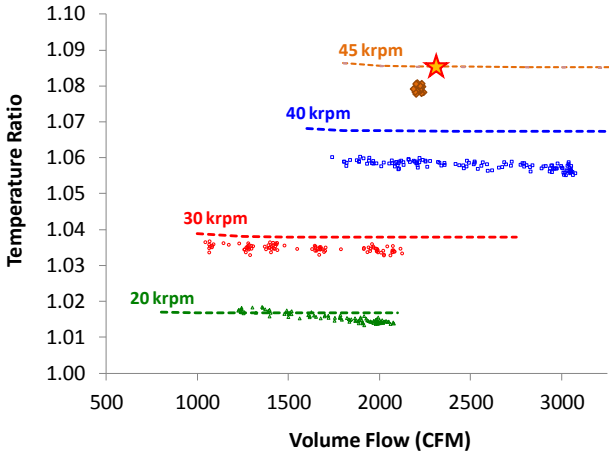

Figure 75. Comparison of theoretical and experimental compressor temperature ratio

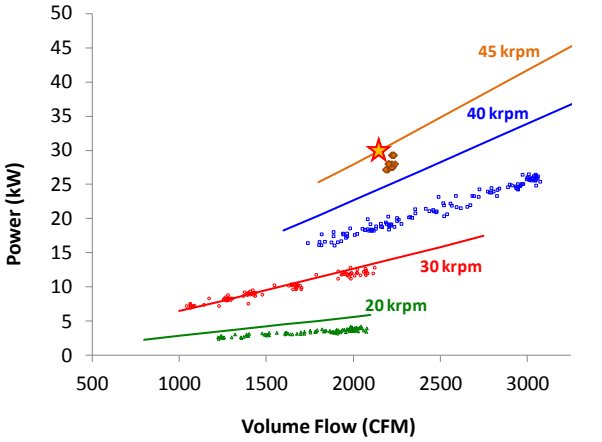

Figure 76. Comparison of theoretical and experimental compressor shaft power required for compressor. Total mechanical efficiency of 85% assumed

During steady state compressor testing, the thermal behavior of the 200 kW electric motors was also monitored. In the closed loop system, a small fraction of helium circulated through the compressor, passing behind the compressor wheel and traveling a torturous path through all eight foil bearings and along the entire rotating shaft. This helium "cooling" flow was returned to the system at the compressor inlet where pressure was lowest. The helium flow through the foil bearings was necessary to prevent stagnation and thermal run-away. The differential

Mohawk Innovative Technology®, Inc.
1037 Watervliet-Shaker Road, Albany, NY 12205
URL: www.miti.cc
Phone: (518) 862-4290, FAX: (518) 862-4291

temperature of foil bearings, relative to the compressor discharge that feeds directly to the bearings, is shown in Figure 77. Differential temperature data is presented for the first thrust bearing and second journal bearing, as positioned relative to the compressor wheel. These two bearings showed the highest operating temperatures of any foil bearings in the motor system and were, therefore, selected for discussion and analysis. Due to heat produced while accelerating the motor, the bearings reached a maximum differential temperature of 5 - 15°F greater than the compressor discharge immediately following a change in speed. After several minutes of operation at constant speed, the foil bearing temperatures converged towards the compressor discharge temperature, indicated by zero differential temperature. These results confirmed that the heat generated by the foil bearings under steady state condition was very low.

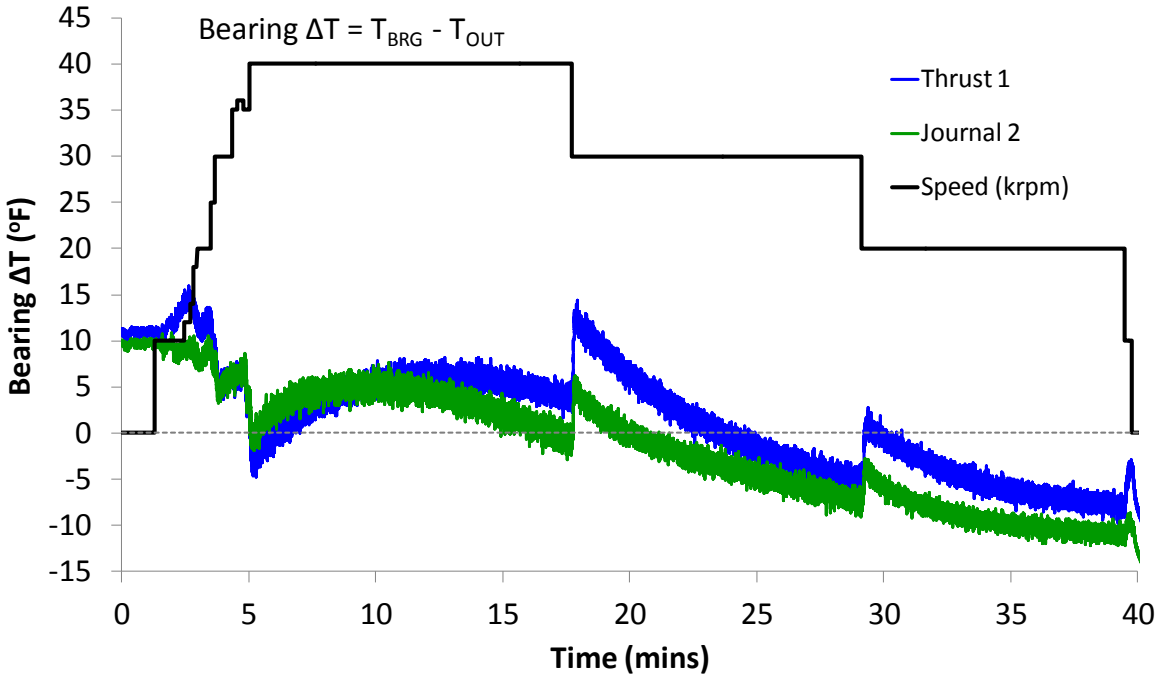

Figure 77. Differential temperature of foil bearing minus compressor discharge temperature. Shown above are the first thrust bearing and second journal bearing closest to the compressor wheel

13.0 System Refinement and Economic Analysis

The successful experimental testing of the single stage compressor per ASME PTC-10 provided validation of MiTi's multi-stage centrifugal compressor for hydrogen pipeline distribution. The results of experimental testing showed actual compressor performance to be slightly better than theoretical predictions. Based upon the analytical and experimental results obtained through the course of this investigation, the entire multi-stage system configuration has been refined and a solid model is shown in Figure 78.

Mohawk Innovative Technology®, Inc.
1037 Watervliet-Shaker Road, Albany, NY 12205
URL: www.miti.cc
Phone: (518) 862-4290, FAX: (518) 862-4291

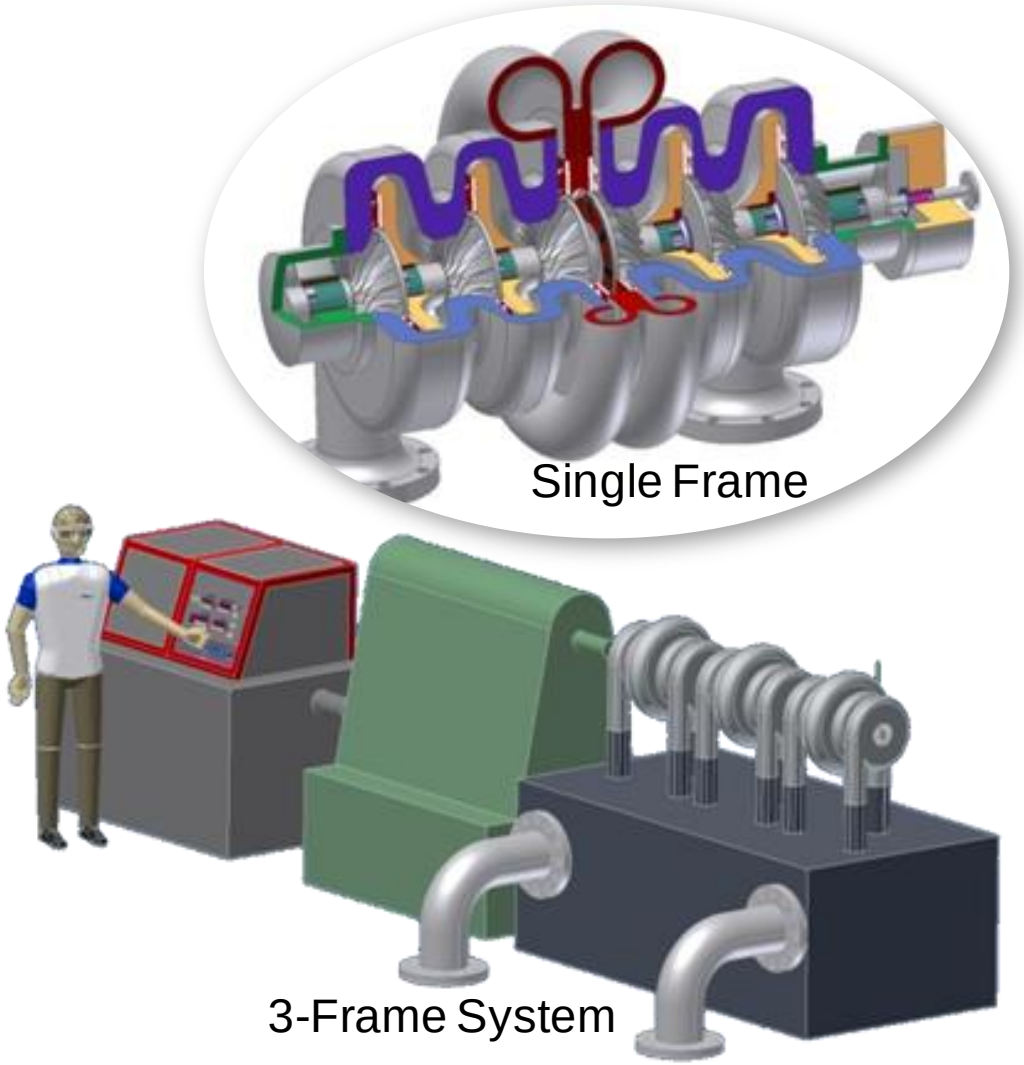

Figure 78. Refined 3D concept of the multi-stage oil-free centrifugal compressor for hydrogen pipeline

While experimental results indicated that output head, efficiency and power were all better than theoretical predictions, MiTi still concluded that a modular 9-stage concept would be the optimum solution. The use of 3 frames, each containing 3 stages, allowed for reduced cost of production and fabrication. Furthermore, should the complete multistage system provide more than the required 1200 psi discharge pressure, the distance between adjacent compressor stations could to be increased and few stations would be required. Given the excellent correlation between theoretical performance and experimental testing, no significant system refinement is needed.

Mohawk Innovative Technology®, Inc.
1037 Watervliet-Shaker Road, Albany, NY 12205
URL: www.miti.cc
Phone: (518) 862-4290, FAX: (518) 862-4291

13.1 Waste-Heat Recovery

As mentioned above, the proposed multi-stage centrifugal compressor system meets the 2012 DOE MYRDD targets. However, in recognition of the continual effort by the DOE to increase energy efficiency standards in this field, MiTi proposes the integration of a novel waste-heat recovery system to further reduce the cost of compression to meet future delivery targets above and beyond the current goals. The hydrogen pipeline compressor station produces large amounts of waste heat that is an optimum opportunity for energy recovery. Inter-cooling strategies have already been discussed previously in Section 7.0. The waste heat of compression and waste heat from the drive system, either electric motor or gas turbine drive, could be recovered to produce useful electricity to off-set the power requirements of the hydrogen pipeline compressor station. Use of water jacketed compressor stages would allow for near isothermal compression and improved system efficiency. The waste-heat would be converted to electric power through implementation of an organic rankine cycle, as depicted in the schematic shown in Figure 79.

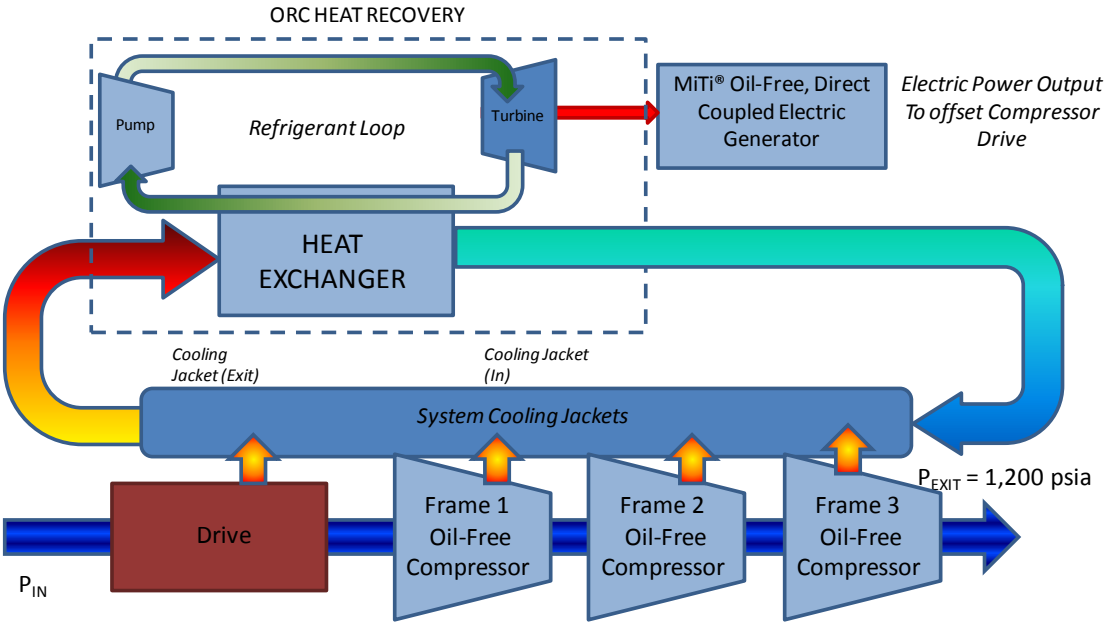

Figure 79. Proposed waste-heat recovery for increased system efficiency and reduced environmental impact

Under isothermal conditions, the power (P_{iso}) of compression can be determined from the following equation: $P_{iso} = RT/M\ ln(P_2/P_1) * \dot{m}$, where R is the universal gas constant, T is the gas temperature and M is the molecular weight of the working fluid. In this example, the isothermal work of compression would be 9,875 HP to achieve a 2.4 pressure ratio with a flow of 500,000 kg/day. By comparison, the compressor configuration with inter-stage cooling requires approximately 12,000 HP for the same pressure and flow condition. This cursory example demonstrates a potential for a reduction of 17% compressor power. Further energy is saved when we consider the output of the turbine generator or the organic rankine cycle used in the heat recovery operation. MiTi is intimately familiar with the design and development of such cycles for similar waste heat recovery and has demonstrated processes that can achieve thermal

Mohawk Innovative Technology®, Inc.
1037 Watervliet-Shaker Road, Albany, NY 12205
URL: www.miti.cc
Phone: (518) 862-4290, FAX: (518) 862-4291

efficiencies of up to 10%. The output power from the organic rankine cycle is an added energy savings on top of the performance gained from isothermal compression.

13.2 Cost Analysis

A preliminary cost analysis has been performed for the proposed multi-stage hydrogen compressor design. This analysis does not include the use of organic rankine cycle for heat recovery. In conducting this cost analysis, several key component quotes from machine shops and subsystem suppliers were obtained and data from trade journals were reviewed. These quotes and industry data were then rolled up into composite system cost estimates presented in Table 15 and Table 16.

Table 15. Costing of the compressor system for various materials of construction

	High-Strength Steel	Titanium Alloy
Compressor only	$4,101,440	$4,204,970
Compressor and Drive	$7,301,440	7,404,970

A breakdown of the costs by component is provided in Figure 80 for high-strength steel and in Figure 81 for titanium. After completing a detailed design of the multi-stage hydrogen compressor, a final review of the MiTi accomplishments relative to both DOE target was performed. Based on MiTi's economic cost projects, this program has shown that the proposed technology is capable of meeting the DOE's 2012 MYRDD performance and cost metrics. For reference, performance and cost analysis of a natural gas pipeline compressor are provided.

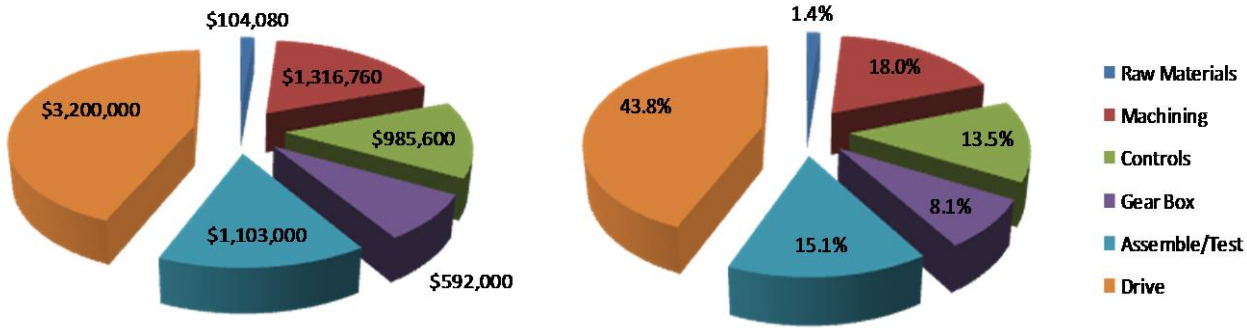

Figure 80. Cost breakdown of the high-strength steel compressor and drive. Costs shown in dollars (left) and as a percentage of the total system price (right)

Mohawk Innovative Technology®, Inc.
1037 Watervliet-Shaker Road, Albany, NY 12205
URL: www.miti.cc
Phone: (518) 862-4290, FAX: (518) 862-4291

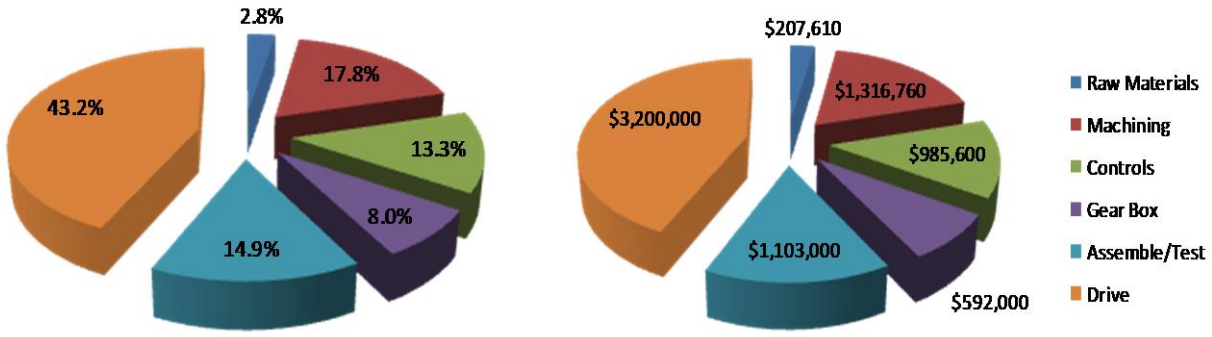

Figure 81. Cost breakdown of the high-strength steel compressor and drive. Costs shown in dollars (left) and as a percentage of the total system price (right)

Table 16. DOE 2012 MYRDD design targets.

Characteristics	Natural Gas Pipelines	DOE Target	MiTi Projection
Efficiency (%)		98%	98%
Hydrogen Capacity (kg/day)		100,000 to 1,000,000	500,000
Hydrogen Leakage		<0.5	0.2
Hydrogen Purity		99.99	99.99
Inlet Pressure (psig)	300-700	300-700	500
Discharge Pressure (psig)	1,000-1,200	1,000-1,200	1,226
Compressor Component Cost ($Million)	$9.2[1]	$9.0	$6.1
Compressor Drive $400/HP ($Million)	$6.4		$6.4
Total Compressor Package (2005 $Million)	$15.6		$12.5
Maintenance Cost (% total Capital Investment)	9.3%[2]	10%...7%..3%	<3%
Maintenance Cost ($/kW-hr)	$0.0157 [3]	$0.007	<$0.005
Package Size (sq-ft)	~1,000	300-350	160
Reliability (# Systems Required)		High - Eliminate Redundant Systems	Very High – Oil-Free Modular System

1 Oil & Gas Journal, Vol. 107.Issue_34,2010, Transportation. Special Report: Pipeline Profits Capacity Expansion Plans Grow Despite Increased Costs

2 DOT/PRCI Pipeline R&D Forum December 11-12, 2003, Washington, DC; 3 Oil & Gas Pipeline Sept 14, 2009, pp77-79

Mohawk Innovative Technology®, Inc.
1037 Watervliet-Shaker Road, Albany, NY 12205
URL: www.miti.cc
Phone: (518) 862-4290, FAX: (518) 862-4291

14.0 Summary

To meet the transmission and delivery compression needs of the DOE, a novel and advanced high-speed, oil-free centrifugal compressor system technology has been designed and experimentally validated. MiTi has shown that with three multi-stage centrifugal compressor frames, operating in series at speeds of 56,000, the DOEs pipeline hydrogen delivery needs can be met. The MiTi system has a flow capacity of 500,000 kg/day of compresses hydrogen with a discharge pressure of 1200 psig. The high operating speeds provide blade tip speeds on the order of 1600 ft/sec (seen in advanced gas turbine engine components) and bearing DNs greater than 3 Million (where D is diameter in mm and N is speed in rpm) to achieve peak efficiency with high power density. This advanced compressor design, enabled through the application of MiTi's compliant foil bearing technology, exceeds the capabilities of state-of-art oil-lubricated bearings by a factor of 2 or more. A double entry, multi-frame design was chosen to minimize thrust loads, machine complexity and power loss. This multi-frame system concept also offers a high degree of modularity to account for differing inlet conditions and requirements. For example, if inlet pressure conditions are lower than our reference inlet condition of 500 psig, then it would be possible to use more frames and or more stages per frame, as needed, to achieve the desired output conditions. This concept also incorporates a novel waste-heat recovery system for improved efficiency to meet the latest DOE efficiency goals. This design meets the DOE's performance targets and achieves an extremely aggressive, specific power metric of 0.48 kW-hr/kg and provides significant improvements in reliability/durability, energy efficiency, sealing and freedom from contamination. The multi-stage compressor system has been validated through full scale performance testing of a single stage with helium similitude gas at full speed in accordance with ASME PTC-10. The experimental results indicated that aerodynamic performance, with respect to compressor discharge pressure, flow, power and efficiency exceeded theoretical prediction. Dynamic testing of a simulator multi-stage compressor was also completed under a parallel program to validate the integrity and viability of the system concept. The results give strong confidence in the feasibility of the multi-stage design for use in hydrogen gas transportation and delivery from production locations to point of use. Finally, a novel waste-heat recovery system has been presented for integration into the proposed multi-stage compressor system. This stat-of-the-art system also features MiTi's high-efficiency turbomachinery and oil-free technology. While the proposed compressor system meets 2012 MYRDD standards without waste heat recovery, MiTi recognizes ever increasing efficiency metrics will make such an approach highly desirable in the near future.

Mohawk Innovative Technology®, Inc.
1037 Watervliet-Shaker Road, Albany, NY 12205
URL: www.miti.cc
Phone: (518) 862-4290, FAX: (518) 862-4291

15.0 Recommendations for Follow on Program

The results from single-stage compressor tests have validated the aerodynamic performance of the proposed hydrogen compressor through similitude testing in helium gas. In parallel, laboratory scale testing and literature surveys have provided data for selection of the most appropriate materials, coatings and manufacturing techniques to provide high confidence that the proposed compressor will be compatible in a hydrogen environment. Therefore, the next step in the development of this compressor concept is to conduct realistic testing in a hydrogen environment. In a program currently in progress through DoD funding, MiTi has developed and tested a smaller scale, multi-stage compressor in a hydrogen environment. This compressor also operated with a compressor tip speed of nearly 1,600 ft/s and combines two stages of compressor on a single shaft. These results will provide valuable data and confidence that can be leveraged by the pipeline compressor program. Based upon the results presented above which show feasibility of a centrifugal multi-stage compressor for pipeline delivery of gaseous hydrogen, Mohawk Innovative Technology recommends the following efforts to continue the development towards a full scale system. The recommended follow-on program includes the three primary objectives 1) testing of the single stage compressor in hydrogen, 2) finalization and detailed design of the multi-stage compressor design to prepare for manufacturing, 3) design of a sub-scale multistage compressor for validation testing and 4) materials testing to address and further understanding of hydrogen embrittlement mechanism as it pertains to centrifugal hydrogen compressors.

The single-stage compressor, with close-loop flow plumbing, instrumentation and dedicated test enclosure has already been validated in helium. In order to test the single-stage compressor in hydrogen, several hardware modifications will be needed. The rotating components (impeller and shaft) are currently constructed of Ti-64. New components will be fabricated from a beta titanium allow and coated with both TiN and CrN for additional safety measure. Other static components, such as o-rings, and instrumentation not capatible with hydrogen will also be upgraded for testing. Compressor testing will be performed under various operating conditions to validate the performance and reliability of the single-stage compressor. The compressor will be instrumented to measure flow, pressure and temperature in various locations. Accelerometers located in various positions will be used to monitor dynamic stability of different regions of the test rig. All components will be disassembled after many hours of operations and start/stops to evaluate the condition of each component.

In parallel with the single-stage hydrogen testing, the detailed design of the multi-stage compressor will be completed. A multi-stage hydrogen compressor frame will be comprised of three identical impeller wheels. While the aerodynamic design is complete, a number of other components such as seals, couplings, housing components and drive systems are needed. Under this task, these details will be resolved and detailed manufacturing drawings will be created. Expected budget limitations make manufacturing of a full scale multi-stage compressor, with drive system, unlikely. However, to address the restrictions of the budget, a sub-scale compressor system can be manufactured for testing. By scaling the multi-stage compressor with regard to mass flow, but maintaining pressure ratio requirements, both cost and power can be reduced. The already tested 200kW drive system which operates at 60,000 rpm can be used to drive a reduce-scale multistage compressor with flow rates on the order of 100,000 kg/day

Mohawk Innovative Technology®, Inc. URL: www.miti.cc
1037 Watervliet-Shaker Road, Albany, NY 12205 Phone: (518) 862-4290, FAX: (518) 862-4291

hydrogen. This subscale compressor will reduce material cost, manufacturing effort and reduced program risk; while at the same time providing dynamic performance in the presence of multi-stage complexities such as inter-stage seals, thermal management and control of assembly tolerances.

One of the key risks which have been identified by MiTi through the course of this research program is the limited understanding of the embrittlement mechanism as it pertains to high-stress rotating equipment. While MiTi has selected beta-titanium allot for the rotating equipment, the basic mechanical properties of these alloys (Ti 10-2-3 and Ti 15-3) when exposed to hydrogen at not well established. The focus of this final task will be to measure baseline mechanical properties for hydrogen-exposed Ti-10-2-3 and Ti-15-3. Product forms of Ti-10-2-3 and Ti-15-3 will be selected to enable the design and fabrication of conventional tensile and fracture mechanics specimens. The mechanical property measurements will emphasize tensile deformation and fracture, as well as fatigue crack growth (FCG). Testing will be conducted through collaboration with both commercial and government sponsored materials laboratories. A combination of TiN and CrN has been tentatively selected for the rotating components. Both coatings are excellent hydrogen permeation barriers based on published literature. The latter also has excellent wear resistance. These coatings will be evaluated for their capability in stopping or slowing permeation of hydrogen into the titanium alloys. Samples coated on all sides will be placed in a high pressure hydrogen chamber at appropriate temperatures and pressures. Hydrogen concentration in the samples will be measured following this treatment. Samples will be also charged with hydrogen, followed by hydrogen concentration measurements. Tensile test sample will be prepared and coated prior to testing. The samples will be stressed either in hydrogen gas or in air, depending on the outcome of previous materials testing. Fatigue testing will be performed with coated thin foil samples.

At the conclusion of this program, the design of a full-scale, multi-stage hydrogen compressor for pipeline delivery will be complete. Validation testing in hydrogen will prove aerodynamics, durability, reliability and compatibility. The subscale multi-stage test rig will validate the necessary seals, thermal management strategies and assembly methods. And finally, materials testing will provide greater understanding of the hydrogen embrittlment mechanism. The above efforts will be extremely beneficial to the development of this technology as it transitions from research to commercialization.

Mohawk Innovative Technology®, Inc.
1037 Watervliet-Shaker Road, Albany, NY 12205
URL: www.miti.cc
Phone: (518) 862-4290, FAX: (518) 862-4291

16.0 References

[1] H. Heshmat, H. Ming Chen, "Principles of Bearing Design, in *Compressor Handbook*, McGraw-Hill Education, New York, NY, 2001.

[2] Japikse D., Baines N.C., "Introduction to Turbomachinery," Concepts ETI, Inc. Norwich, VT and Oxford University Press, Oxford, England, 1994.

[3] Japikse D., "Centrifugal Compressor Design and Performance," Concepts ETI, Inc. Wilder, VT, 1996.

[4] RP Gangloff, "Hydrogen Assisted Cracking of High Strength Alloys," in Comprehensive Structural Integrity, I. Milne, R.O. Ritchie and B. Karihaloo, Editors-in-Chief, J. Petit and P. Scott, Volume Editors, Vol. 6, Elsevier Science, New York, NY, pp. 31-101 (2003).

[5] Anonymous, "Safety Standards for Hydrogen and Hydrogen Systems," NSS 1740.16, NASA.

[6] RP Jewett, RJ Water, WT Chandler and RP Frohmberg, "Hydrogen Environment Embrittlement of Metals," NASA CR-2163, 1973.

[7] BP Sommerday, NR Moody, JE Costa and RP Gangloff, "Environment-Induced Cracking in Structural Titanium Alloys," Corrosion, (1998) Paper No. 267.

[8] BP Sommerday and C San Marchi, "Technical Reference on Hydrogen Compatibility of Materials," Sandia National Laboratory, 20011.

[9] C San Marchi, BP Sommerday, X Tang and GH Schirosky, "Effects of Alloy Composition and Strain Hardening on Tensile Fracture of Hydrogen Precharged Type 316 Stainless Steels," International Journal of Hydrogen Energy, 33(2008)889-904.

[10] RR Boyer, An Overview on the Use of Titanium Alloys in the Aerospace Industry," Materials Science and Engineering, A213(1996)103-114.

[11] RR Boyer and RD Briggs, "The Use of Beta Titanium Alloys in Aerospace Industry," Journal of Materials Engineering and Performance, 14(2005)681-685.

[12] E Tal-Gutelmacher and D Ervin, "The Hydrogen Embrittlement of Titanium Based Alloys," JOM, 57(2005)46-49.

[13] HJ Christ, A Senemmar, M. Decker and K Prubner, "Effect of Hydrogen on Mechanical Properties of Beta-Titanium Alloys," Sadhana, 28(2003)453-465.

[14] AM Alvarez, IM Robertson and HK Birnbaum, "Hydrogen Embrittlement of a Metastable Beta Titanium Alloy," Acta Materialia, 52(2004)4161-4175.

[15] International Titanium Association, "Specification Book," 4th Edition, 2005.

[16] BP Sommerday and RP Gangloff, "Effect of Strength on Environment-Assisted Cracking of Ti-8V-6Cr-4Mo-4Zr-3Al in Aqueous NaCl," Materials Science and Engineering A254(1998)166-178.

[17] JE Costa, JC Williams and AW Thompson, "The Effect of Hydrogen on Mechanical Properties of Ti-10V-2Fe-3Al," Metallurgical Transactions A, 18(1987)1421-1430.

[18] HG Nelson, "Hydrogen Environment Effects on Advanced Alloys and Composites in Aerospace Structures," Thermal Structures Conference, 13-15- Nov. 1990, pp.301-311, Charlottesville, VA.

[19] SC Lee, WY Ho, CC Huang, EI Meletis and Y Liu, "Hydrogen Embrittlement and Fracture Toughness of a Titanium Alloy with Surface Modification by Hard Coatings," J. Materials Eng. And Performance, 5(1996)64-70.

[20] YY Takamura, F. Koch, H Maier and H Bplt, "Hydrogen Permeation Barrier Performance Characterization of Vapor Deposited Amorphous Aluminum Oxide Films," Surface and Coatings Technology, 153(2002)114-118.

[21] T Nishikiori, T Nohira and Y Ito, "Electrochemical Evaluation of High Temperature Hydrogen Impermeability of TiN Films and it's Dependence on Film Thickness," Thin Solid Films, 408(2002)148-154.

[22] C H Henager, "Hydrogen Permeation Barrier Coatings," Materials for the Hydrogen Economy, R H Jones and G J Thomas, Eds., CRC Press, 2008, 181-190.

[23] G T Murray, "Prevention of Hydrogen Embrittlement by Surface Films," Hydrogen Embrittlement: Prevention and Control, ASTM STP 962, L Raymond, Ed. ASTM, Philadelphia, PA 1988, 304-317.

[24] DM Symons and AW Thompson, "The Effect of Hydrogen on the Fracture Toughness of Alloy X-750," Metallurgical and Materials Transactions, 28(19+97)817-823.

[25] G.A. Young and J. R. Scully, "Hydrogen Embrittlement of Solution Heat Treated and Aged Beta-Titanium Alloys," Corrosion, 50 (1994) 919-933.

[26] DF Teter, IM Robertson, and HK Birnbaum, "The Effects of Hydrogen on the Deformation and Fracture of Beta Titanium Alloys," Acta Materilia, 49(2001)4313-4323.

[27] D. H Buckley, Surface Effects in Adhesion, Friction, Wear and Lubrication, Elsevier, New York, 1981.

[28] D V Keller, "Adhesion, Friction, and Lubrication Research by Modern Surface Science Techniques," J Vacuum Sci. and Tech, 9(1972)133-142.

[29] R Erck, GF Fenske and O Eryilmaz, "Friction and Wear of Metals and Coatings Used in Hydrogen," Proceedings of 2008 International Hydrogen Conference, Effects of Hydrogen on Materials, B Somerday, P Sofranis and R Jones (eds), ASME International, Materials Park, OH, 2009.

[30] K Fukuda and J Sugimura, "Sliding Properties of Pure Metals in Hydrogen Environment," Proceedings of ASME/STLE IJTC 2008-71210.

[31] K Fukuda, M Hashimoto and J Sugimura, "Friction and Wear of Ferrous Materials in a Hydrogen Gas Environment," Tribology Online, 6(2011)142-147.

[32] K Fukuda and J Sugimura, "Influence of Trace Water in a Hydrogen Environment on the Tribological Properties of Pure Iron," International Tribology Conference, Hiroshima, Japan, Oct 30-Nov 3, 2011. Paper No. B3-01.

[33] T Morita, H Tanaka, Y Sawae and J Sugimura, "Effects of Water Concentration and Sliding Conditions on Friction and Wear of Some Alloys in Hydrogen," International Tribology Conference, Hiroshima, Japan, Oct 30-Nov 3, 2011. Paper No. G2-08.

[34] T Gradt and G Theiler, "Tribological Behavior of Solid Lubricants in Hydrogen Environment," Tribology Online, 6 (2011) 117-122.

[35] K Nakashima and C Morillo, "Wear Mechanisms on PTFE in Humidified Hydrogen Gas," Proceedings of ASME/STLE ITTC2011-61180.

[36] R Erk and GR Fenske, "Polymers and Coatings for Tribological Application in Hydrogen Environment," in press. 2012

[37] T Murakami, H Mano, K Kaneda, M Hata, S Sasaki and J Sugimura, "Friction and Wear Properties of Zirconium and Niobium in a Hydrogen Environment," Wear, 268(2010)721-729.

[38] K Nakashima, A Yamaguchi, Y Kurono, Y Sawae, T. Murakami and J Sugimura, "Effect of High Pressure Hydrogen Exposure on Wear of Polytetrafluoroethylene Sliding Against Stainless Steel," J Eng. Tribology, 224(2010)285-292.

[39] T Iwai, Y Sakano and Y Shokaku, "Friction and Wear Properties of Polyamide-imide Composites Under Hydrogen Atmosphere," Hydrogenius Tribology Sysmp[osium, Kyushu University, Feb 3, 2011.

[40] Y Sawae, E Myakoshi, S Doi, H Wanatabe, K Kurono and J Sugimura, "Friction and Wear of PTFE and PTFE Composites in 40 MPa Hydrogen Gas," International Tribology Conference, Hiroshima, Japan, Oct 30-Nov 3, 2011. Paper No. B3-09.

[41] Y Sakano, T Iwai amd Y Shokaku, "Friction and Wear Properties of PTFE Composites Against 6061-T6 Aluminum Ally under Hydrogen Environment," International Tribology Conference, Hiroshima, Japan, Oct 30-Nov 3, 2011. Paper No. B3-08

[42] C Donnet, J fontaine, A Grill, T Le Mogne, "The Role of Hydrogen on The Friction Mechanisms of Diamond-Like Carbon Films," Tribology Letters, 9(2000)137-142.

[43] A Erdemir and O L Eryilmaz, "On the Hydrogen and Deuterium Lubrication Mechanisms of Diamond Like Carbon Film," International Tribology Conference, Hiroshima, Japan, October 2011, ITC-B3-02.

[44] RP Jewett, RJ Water, WT Chandler and RP Frohmberg, "Hydrogen Environment Embrittlement of Metals," NASA CR-2163, 1973.

[45] HG Nelson, "Hydrogen Environment Effects on Advanced Alloys and Composites in Aerospace Structures," Thermal Structures Conference, 13-15- Nov. 1990, pp.301-311, Charlottesville, VA.

[46] SC Lee, WY Ho, CC Huang, EI Meletis and Y Liu, "Hydrogen Embrittlement and Fracture Toughness of a Titanium Alloy with Surface Modification by Hard Coatings," J. Materials Eng. And Performance, 5(1996)64-70.

Mohawk Innovative Technology®, Inc. URL: www.miti.cc
1037 Watervliet-Shaker Road, Albany, NY 12205 Phone: (518) 862-4290, FAX: (518) 862-4291

[47] YY Takamura, F. Koch, H Maier and H Bplt, "Hydrogen Permeation Barrier Performance Characterization of Vapor Deposited Amorphous Aluminum Oxide Films," Surface and Coatings Technology, 153(2002)114-118.

[48] T Nishikiori, T Nohira and Y Ito, "Electrochemical Evaluation of High Temperature Hydrogen Impermeability of TiN Films and its Dependence on Film Thickness," Thin Solid Films, 408(2002)148-154.

[49] C H Henager, "Hydrogen Permeation Barrier Coatings," Materials for the Hydrogen Economy, R H Jones and G J Thomas, Eds., CRC Press, 2008, 181-190.

[50] G T Murray, "Prevention of Hydrogen Embrittlement by Surface Films," Hydrogen Embrittlement: Prevention and Control, ASTM STP 962, L Raymond, Ed. ASTM, Philadelphia, PA 1988, 304-317.

[51] S. Jahanmir, H. Heshmat, and C. Heshmat, "Assessment of Tribological Coatings for Foil Bearing Applications," *Tribology Trans.,* 52 (2009) 231-242

[52] S. Jahanmir, H. Heshmat, and C. Heshmat, "Evaluation of DLC Coatings for High-Temperature Foil Bearings," *Journal of Tribology,* 131 (2009) 21-32.

[53] Heshmat, H. "Operation of Foil Bearings Beyond the Bending Critical Mode," ASME/STLE Joint Tribology Conference, Orlando, FL, October 10-13, 1999, (2000) Journal of Tribology, Volume 122 (1), pp. 192-198.

[54] Swanson, E.E., Heshmat, H. and Shin, J.S. "The Role of High Performance Foil Bearings in an Advanced, Oil-Free, Integral Permanent Magnet Motor Driven, High-Speed Turbo-Compressor Operating Above the First Bending Critical Speed," ASME Paper GT2002-30579, 2002 ASME Turbo Expo: Land, Sea and Air, June 2002, Amsterdam, The Netherlands, (2002) American Society of Mechanical Engineers, International Gas Turbine Institute, Turbo Expo (Publication) IGTI, Volume 1, pp. 1119-1125.

Mohawk Innovative Technology®, Inc. URL: www.miti.cc
1037 Watervliet-Shaker Road, Albany, NY 12205 Phone: (518) 862-4290, FAX: (518) 862-4291

17.0 Partial List of Visits

- In December, Dr. Said Jahanmir (MiTi Program Manager) and Ms. Melissa Heshmat (MiTi CFO) traveled to Hiroshima, Japan to meet with Mitsubishi staff to finalize the subcontract with MHI and plan the technical collaboration.

- Dr. Hooshang Heshmat (MiTi PI) traveled to Hiroshima, Japan to meet with Mitsubishi staff and discuss the technical collaboration plan.

- During this reporting period, Mr. Masayuki Kita of MHI visited Mohawk Innovative Technology, Inc, in Albany, NY to discuss the technical plans for the second and third year of the project

- NIST Boulder Hydrogen Compatibility Laboratory, August 2010

- Tech Team Review, Dec 9th 2010, Detroit, MI.

- Dr. Hooshang Heshmat (MiTi PI) Carbon-Neutral Energy Research Institute Kickoff Symposium, February, 1st, 2011, Kyushu University, Fukuoka, Japan

- Dr. Hooshang Heshmat (MiTi PI) as keynote speaker attended International Hydrogen Energy Development Forum 2011 – 2011 Hydrogenius Tribology Symposium, February 3rd, 2001, Kyushu University, Fukuoka, Japan

- Dr. Hooshang Heshmat (MiTi PI) Visitation and Program Review at MHI Facility, February 7, 2001, Hiroshima, Japan

- Dr. Sunita Satyapal, Program Manager, Fuel Cell Technologies and Dr. Antonio Ruiz, Team Lead, Safety, Codes &Standards visited MiTi in September for a brief tour of the facilities.

- Dr. Said Jahanmir attended a local workshop held at College of Nano Science in Albany, NY on fuel cell and hydrogen infrastructure in September.

- Dr. Said Jahanmir visited the DOE HQ and briefed the Program Managers of the status of the project and discussed the remaining testing plan (November 2012)
- Dr. Hooshang Heshmat (MiTi PI) attended each and every Tech Team Meetings as well as AMR Meetings held by DOE, every year throughout the Program period

18.0 Publications / Presentations

1. "Oil-Free Centrifugal Hydrogen Compression Technology Demonstration," DOE Hydrogen Program Annual Review and Peer Evaluation Meeting, June 2008, Arlington, VA.
2. "Oil-Free Centrifugal Hydrogen Compression Technology Demonstration," DOE Hydrogen Program Annual Review and Peer Evaluation Meeting, May 2009, Arlington, VA.
3. DOE Hydrogen Delivery Tech Team Meeting December 15th, 2009, Washington DC.
4. DOE Pipeline Materials Workshop, NIST, Boulder Co, August 2010.
5. Heshmat H., Hunsberger AZ., Ren Z., Jahanmir S., Walton JF., "On the Design of a Multi-Megawatt Oil-Free Centrifugal Compressor for Hydrogen Gas Transportation and Delivery – Operation Beyond Supercritical Speeds", November 12-18, 2010, Vancouver, British Columbia, Canada.
6. Heshmat H., *Invited Keynote*, "Tribological Requirements of High-Speed Oil-Free Rotating Machinery for Hydrogen Applications," 2011 Hydrogenous Tribology Symposium, February 3, 2011, Fukuoka, Japan.
7. Heshmat H., "Design of a Multi-Megawatt Oil-Free Centrifugal Compressor for Hydrogen Gas Transportation and Delivery," Fuel Cell and Hydrogen Energy Expo, February 15, 2011, National Harbor, Md.
8. Heshmat H., "Oil-Free Centrifugal Hydrogen Compression Technology Demonstration", Annual Merit Review, DOE Hydrogen and Fuel Cells Program Annual Merit Review and Peer Evaluation Meeting, May 9-13, 2011, Washington, D.C.
9. Delivery Tech Team Meeting, Energetics Offices, Columbia Md., January 5th, 2012.
10. Invited presentation, on Hydrogen Compressor, International Tribology Conference, Hiroshima, Japan, Decemberr 2011
11. ARPA-E Energy Innovation Summit: MiTi visited and presented at the ARPA-E Convention; February 27-29, 2012 in National Harbor, MD. The mock-up of a single-frame of the hydrogen compressor was demonstrated at this event, Figure 82.
12. World Hydrogen Energy Conference (WHEC): Toronto Ontario, Canada, June 3-7. MiTi attended the WHEC in Toronto Canada and exhibited the full-scale mock-up of the hydrogen compressor being developed under this program.
13. Walton, JF, "Design of a Multi-Megawatt Oil-Free Centrifugal Compressor for Hydrogen Gas Transportation and Delivery", presented at the World Hydrogen Energy Conference, Toronto, Canada, June 6, 2012.

Mohawk Innovative Technology®, Inc. URL: www.miti.cc
1037 Watervliet-Shaker Road, Albany, NY 12205 Phone: (518) 862-4290, FAX: (518) 862-4291

14. Heshmat, H, "Oil-Free Centrifugal Hydrogen Compression Technology Demonstration". Presented at the Hydrogen and Fuel Cells Program Annual Merit Review and Peer Evaluation Meeting, May 17, 2012, Arlington VA.
15. MiTi presents, "Operation of the single stage compressor". Multimedia video can be viewed at the following site: (http://www.youtube.com/watch?v=dPn0uLIdtS8).
16. H. Heshmat, A. Hunsberger, Z. Ren, S. Jahanmir, and J. F. Walton, "Oil-Free Foil-Bearings for Centrifugal Hydrogen Compressor," Tribology Online, January 2013.
17. Heshmat H., Walton JF., "Oil-Free Modular System Designs for Industrial Compressors and Renewable Energy Turbine Generator Systems," Clean Technology Conference and Expo, June 21, 2010, Anaheim, CA
18. Jahanmir S., "Hydrogen Compressor Material Selection Challenges," DOE Pipeline Materials Workshop, NIST, Boulder Co, August 17, 2010.
19. Heshmat H., Hunsberger AZ., Ren Z., Jahanmir S., Walton JF., "On the Design of a Multi-Megawatt Oil-Free Centrifugal Compressor for Hydrogen Gas Transportation and Delivery – Operation Beyond Supercritical Speeds", Proceedings of the ASME International Mechanical Engineering Congress and Expo, November 12-18, 2010, Vancouver, BC, Canada.
20. Heshmat H., Jahanmir S., "Oil-Free Centrifugal Compression Technology Demonstrations," Hydrogen Delivery Tech Team, December 9, 2010, Southfield, MI.
21. Heshmat H., *Invited Keynote*, "Tribological Requirements of High-Speed Oil-Free Rotating Machinery for Hydrogen Applications," 2011 Hydrogenous Tribology Symposium, February 3, 2011, Fukuoka, Japan.
22. Heshmat H., "Design of a Multi-Megawatt Oil-Free Centrifugal Compressor for Hydrogen Gas Transportation and Delivery," Fuel Cell and Hydrogen Energy Expo, February 15, 2011, National Harbor, Md.
23. Heshmat, H., "Centrifugal Hydrogen Compressor," DOE Merit Review, Crystal City, May 10, 2011
24. Heshmat, H., Hunsberger, A., Ren, Z., Jahanmir, S., and Walton, J., "Oil-Free Bearings and Seals for Centrifugal Hydrogen Compressor," International Tribology Conference, Hiroshima, Japan, December 5, 2011.

Mohawk Innovative Technology®, Inc.
1037 Watervliet-Shaker Road, Albany, NY 12205
URL: www.miti.cc
Phone: (518) 862-4290, FAX: (518) 862-4291

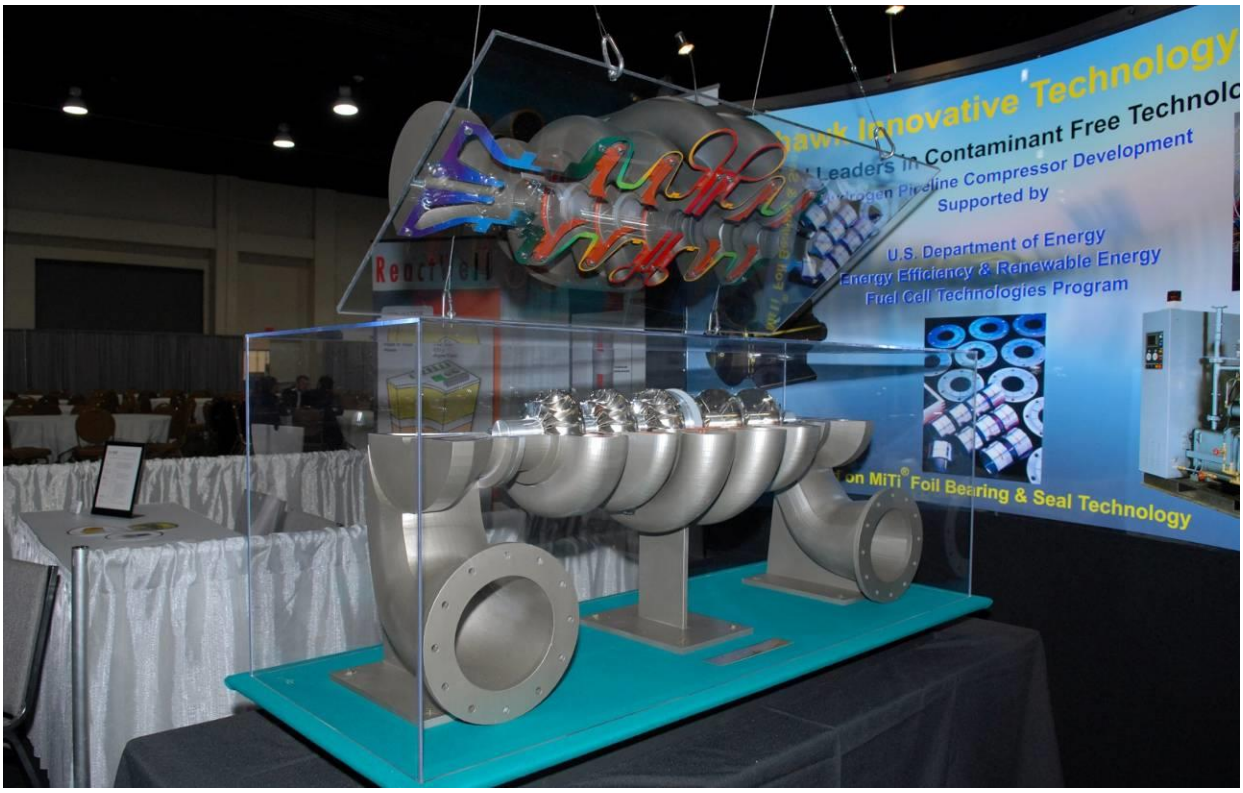

Figure 82. MiTi exhibit booth at the 2012 ARPA-E Energy Innovation Summit at the Gaylord National Convention Center in National Harbor, MD

Mohawk Innovative Technology®, Inc.
1037 Watervliet-Shaker Road, Albany, NY 12205
URL: www.miti.cc
Phone: (518) 862-4290, FAX: (518) 862-4291

19.0 Appendix

Mohawk Innovative Technology®, Inc.
1037 Watervliet-Shaker Road, Albany, NY 12205
URL: www.miti.cc
Phone: (518) 862-4290, FAX: (518) 862-4291

19.1 APPENDIX A: Subcontractor Report – PTC 10 Compliance

Redmond, WA:
(425) 883-2058
18378 Redmond Way
Redmond, WA 98052

Portland, ME:
(207) 874-2802
70 Center Street
Portland, ME 04101

July 24, 2012

Andrew Z. Hunsberger
Sr. Research Engineer.
Mohawk Innovative Technology Inc.
1037 Watervliet-Shker Road
Albany, NY 122905
Via Email- ahunsberger@miti.cc

Subject" Task 1 Evaluation for PTC -10 test

Dear Andrew

Attached is the Task 1 reports covering the evaluation of surge requirements, evaluation of the proposed test set up and preliminary uncertainty budgets for the instruments and instrument installation. This is an interesting project and I expect the later phases will continue to be interesting. I expect that once you have had a chance to review the attached document, you will have questions, fell free to contact me. I expect the Fischer valve quote will be available within the next few days.

Dennis W. Pednault
dennis.pednault @mchale.org
603-466-1111

CC: P.Brad Woods

Attachments: Task 1 report

Mohawk Innovative Technologies
Review of Test Instrumentation and Test Loop Hardware

Introduction

Mohawk Innovative Technologies has developed a high speed centrifugal compressor. They have requested assistance from McHale and Associates in developing and executing a PTC 10 - 1997 performance test to develop performance of the unit at a specific operating point. The compressor is ultimately intended to compress hydrogen gas. In order to test the unit, the client intends to test the unit with a closed loop system with helium gas using the provisions in the PTC 10 -1997 for a Type 2 test. The initial task requested by Mohawk was a review of the proposed test configuration

- Review the project requirements for anti-surge hardware. Perform calculations for surge volume required.
- Review the test loop components for capacity and sizing.
- Review the test instrumentation selection and accuracy based on ASME PTC-10 requirements.

Surge Control

After a review of the various industry recommendations for surge protection, the installation of a surge control bypass does not appear to be needed for the low pressure ratio single stage test. A traditional compressor station surge control strategy is primarily oriented to operating compressor stations that have the potential of being rapidly shut down for reasons out of their control. In that case, the compressor could be exposed to a rapid pressure spike well above the normal operating pressure of the system due to "hammer" in the line related to the mass flow of the gas being stopped rapidly. This propagates a pressure wave that is reflected off a rapidly closed downstream valve back to the compressor inlet, potentially causing a surge event. In that case an internal surge control system must be in place to deal with the rapid transient change in pressure while keeping the plant isolated from the gas pipeline.

The proposed test stand will be operated always as a closed loop; all of the input power will either be absorbed by the helium and then cooled or radiated out into the test cell. The control valve used to maintain the compressor inlet pressure operates as a "surge control valve" during normal operation. There is no need to have provisions for emergency shutdown surge control as there is no external way of shutting off the flow through the system. Although a surge recycle valve and line could be installed, its only reason for operation would be the failure of the system control valve or over speeding of the drive motor. The system control valve could be equipped with a spring assisted operator that would "fail" open. The control valve actuator would drive the valve closed against the spring. If there was a controller failure or loss of

Mohawk Innovative Technology®, Inc.
1037 Watervliet-Shaker Road, Albany, NY 12205
URL: www.miti.cc
Phone: (518) 862-4290, FAX: (518) 862-4291

instrument air, the valve would open 100% dropping the pressure differential to zero across the compressor causing it to increase the flow to the point where the overall system pressure drop would exceed the capability of the control valve

A surge tank volume is generally needed for a system that has a reciprocating driver where the system flow varies cyclically. The surge volume is intended to act as an accumulator to buffer out the cyclical pulses from the compressor. It also acts as an area of low gas velocity where condensable liquids may accumulate for removal. The final use is to add surface area to the system to radiate heat to the environment. As the Mohawk unit is a high speed radial design with a low pressure ratio, it is assumed that the pressure output is constant with minimal detectible pulsation. The working gas is commercial helium, it is not expected that vapor will build up unless the gas cooler is leaking. The only remaining use for surge volume would be to buffer out oscillations introduced into the system by the system control valve. As this is highly dependent on the valve and controller selected, there is no recommendation on tank sizing.

Test Loop Components and Sizing

The design of the test loop components is dependent upon the planned test. As the pressure ratio is low, the frictional pressure loss of the system components impact the range of operational testing. As the proposed test is for one single design point, the components can be optimized to allow testing for this value and the two test points that bracket the specified capacity within a range of 96 to 104 percent. Although there is some operating margin for a range of flows, testing a full range of flows from predicted surge to predicted choke is not achievable with one set of components at the low pressure ratio of the test. This limitation is not present during the high speed test as the control valve is in range for the full flow range from predicted surge to predicted choke.

Major components

The test rig as proposed consists of compressor, outlet check valve, nozzle type flow meter with diffusing cone, three gas coolers in parallel, storage tank, filter, and control valve. A flow straightener may additionally be included. Mohawk has supplied some information on the proposed system components as shown in Table 1. There was no information on the filter shown on the proposed test loop drawing, Figure 8 of the Mohawk package. As a means of reducing the overall friction loss, it may be advisable to operate the system with a filter for a period of time to capture any fine particulate and then remove the filter for the actual test. The Figure 8 drawing does not show a location for the proposed control valve. As the copy supplied is not drawn to scale and lacks dimensions, it is difficult to determine if the test code required minimum distances for the components are maintained.

Mohawk Innovative Technology®, Inc.
1037 Watervliet-Shaker Road, Albany, NY 12205
URL: www.miti.cc
Phone: (518) 862-4290, FAX: (518) 862-4291

Mohawk Innovative Technologies
Review of Test Instrumentation and Test Loop Hardware

Table 1 Equipment Pressure Loss at Design Flow

	Type	Quantity	Units	Pressure drop
Flow meter	Flow Systems	1	Inches H20	225
Check Valve	Milwaukee Valve	1	psi	<3
Gas Cooler	Thermal Transfer Products	3	psi	.91
Flow Straightener	Unknown	1	psi	?
Filter	Unknown	?	psi	?

Figure 1 shows a possible arrangement to minimize the foot print of the test. It is not intended to be a required layout, as long as the minimum distances are maintained or exceeded. Alternative layouts are possible as long the PTC 19.5 and PTC 10 required clearances are met or exceeded. If the test site has high ceilings, there may be additional options to use a vertical layout to minimize the equipment footprint. Should there be clearance issues, some of the distances could be reduced although that would increase the overall uncertainty.

If a similar layout to Figure 1 is used, the supply to the coolers should be routed to one end of the row of cooler inlets while the discharge is located at the opposite end to equalize the flow through the coolers. I have shown the control valve upstream of the coolers. The installation of a control valve immediately upstream of the flow meter would be considered in Table 7-1.2-1 in PTC 19.5 -2004 as an "Abrupt symmetrical reduction" with a ratio of excess of 0.5 which requires 30 pipe diameters upstream. Dependent on the opening of the valve selected, the ratio could be less than 0.5 which would reasonably require even longer distances or a flow equalizer upstream of a flow meter. The siting of the coolers downstream of the valve would redistribute any turbulence introduced by the control valve, acting as a means of redistributing the flow.

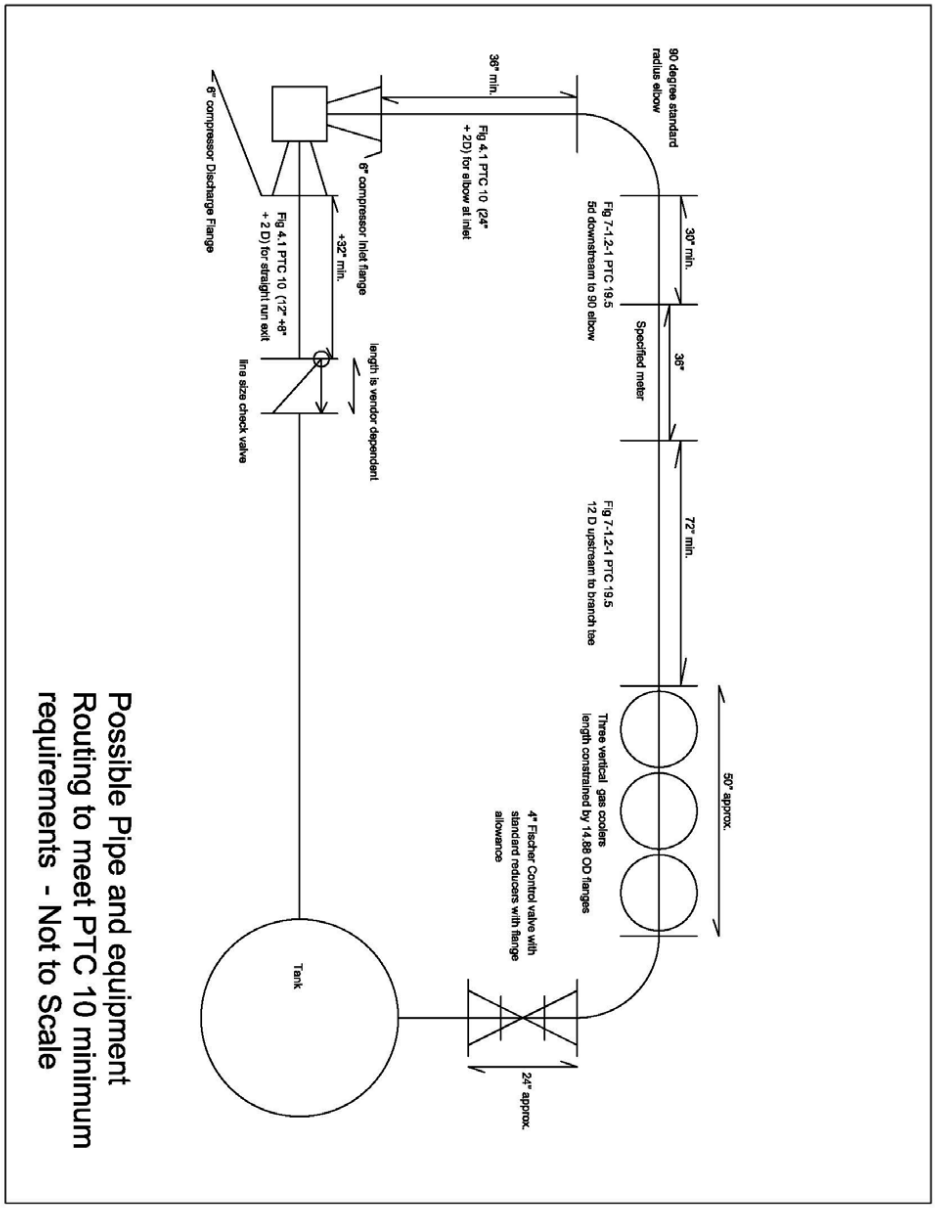

Figure 1

Mohawk Innovative Technology®, Inc.
1037 Watervliet-Shaker Road, Albany, NY 12205
URL: www.miti.cc
Phone: (518) 862-4290, FAX: (518) 862-4291

As shown in Figure 1, the coolers are vertical which most likely will require a double offset in the piping to account for the cooler inlet height. If floor space is available they could be laid out horizontally.

Note that the flow meter section distances would increase if the PTC 19.5 recommendations for a Primary Flow Section shown in Figure 5-0 of the code were used. The Primary Flow section has a total length of 30 pipe diameters which would require an addition straight run of pipe on either side of the flow meter. This pipe section yields the "highest accuracy and confidence" for a flow nozzle type flow meter. The flow meter selected by the MITI is expected to have adequate accuracy to meet the constraints of the test. If higher accuracy is desired, an additional 42" would be added to the length of the current flow section to accommodate an ASME primary flow section.

Control Valve

The control valve is characterized by the manufacturer with a C_v value which is a dimensionless factor that correlates the amount of valve opening to a specific pressure drop. The control valve would be controlled by a Mohawk supplied pressure controller equipped with appropriate PID control algorithms. In order to obtain a smooth response to changes in control inputs, the control valve should be specified as an equal percentage valve where an increase in valve opening will supply an equal increase in valve C_v.

Using data supplied by Mohawk shown in Table 1 (Figure 2 in Mohawk's March 2012, document), a series of values were obtained from the 39,233, 30,000 and 20,000 RPM curves from predicted surge to predicted choke.

Table 2 – Design Point Data

Design Variable	Units	Value
Test Gas		Helium
Speed	rpm	39,323
Inlet Pressure	psia	100
Outlet Pressure	psia	113.8
Pressure Ratio		1.138
Inlet Temperature	Deg F	100
Predicted Design Flow	lbm/min	128
Bracket Value for PTC 10 Test		
96% of design flow	lbm/min	122.88
104% of design flow	lbm/min	133.14

Mohawk Innovative Technology®, Inc.
1037 Watervliet-Shaker Road, Albany, NY 12205
URL: www.miti.cc
Phone: (518) 862-4290, FAX: (518) 862-4291

The friction loss of four pipe sizes, 4″, 6″ 8″ and 10″ were calculated at the design flow rate in order to determine the optimal sizing. Within the proposed flow range, 6″nominal pipe size appears appropriate for the design flows as there is a significant increase in frictional loss if 4″ pipe is used.

The frictional loss values at the equipment design flow in table 3 were added to come up with an estimated overall pressure drop. In order to determine an estimated pressure drop at other operating conditions, the flow at a specific operating point was divided by the design flow and squared to obtain a ratio of the pressure drop from the design point to the new flow rate. A control valve C_v value was calculated for each point on the three RPM curves. The results of the calculations are shown in Table 4. In order to verify that the valve would be appropriate for the high speed operational testing, a C_v at the predicted surge flow and choke flow at 60,000 rpm were also calculated and are shown in table 5.

Table 4 – Valve C_v for Operating at Design Point and other flows

39323 RPM						30000 RPM						20000RPM					
Flow	ACFH	SCFM	Valve Inlet pressure	Gas	Cv	Flow	ACFH	SCFM	Valve Inlet pressure	Gas	Cv	Flow	ACFH	SCFM	Valve Inlet pressure	Gas	Cv
lb/min			psia	pressure					psia	pressure					psia	pressure	
95	85,794	12,795	114	103.2	146	75.8	68,455	9,665	107.92	101.8	151	50	45,155	6,110	103.44	100.7	146
125	112,887	16,821	113.9	105.4	218	90.32	81,568	11,503	107.8	102.5	194	60.48	54,619	7,390	103.42	101.1	190
150	135,465	20,114	113.5	107.8	317	100	90,310	12,712	107.6	103.1	232	70.5	63,668	8,604	103.3	101.4	248
175	158,042	23,053	111.5	110.2	778	119.35	107,785	15,103	107.11	104.4	355	80.8	72,970	9,842	103.1	101.9	350
200	180,620	25,874	109.5	112.9	#NUM!	140.3	126,705	17,602	106.19	106.0	1445	90.32	81,568	10,959	102.7	102.3	697
220	198,682	27,931	107.46	115.0	#NUM!	159.6	144,134	19,761	104.8	107.5	#NUM!	100	90,310	12,098	102.4	102.8	#NUM!
230.6	208,254	28,879	106	116.1	#NUM!	176	158,945	21,459	103.2	108.9	#NUM!	124.19	112,156	14,863	101.3	104.3	#NUM!
						195	176,104	23,430	101.7	110.6	#NUM!	140.32	126,723	16,603	100.15	105.3	#NUM!

Table 5 – Valve C_v for 60,000 RPM test

Valve Cv for 60,000 RPM operation					
			Valve Inlet		
Flow	ACFH	SCFM	Pressure	Gas	Cv
			psia	pressure	
84	121176	10,621	67	50.7	129
144	207730	17,121	63	52.73	270

Mohawk Innovative Technology®, Inc.
1037 Watervliet-Shaker Road, Albany, NY 12205
URL: www.miti.cc
Phone: (518) 862-4290, FAX: (518) 862-4291

The valve C_v is subject to change as the system configuration changes. The following numeric values are based on the equipment selection and piping configuration as it is known today. As the design gets firmed up, the calculated values may change and could be recalculated although barring major alterations, they aren't expected to change substantially. For purposes of a single point test, a valve with a C_v capacity 146 to 317 within an operating range of 20% to 80% is adequate for the PTC 10 test. A C_v range of 129 to 270 would be adequate for the high speed rotation test to confirm flows from the predicted choke to the predicted surge points at the specified pressure input pressure The use of a larger valve with additional C_v capacity would increase the flow range at the 39323 RPM test speed approximately 25 lbs per minute from 150 to 175 lb/min.

The actual size of the valve over the minimum required to obtain the C_v is dependent upon the interest of the client in operating the compressor at flow points other than the design point and the response required of the valve. A large valve increases the range of flows, while a small valve allows more precise control at a given operating point and lowers up front cost.

In some cases at high flow rates, the friction loss in the piping and equipment exceeds the operating pressure of the fan leading to a "num" error in the spreadsheet. This indicates that unless the system friction loss is decreased by increasing the pipe line size or decreasing the friction loss though the equipment, the system will not operate at the specific flow and inlet pressure as the control valve is 100% open. With the control valve wide open, the system pressure loss will determine the highest flow rate for a given inlet pressure. This is not expected to be an issue during the high speed rotational test as the pressure ratio of the unit is higher and the control valve will be in its operational range.

Over Pressure Protection

The pipe yield strength of Schedule 40 carbon steel pipe is well in excess of the test pressure. A pressure relief device will be required for the storage tank and possibly other components if they are rated for less than the safety tank. There may be other local codes and standards that will add additional requirements.

System Control at Operating Point

The control of the system pressure in the area approaching the surge point at any speed is important; a control loop with fast response with no overshoot is required to maintain the flow through the system below the predicted surge flows. The control valve may require an oversized actuator and high accuracy positioner to minimize response time. A preliminary quote is being prepared by the local Emerson representative for the most cost effective control valve equipped for fast response with minimal overshoot potential.

Mohawk Innovative Technology®, Inc.
1037 Watervliet-Shaker Road, Albany, NY 12205
URL: www.miti.cc
Phone: (518) 862-4290, FAX: (518) 862-4291

The system flow pressure curve in the region between the operating point and the predicted surge line is nearly "flat" where a small pressure change yields a large change in flow. In this area of operation the friction loss in the equipment and piping serves an important purpose in that it imposes a change in pressure drop that varies with the square of the flow. Using a 6" diameter sch. 40 pipe, the change in system pressure from the expected surge point of 95 lb/min to the design point of 125 lb/min yields a predicted change in system pressure due to frictional losses of 2.3 psia with a corresponding C_v change from 146 to 218. Although a specific control valve has not been selected a 4" Fisher Cam Vee Valve, a modified ball type valve, would require just over 10 degrees of valve rotation to obtain the change in C_v from the predicted surge point to the design point. The 4" valve would limit the full speed flow rate to some point between 150 and 175 lb/min. A smaller 3" valve would be too restrictive to allow the system to operate at the design point

Proposed Instrumentation Configuration

The described location of the pressure and temperature transmitters on the discharge of the fan in the Mohawk description is reversed. The four pressure measurement ports are to be located upstream of the temperature measurement ports on both the inlet and outlet. The reference to Fig 4.1 in PTC 10-1997 is correct and shows the correct orientation. The vertical centerline of the pressure taps should be rotated 45 degrees from the centerline of the upstream 90 degree elbow to minimize pressure variations related to the upstream elbow. As shown in Figure 4.1 the temperature probes will be further rotated 45 degrees so that one set of temperature probes will be aligned with the elbow centerline. The pressure taps should be installed and drilled to the specification in 4.6.7. It is important to note that the hole size is less than 1/8 of an inch as the requirement of no larger than 4/10 of the wall size must be followed. The holes must be smooth so the pressure transmitter will need to be attached to a coupling with mating threads attached to the exterior of the pipe rather than direct threading the pipe wall.

Cooling water control

The sizing and response of the cooling water control system must be capable of meeting the 8% maximum permissible deviation called out in table 3.1. of PTC 10-1997. The configuration of the system is not specified by the code unless the system is used to establish shaft power by heat balance.

Pipe Insulation

As a manner of measuring power input has not been established, the matter of pipe insulation will need to be resolved. If the shaft power by electrical method is used there is no requirement for insulation as long as the temperatures recorded are uniform. If the Heat Balance method is used, the piping and casing will be insulated at a minimum between the two sets of temperature transmitters.

Mohawk Innovative Technology®, Inc.
1037 Watervliet-Shaker Road, Albany, NY 12205
URL: www.miti.cc
Phone: (518) 862-4290, FAX: (518) 862-4291

Instrument Selection and Uncertainty

The most current Performance test Code – PTC10-97 does not establish an overall required uncertainty result required to declare a successful test. The PTC 10-1997 approach is to establish permissible maximum deviation values for operating conditions in table 3.2. If the test is performed within these limits, the resultant test results are stated for a mean value plus or minus a calculated uncertainty. As the test is intended to establish a specific operating point on a plot of pressure versus flow, the reported result will be mass flow (lb/min) plus or minus a flow meter uncertainty at an indicated pressure. The initial uncertainty budget will be specific to the test speed only. Additional uncertainty will be introduced when the pressure and temperature measurements at the compressor inlet and outlet are used to calculate the flow for hydrogen instead of helium test gas at a given inlet pressure at the operating speed of 60,000 RPM.

The initial set up of the model and the uncertainty is based on the use of Real gas values obtained from the NIST REFPROP program. The uncertainty for using ideal gas equations has not been included in this analysis.

The pretest un-certainty budget utilizes an assumed value for the Standard Deviation of the Mean as no test data has been collected to analyze. In order to have a starting point for the pretest estimates, the permissible fluctuations from specified operating conditions in Table 3.4 were used to generate a random set of 30 data points for each measured value from which the standard deviation of the mean for each instrument was generated. Once testing data is available, these assumed values will be replaced with actual values and a new actual standard deviation of the mean will replace the assumed value. In most cases this is a conservative approach if the system can be operated at a stable flow.

The predicted pretest uncertainty budget with uncorrelated data is expected be in the range of ±0.83% while operating with helium gas at the test speed of 39,323 RPM. The tabulation of the uncertainty is shown in Table 6. The expected uncertainty budget with uncorrelated data for the flow rate utilizing hydrogen at the operating RPM of 60,000 RPM is plus or minus 0.98 %. The tabulation of this uncertainty is shown in Table 7.

Mohawk Innovative Technology®, Inc.
1037 Watervliet-Shaker Road, Albany, NY 12205
URL: www.miti.cc
Phone: (518) 862-4290, FAX: (518) 862-4291

Mohawk Innovative Technologies
Review of Test Instrumentation and Test Loop Hardware

Table 6 – Flow Meter Uncertainty

FLOWMETER UNCERTAINTY ANALYSIS															
	Measurement Uncertainty (95% Confidence Level)											Uncertainty of Test Results (@5% Confidence Level)			
	Test Value				Systematic			Random			Total				
TEST RUN 1 (Relative Basis)	Mean, $\bar{X}$	Description	Units	Quantity	B_{inst} Instrument Systematic Uncertainty	$B_{spatial}$ Spatial Systematic Uncertainty	$U_{95,SYS}$ Overall Systematic Uncertainty	$S_{\bar{X}}$ Standard Deviation of the Mean	$t_{95,\nu}$ Student's t	$U_{95,RAND}$ Random Uncertainty	$U_{95,TOT}$ Total Measurement Uncertainty	q Relative Sensitivity	$U_{PI,SYS}$ lbm/min Systematic Uncertainty of Corrected Output	$U_{PI,RAND}$ lbm/min Random Uncertainty of Corrected Output	U_{PI} lbm/min Total Uncertainty of Corrected Output
	0.966	Flow Coefficient - C	unit less	1	0.005	0.000	0.005	0.0000	2.000	0.000	0.005	1.00	0.0050000	0.0000000	0.0050000
	0.193	Throat Diameter -d *1	inches	1	0.000	0.000	0.000	0.0000	2.000	0.000	0.000	-	0.0000000	0.0000000	0.0000000
	0.305	Body Diameter -D *1	inches	1	0.000	0.000	0.000	0.0000	2.000	0.000	0.000	-	0.0000000	0.0000000	0.0000000
	0.066	Gas Density - pressure input	lbm/ft	1	0.0030	0.000	0.00299	0.0000	2.000	0.012	0.012	0.50	0.0014950	0.0060248	0.0062075
	0.066	Gas Density - temp Input*4	lbm/ft	1	0.00333	0.000	0.00333	0.0005	2.000	0.001	0.004	0.50	0.0001740	0.0004633	0.0018335
	0.066	Gas Density - REFPROP VALUES *3	lbm/ft	1	0.003	0.000	0.003	0.0000	2.000	0.000	0.003	0.50	0.0024994	0.0000000	0.0024994
	225.000	Differential Pressure	lbf/in2	1	0.003	0.000	0.003	0.0019	2.000	0.004	0.005	0.50	0.0014996	0.0019119	0.0024299
													Total Relative Uncertainty		0.0089
													Total Relative Uncertainty	%	0.89%
*1 - diameters are included in overall error for flow meters															
*2 - Instrument Uncertainty for density is established by perturbing the temperature values that are used by REPROP to calculate density.															
*3- REFPROP has a stated accuracy for density of .5% in the range of the test, this value is used as an "instrument sensitivity"															
*4 - special grade thermocouples 2.0% accuracy															

Table 7 - Compressor Uncertainty

COMPRESSOR UNCERTAINTY ANALYSIS															
	Measurement Uncertainty (95% Confidence Level)											Uncertainty of Test Results (@5% Confidence Level)			
	Test Value				Systematic			Random			Total				
TEST RUN 1 (Relative Basis)	Mean, $\bar{X}$	Description	Units	Quantity	B_{inst} Instrument Systematic Uncertainty	$B_{spatial}$ Spatial Systematic Uncertainty	$U_{95,SYS}$ Overall Systematic Uncertainty	$S_{\bar{X}}$ Standard Deviation of the Mean	$t_{95,\nu}$ Student's t	$U_{95,RAND}$ Random Uncertainty	$U_{95,TOT}$ Total Measurement Uncertainty	q Relative Sensitivity	$U_{PI,SYS}$ lbm/min Systematic Uncertainty of Corrected Output	$U_{PI,RAND}$ lbm/min Random Uncertainty of Corrected Output	U_{PI} lbm/min Total Uncertainty of Corrected Output
		Flow													
	128.000	Flowmeter accuracy	lb/min	1	0.00889	0.000	0.009	0.000000	2.000	0.000	0.009	1.000	0.0088908	0.0000000	0.0088908
	108.000	Inlet Pressure *1	lb/in2	4	0.00019	0.000	0.000	0.002481	2.000	0.005	0.005	0.997	0.0001869	0.0049462	0.0049497
	100.000	Outlet Pressure *1	deg F	4	0.00019	0.000	0.000	0.000597	2.000	0.001	0.001	0.997	0.0001869	0.0011909	0.0012055
	120.000	Inlet Temperature *2	deg F	4	0.00248	0.000	0.002	0.000491	2.000	0.001	0.003	0.178	0.0004408	0.0001749	0.0004742
	120.000	Outlet Temprature *2	deg F	4	0.00248	0.000	0.002	0.000491	2.000	0.001	0.003	0.178	0.0004408	0.0001749	0.0004742
													Relative Error		0.01027
													Relative Error	%	1.03%
*1 pressure transmiter accuracy .3% per Omega data sheet															
*2 thermocouples 3.96 % accuracy															

The most significant source of error is the flow meter with its associated flow coefficient. It accounts for more than 60% of the error for the test case and 88% of the error for the normal operating case. The only real option for improving this accuracy is to determine if the vendor could supply a special calibration more accurate than the quoted 0.5%. This may require calibration of the entire flow section including the upstream and downstream entrance and exit section. The expected accuracy of a calibrated flow section is about 0.2% using typical data from Alden Labs in Worcester, MA. ASME PTC 5-2004 has a recommended Primary Flow Section discussed in section 5-1 and illustrated in Fig 5-0. The longer flow section would require a longer straight line distance than shown on Fig 1 of this report. It is important to note the discussion in the opening section of Section 5 of PTC 19.5 that a flow section is best calibrated and left assembled or constructed in a way that provision for accurate realignment and reassembly must be built into the section. Alternatively a second flow meter operated in parallel to the primary unit could be utilized although this option would increase the overall length as

appropriate piping would be needed to split the flow and recombine it at the downstream end of the meters.

Another significant source of error is the measurement of the inlet pressure to the flow meter. It directly impacts the calculation of density and the large pretest standard deviation of the mean for assumed test value variation leads to a high total uncertainty. This value can be decreased by the installation of multiple pressure transmitters to reduce the pressure measurement uncertainty.

There is some opportunity to reduce the overall uncertainty budget at possibly a low cost by substituting differential pressure transmitters for the selected pressure transmitters on either side of the compressor.

Answers to Mohawk questions

1. *Do the proposed operating conditions for this helium test Table 3 satisfy the requirements of PTC-10 Type 2 test?* – Yes, based on the proposed values supplied by MITI, the proposed test falls within the permissible deviations.
2. *Is the use of an anti-surge loop necessary in this single stage compressor application?* - As discussed in the report, a surge loop is not required as the occurrence of a rapid increase in operating pressure can be avoided by appropriate selection of the control valve. Note that the operation of the valve controller is within Mohawk's scope, although controllers are available that can meet the requirements, the type of the controller and the response of the controller is not known by McHale. The controller selected will need to be tuned to prevent overshoot and provide rapid response by the selection of appropriate PID constants.
3. *Is the interpretation of PTC-10 correct regarding the placement of thermocouples, pressure transducers, elbow, valves, flow meters and straight sections, with respect to compressor inlet and discharge?* As discussed in the report, the control valve was not shown on Mohawk supplied piping drawings. Figure 1 is included for a possible layout.

4. *Are there ways to optimize the layout of the closed loop test rig pictured in Figure 7 and are the dimensions of the dedicated test cell appropriate to contain the flow loop?* - As discussed in the report, mounting the three coolers vertically and using them as a flow conditioner will reduce the dimensions somewhat.

5. *Is a 1,000 gallon capacity pressure vessel sufficient for this flow loop?* - Despite extensive effort, a method of calculation of storage volume was not determined for a centrifugal type compressor.

6. *Does the venture flow meter quoted by Flow Systems Inc. meet the needs of this test loop?* As discussed, the overall pretest uncertainty for the standard operating output is estimated at plus or minus 0.98%. If a lower level of uncertainty is required, the flow meter most likely would need to be replaced with a unit with higher accuracy, the flow element can be provided a calibrated flow section, or meters in series could be used.

7. *Will the after cooler specified by Thermal Transfer Products meet the needs of this test loop? -* The after cooler proposal calls out the need for three units in parallel. The overall heat generated by the system is below the capacity available with the three coolers. There is additional error introduced into the test by the use of three units and therefore that is a economic decision on MITI's part. It is important to note that if alternatives are investigated that the pressure loss through any proposed unit should not be increased.

8. *Does Fisher offer an appropriate throttle valve and control for the application? Can a more affordable option be found? -* A vendor proposal is forthcoming. It is unlikely that a low cost control valve is available given the accurate control required to stay below the surge point and the suggested spring loaded positioner. As discussed a four inch valve can be used with some restriction in the test operating range.

9. *What other instrumentation would be recommended for this loop? -* The type of speed measurement was not stated. The code requires a minimum of one independent method of speed measurement. If there is a desire to predict an operating horsepower at the specified point, a means of electrical input (kW) or shaft horsepower measurement is required.

10. *Are there other general oversights that have been made in the design of this test loop? -* Beyond the reported recommendations, the test loop and the decision to use a Type 2 test with an inert gas appears to be good approach to establishing the system performance.

This concludes the Task 1 review.

Mohawk Innovative Technology®, Inc.
1037 Watervliet-Shaker Road, Albany, NY 12205
URL: www.miti.cc
Phone: (518) 862-4290, FAX: (518) 862-4291

19.2 APPENDIX B: Subcontractor Report - CFD

Turbo Solutions ENGINEERING

Hydrogen Compressor CFD Analysis

Summary Presentation

Prepared for Mohawk Innovative Technology, Inc.
Albany, NY

By

Turbo Solutions Engineering LLC
Norwich, VT

Turbo Solutions Proposal P0226
Turbo Solutions Contract Number 1147
Mohawk Innovative Technology, Inc. Purchase Order 1090672

01 March 2010

1

Turbo Solutions ENGINEERING

Overview

- Program Scope
- Design Point Performance Prediction
- Computational Fluid Dynamics Results
  - Analysis Package
  - Geometry and Mesh
  - Mass-Averaged Performance Maps
  - Mass-Averaged Design Point Performance
  - Flowfield Plots
- Summary

2

Mohawk Innovative Technology®, Inc.
1037 Watervliet-Shaker Road, Albany, NY 12205
URL: www.miti.cc
Phone: (518) 862-4290, FAX: (518) 862-4291

Turbo Solutions ENGINEERING

Design Point Performance Prediction

- Gas = H2
- Inlet total pressure = 500.0 psia
- Inlet total temperature = 212.0 °F
- Inlet mass flow = 382 lbm/min
- Inlet volume flow = 2773 cfm
- Rotational speed = 56,414 rpm
- Discharge total pressure = 558.8 psia
- Pressure ratio (tt) = 1.118
- Polytropic head (tt) = 59,327 ft lbf/lbm
- Φ = 0.125
- Ψ = 0.913
- μp (tt) = 0.746
- ηp (tt) = 0.817
- Power = 840.9 hp

3

Turbo Solutions ENGINEERING

Computational Fluid Dynamics Analysis
Analysis Package

- ANSYS-CFX V11.1
  - ANSYS-BladeModeler
    - Import geometry from CompAero suite of tools
    - Create ANSYS-TurboGrid geometry input file
  - ANSYS-TurboGrid
    - Import geometry from ANSYS-BladeModeler
    - Create structured mesh of impeller, diffuser, and return channel
  - ANSYS-Pre
    - Import mesh from ANSYS-TurboGrid
    - Apply periodics, interfaces, and boundary conditions
    - Create ANSYS-Solver input file
  - ANSYS-Solver
    - Navier-Stokes flow solver
  - ANSYS-Post
    - Post-process results from ANSYS-Solver
    - Mass- and area-average fluid quantities
    - Three-dimensional flowfield plots

4

Mohawk Innovative Technology®, Inc.
1037 Watervliet-Shaker Road, Albany, NY 12205
URL: www.miti.cc
Phone: (518) 862-4290, FAX: (518) 862-4291

Turbo Solutions ENGINEERING

Computational Fluid Dynamics Analysis
Convergence

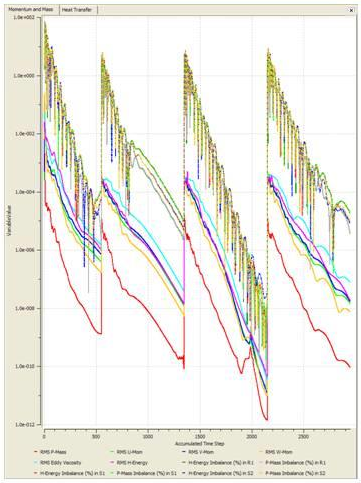

- Initial CFD analyses would not converge due to large areas of flow recirculation in the impeller, vane diffuser, and return channel
- Well converged CFD solutions were obtained by using a fixed inlet mass flow, fixed inlet total temperature, fixed exit static pressure boundary condition
- CFD results in following sections had inlet total pressures varying from 504 to 523 psia
- All mass-averaged quantities were properly referenced to an inlet total pressure of 500 psia

5

Turbo Solutions ENGINEERING

Computational Fluid Dynamics Analysis
Geometry

Front View

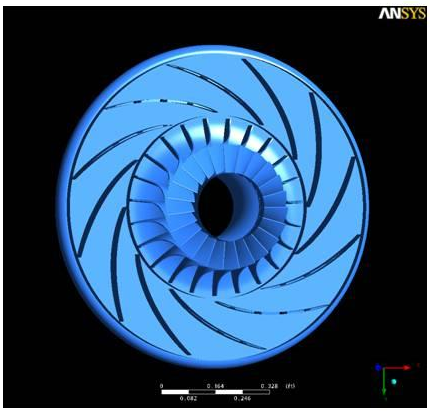

Rear View

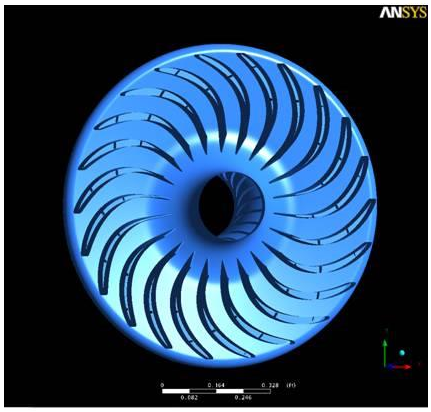

6

Mohawk Innovative Technology®, Inc.
1037 Watervliet-Shaker Road, Albany, NY 12205
URL: www.miti.cc
Phone: (518) 862-4290, FAX: (518) 862-4291

Turbo Solutions ENGINEERING

Computational Fluid Dynamics Analysis
Mesh

Front View

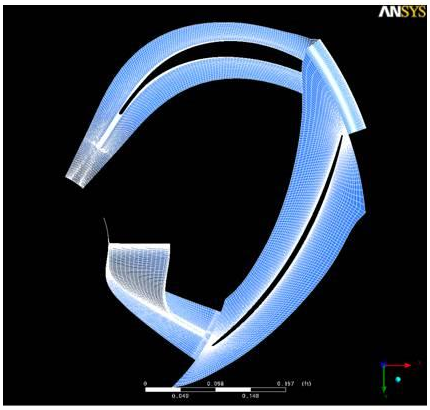

Rear View

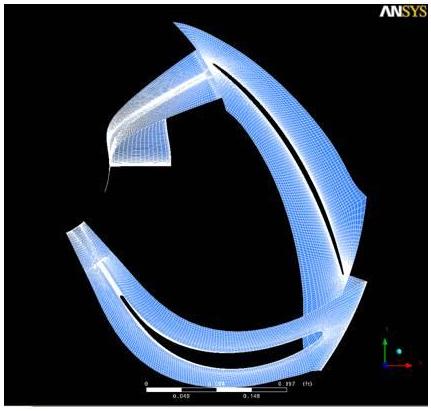

7

Turbo Solutions ENGINEERING

Computational Fluid Dynamics Analysis
Mesh

Impeller Detail

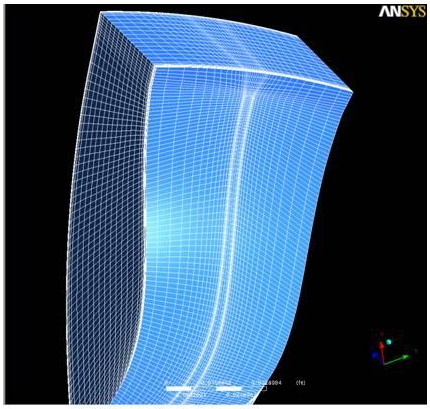

Summary

- Total nodes = 424,654
- Total elements = 382,632
  - Tetrahedra = 0
  - Wedges = 0
  - Pyramids = 0
  - Hexahedra = 382,632

8

Mohawk Innovative Technology®, Inc.
1037 Watervliet-Shaker Road, Albany, NY 12205
URL: www.miti.cc
Phone: (518) 862-4290, FAX: (518) 862-4291

Turbo Solutions ENGINEERING

Computational Fluid Dynamics Analysis
Mass-Averaged Performance Maps

Stage Work vs. Flow

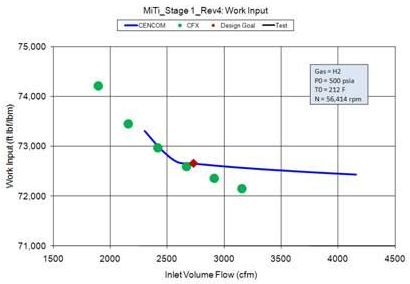

Diffuser Exit Head vs. Flow

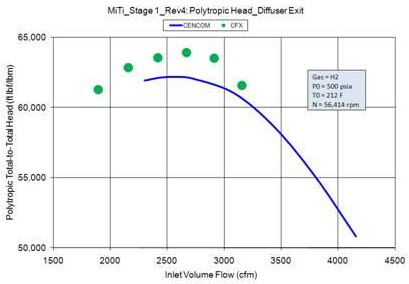

9

Turbo Solutions ENGINEERING

Computational Fluid Dynamics Analysis
Mass-Averaged Performance Maps

Stage Exit Head vs. Flow

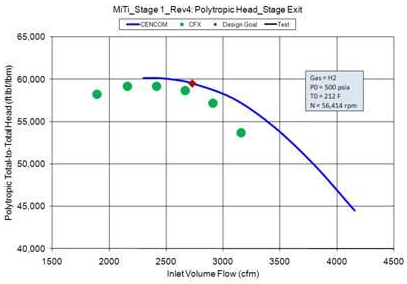

Diffuser Exit ηp_tt vs. Flow

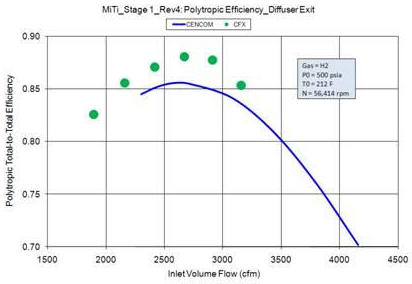

10

Mohawk Innovative Technology®, Inc.
1037 Watervliet-Shaker Road, Albany, NY 12205
URL: www.miti.cc
Phone: (518) 862-4290, FAX: (518) 862-4291

Turbo Solutions ENGINEERING

Computational Fluid Dynamics Analysis
Mass-Averaged Performance Maps

Stage Exit ηp_tt vs. Flow

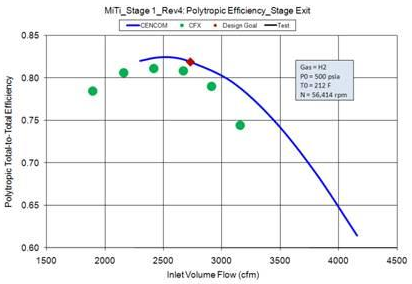

Design Point Summary

1147: MiTi_Stage 1_Rev4

		CENCOM[1]	CFX[2]	Test[3]
Impeller Inlet				
Fluid		H2	H2	
Q	cfm	2672	2670	
N	rpm	56,414	56,414	
P0	psia	500.00	500.00	
T0	F	212.00	212.00	
Impeller Exit				
P02	psia	568.15	569.28	
T02	F	239.09	239.06	
Work	ft lbf/lbm	72662	72587	
Head_p	ft lbf/lbm	67048	68089	
η_p		0.923	0.938	
Diffuser Exit				
P05	psia	562.94	564.77	
T05	F	239.09	239.06	
Work	ft lbf/lbm	72662	72587	
Head_p	ft lbf/lbm	62213	63915	
η_p		0.856	0.881	
Stage Exit				
P0ex	psia	560.23	559.15	
T0ex	F	239.09	239.06	
Work	ft lbf/lbm	72662	72587	
Head_p	ft lbf/lbm	59681	58667	
η_p		0.821	0.808	

11

Turbo Solutions ENGINEERING

Computational Fluid Dynamics Analysis
Flowfield Plots – Meridional View

Velocity Contours

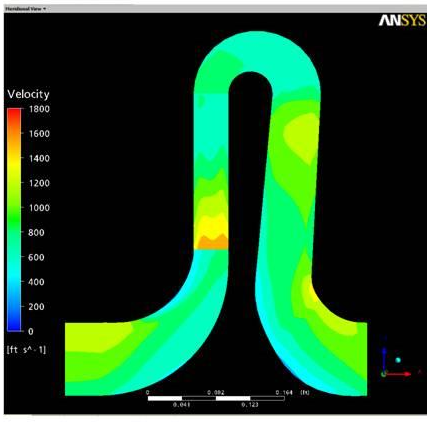

Velocity Vectors

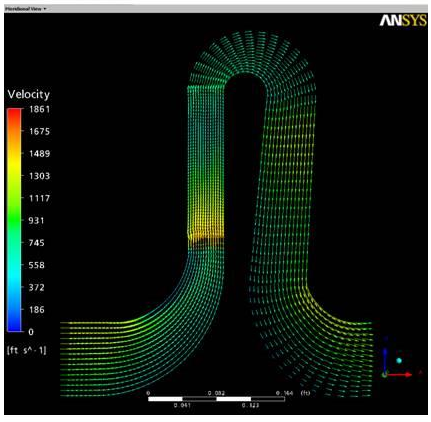

12

Mohawk Innovative Technology®, Inc.
1037 Watervliet-Shaker Road, Albany, NY 12205
URL: www.miti.cc
Phone: (518) 862-4290, FAX: (518) 862-4291

Turbo Solutions ENGINEERING

Computational Fluid Dynamics Analysis
Flowfield Plots – Meridional View

Total Pressure Contours

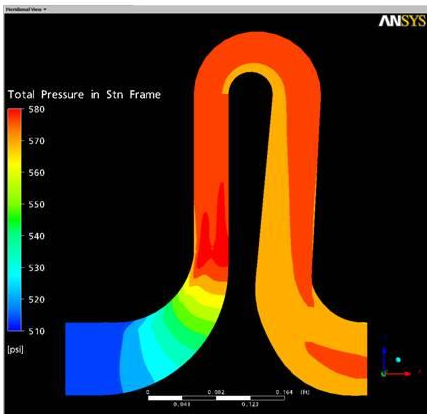

Static Pressure Contours

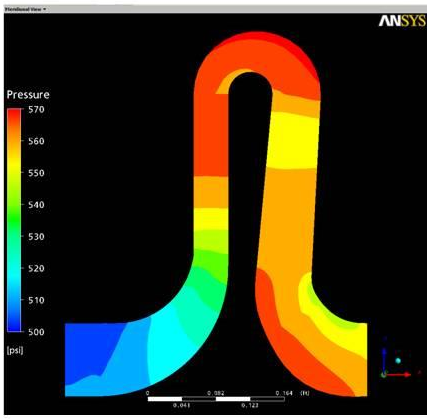

13

Turbo Solutions ENGINEERING

Computational Fluid Dynamics Analysis
Flowfield Plots – Blade-to-Blade View

Velocity Contours - Mean

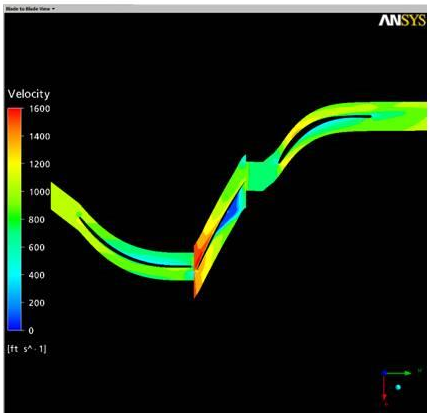

Velocity Vectors - Mean

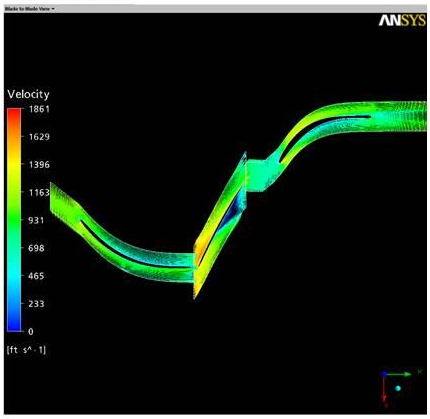

14

Mohawk Innovative Technology®, Inc.
1037 Watervliet-Shaker Road, Albany, NY 12205
URL: www.miti.cc
Phone: (518) 862-4290, FAX: (518) 862-4291

Turbo Solutions ENGINEERING

Computational Fluid Dynamics Analysis
Flowfield Plots – Blade-to-Blade View

Total Pressure Contours - Mean

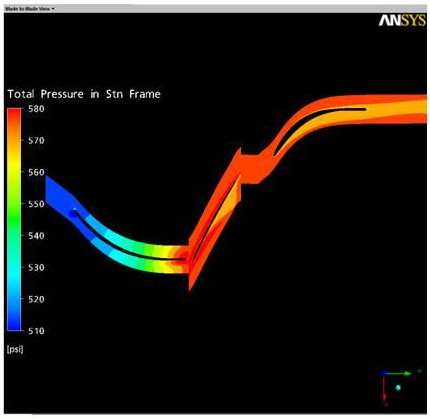

Static Pressure Contours - Mean

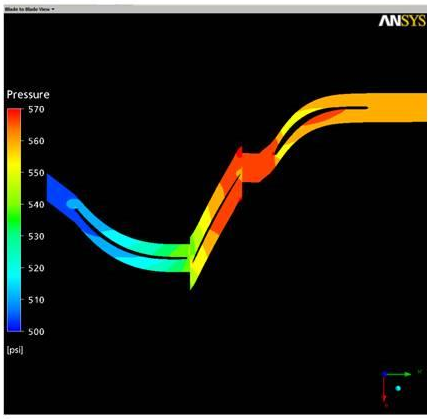

15

Turbo Solutions ENGINEERING

Computational Fluid Dynamics Analysis
Flowfield Plots – 3D View

Velocity Streamlines – Front

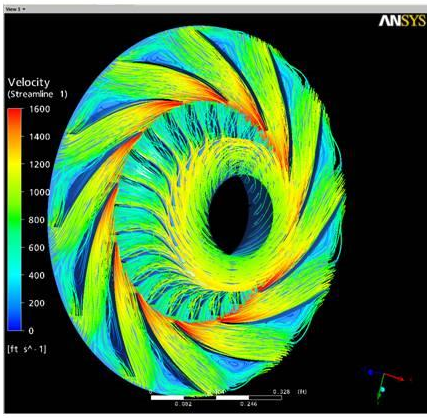

Velocity Streamlines - Rear

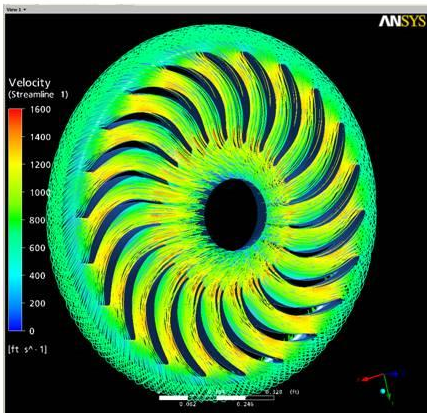

16

Mohawk Innovative Technology®, Inc.
1037 Watervliet-Shaker Road, Albany, NY 12205
URL: www.miti.cc
Phone: (518) 862-4290, FAX: (518) 862-4291

Turbo Solutions ENGINEERING

Computational Fluid Dynamics Analysis
Flowfield Plots – 3D View

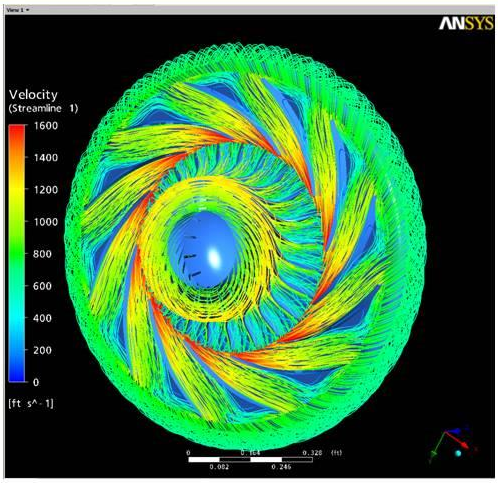

17

Turbo Solutions ENGINEERING

Computational Fluid Dynamics Analysis
Flowfield Plots – 3D View

Velocity Vectors – Impeller

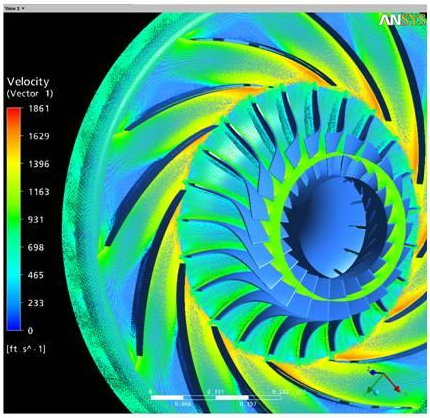

Velocity Vectors – Return Channel

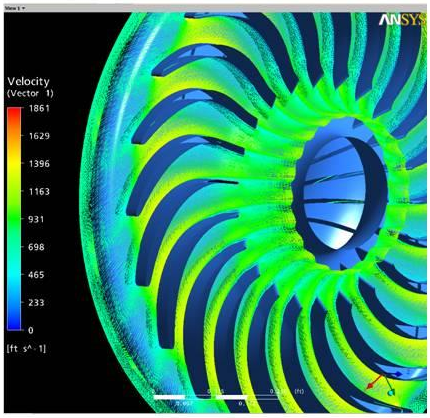

18

Mohawk Innovative Technology®, Inc.
1037 Watervliet-Shaker Road, Albany, NY 12205
URL: www.miti.cc
Phone: (518) 862-4290, FAX: (518) 862-4291

Turbo Solutions ENGINEERING

Computational Fluid Dynamics Analysis
Flowfield Plots – 3D View

Velocity Vectors Impeller Inlet

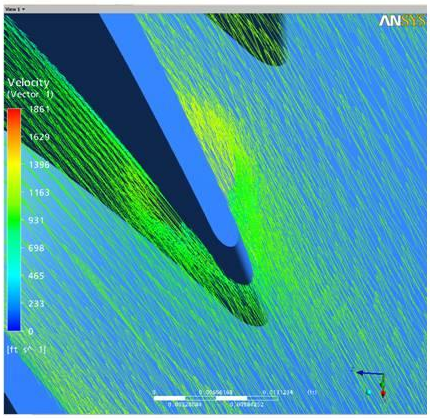

Velocity Vectors Impeller Exit

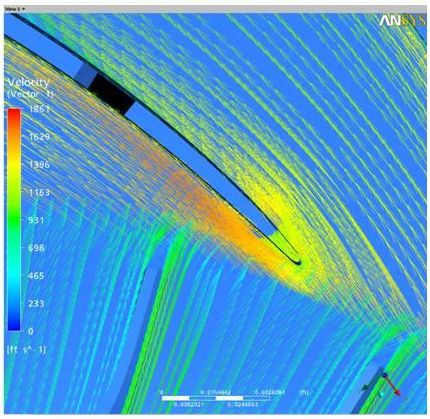

19

Turbo Solutions ENGINEERING

Summary

- CFD analysis of Mohawk Innovative Technology, Inc. hydrogen compressor is complete
- CFD model included impeller with tip clearance, vane diffuser, and return channel
- Work, head, and efficiency from meanline analysis (CENCOM) and CFD analysis (ANSYS-CFX) agree quite well from 70% to 120% design flow
- At the design condition, CFD predicts the stage will be about 1.7% low in total-to-total polytropic head and about 1.3 points low in total-to-total polytropic efficiency when compared to meanline predictions
- Detailed plots of the flowfield from CFD show some areas for potential performance improvement, but overall the flow patterns are quite good given the high work input coefficient and high polytropic head coefficient of the stage
- During the detailed design phase, it is recommended that comprehensive redesign iterations including meanline design, 3D blading design, CFD analysis, and structural analysis be completed

20

Mohawk Innovative Technology®, Inc.
1037 Watervliet-Shaker Road, Albany, NY 12205
URL: www.miti.cc
Phone: (518) 862-4290, FAX: (518) 862-4291